Value4Farm

VALUE4FARM

D2.6 Modelling study to optimise the design and management of agrivoltaic systems

Start date of the project:	01/09/2023
Duration of the project:	42 months
Deliverable n° & name	D2.6
Version:	1
Work-package n°:	2
Due date of D:	M12, 31/08/2024
Actual date of D:	20/12/2024
Participant responsible:	UCSC
Main authors:	Stefano Amaducci, Amirhossein Nik Zad, Giorgio Impollonia
Project website address:	www.value4farm.eu

Nature of the Deliverable		
R	Document, report	X
DEM	Demonstrator, pilot, prototype	
DATA	Data sets, microdata, etc.	
OTHER	Software, technical diagram, etc.	

Dissemination Level		
PU	Public, fully open and automatically posted online	X
SEN	Sensitive, limited under the conditions of the Grand Agreement	
CI	Classified information: RESTREINT UE (Commission Decision 2015/444/EC)	
	Classified information: CONFIDENTIAL UE (Commission Decision 2015/444/EC)	
	Classified information: SECRET UE (Commission Decision 2015/444/EC)	

Quality procedure			
Date	Version	Reviewers	Comments
07/11/2024	V1	Sander Vandendriessche (INA), Esperanza Huerta Lwanga (WUR), Danish Rehmann (MITIS), Uffe Jørgensen (AU)	General comments on structure and typos; Feedback on modelling approach and some numbers
11/12/2024	V2	Sander Vandendriessche (INA)	
20/12/2024	Final Version		

TABLE OF CONTENTS

LIST OF ABBREVIATIONS

AD	Anaerobic Digestion
APV	Agrivoltaics
BESS	Battery Energy Storage System
BHE	Borehole Heat Exchanger
$BioCH_4$	Biomethane
CAPEX	Capital Expenditure (implied by context)
CHP	Combined Heat and Power
COP	Coefficient of Performance
CPVT	Concentrated Photovoltaic Thermal
CSP	Concentrating Solar Power
ER	Electricity Reliability
FL	Full Light
GCR	Ground Cover Ratio
GSHP	Ground-Source Heat Pump
HP	Heat Pump
KPI	Key performance indicator
LCC	Life Cycle Cost
LCR	Life Cycle Revenue
LHV	Lower Heating Value
MPPT	Maximum Power Point Tracking
Nm^3	Normal Cubic Meters
O&M	Operation and Maintenance (implied by context)
PAR	Photosynthetically active radiation
PSH	Peak Sun Hours
PV	Photovoltaic
Sm^3	Standard Cubic Meters
SOC	State of Charge
UFL	Milk fodder units
WS	Water Stress
WUE	Water Use Efficiency

LIST OF FIGURES

LIST OF TABLES

KEYWORDS LIST

Agrivoltaics; Biomethane; Optimisation; KPIs; Modelling

EXECUTIVE SUMMARY

This report, Deliverable D2.6, presents the outcomes of Task 2.3, which focuses on the integration of agrivoltaics (APV) with biomethane production to create off-grid and grid-connected renewable energy solutions. The study investigates two scales: small-scale applications for off-grid biomethane plants and larger-scale applications aimed at enhancing agricultural sustainability and energy generation. The primary objective is to evaluate the techno-economic feasibility of combining these renewable technologies to optimize energy production, reduce reliance on fossil fuels, and support sustainable agricultural practices.

At the small scale, the study evaluates various configurations of APV systems integrated with biogas production for a biomethane plant located in Piacenza, Italy. The most economically viable option is found in Scenario 7, which integrates a vertical bifacial APV system (327 kW_p capacity), the power grid, and a biogas boiler. This configuration provides a 30% energy recovery (ER) and achieves the highest Life Cycle Revenue to Life Cycle Cost (LCR/LCC) ratio. By utilizing a biogas boiler for heat production rather than a combined heat and power (CHP) unit, the system minimizes capital and operational costs while ensuring reliable energy supply, with the added benefit of increased biomethane production for sale.

The adaptability of this optimal configuration was further validated by its application in Denmark, demonstrating how region-specific factors influence system performance. In the Danish context, the vertical bifacial APV system with a capacity of 506 kW_p achieved its optimal performance at a slightly higher ER of 35%, primarily due to lower solar intensity and regional energy tariffs. While this required a higher PV capacity compared to Italy, the findings highlight the scalability and transferability of the methodology when tailored to local climatic, economic, and spatial conditions. This emphasizes the importance of region-specific analyses in maximizing the cost-effectiveness and efficiency of integrated renewable energy systems.

At the larger scale, the study examines the potential of APV systems for enhancing the sustainability of agricultural operations, particularly in regions like the Po Valley in northern Italy. APV systems enable dual land use, generating both renewable energy and agricultural products. The study reveals that PV systems, integrated with agricultural practices, provide higher energy yields compared to biomethane production alone, making them a more efficient option for meeting energy demands. The performance of various crops under different irrigation conditions highlights the importance of tailored agricultural practices to maximize the benefits of APV systems. While crop yields vary, the integration of APV technology demonstrates significant advantages in terms of water-use efficiency, resilience to water stress, and overall energy production.

Overall, this research underscores the importance of integrating APVs and biomethane systems to create sustainable, energy-efficient solutions for rural and agricultural regions. The study calls for further exploration and policy support to promote these integrated systems, which offer a pathway to a more resilient and sustainable energy future.

1 INTRODUCTION

This deliverable (D 2.6) is the main outcome of Task 2.3 (Comprehensive study for off-grid biomethane ($BioCH_4$) plants), which investigates the potential integration of $BioCH_4$ production and agrivoltaics (APV) to create off-grid $BioCH_4$ plants or to identify the optimal synergy between these renewable energy technologies. The study is divided into two parts: the first focuses on small-scale APV systems and their ability to generate the electricity needed for off-grid $BioCH_4$ production; the second explores the scalability of APV systems to medium and large farms (20 hectares and beyond) to enhance renewable energy production at the farm level and feed surplus electricity into the grid.

The first part of the study develops an integrated energy model to meet the thermal and electrical demands of an anaerobic digestion (AD) facility in Piacenza (Italy). While achieving a fully off-grid system remains challenging, this research evaluates the feasibility of such systems by assessing the balance between energy independence and practical reliance on the grid. The focus on a small-scale system is motivated by the increasing importance of localized energy solutions, which not only support sustainability in small agricultural operations but also offer economic benefits, such as $BioCH_4$ sales to the gas grid. This comprehensive approach aligns with the broader goals of optimizing land use, enhancing energy efficiency, and ensuring the scalability of renewable energy solutions in agricultural contexts.

The second part of the study investigates the integration of large-scale APV systems into biogas farms to enhance the sustainability and productivity of agricultural systems. A case study conducted at a dairy farm in northern Italy explores the use of agricultural land to produce energy carriers for mobility (e.g., vehicles running on electricity or $BioCH_4$), while also producing food and feed. A crop model was applied to evaluate different *BiogasDoneRight* crop rotations under an APV system. The study examined various simulation scenarios to optimize APV design parameters (such as pitch) and crop management practices (e.g., irrigation). Several scenarios were analysed, including those focused on milk production alone, milk production combined with $BioCH_4$ production, and milk production combined with APV energy production. These scenarios were evaluated through different crop rotations to assess the trade-offs between food/feed production and energy generation. In this context, the study focuses on understanding the interplay between renewable energy technologies and agricultural practices, with a goal of developing a framework for optimizing APV systems that meet both food and energy demands in agricultural settings.

2 SMALL-SCALE AGRIVOLTAIC INSTALLATION IN BIOGAS FARMS

2.1 INTRODUCTION

The integration of renewable energy technologies into small-scale agricultural operations, defined as those up to 2 hectares (Lowder et al., 2016), is crucial for achieving sustainability, reducing greenhouse gas emissions, and improving energy access in rural areas (Fiorentino et al., 2024). Biomethane ($BioCH_4$) production from anaerobic digestion (AD) of organic matter plays a significant role in this context, offering a sustainable waste management solution while generating renewable energy (EBA Statistical Report, 2023) Upgraded $BioCH_4$ can be injected into the gas grid or used as fuel for combined heat and power (CHP) systems or biogas boilers, making it versatile for different energy needs.

Several studies have explored renewable energy integration strategies that enhance energy self-sufficiency and economic feasibility. (Temiz et al., 2022) demonstrated an integrated agrivoltaic (APV)-biogas system in Thailand that efficiently supplies electricity, heating, and cooling, while (Bambokela et al., 2020) highlighted the reliability of biogas-solar photovoltaic (PV) hybrid mini-grids for agricultural communities in Sub-Saharan Africa. Research on advanced configurations, such as PV-driven biomethanation (Sieborg et al., 2024) and concentrated PV thermal (CPVT) collectors paired with AD systems (Su et al., 2021) has shown the potential to increase $BioCH_4$ yields and reduce reliance on fossil fuels.

In Italy, favourable policies promoting renewable energy have driven significant growth in the biogas sector, positioning it as a crucial contributor to the country's electricity generation (Fiorentino et al., 2024) Figure 2.1 shows the position of Italy and Denmark among the top 10 countries in Europe in terms of upgraded biogas production (EBA Statistical Report, 2023).

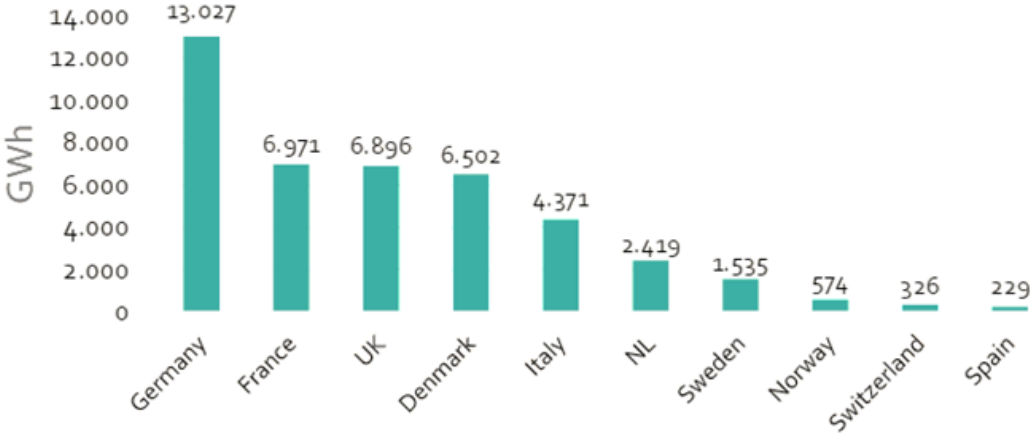

Figure 2-1 Upgraded biogas production in gigawatt hours for the ten leading EU countries in 2022 (EBA Statistical Report, 2023).Despite this progress and Italy's leadership in renewable energy integration (Taramasso et al., 2024) the potential of combining biogas with solar energy technologies, such as APV systems, remains underexplored, even though such integration could significantly enhance energy self-sufficiency and sustainability. Innovations such as hybrid energy systems using heat pumps (HP), PV panels, and biogas boilers (Álvaro et al., 2023; Hao et al., 2018) have proven effective in reducing emissions and improving economic viability. Studies on concentrating solar power (CSP)-biogas

hybridization (Calise et al., 2023), PV-biomethanation systems (Villarroel-Schneider et al., 2023), and biogas-PV-wind hybrid setups (Akarsu and Demir, 2024) underscore the importance of multi-energy approaches to optimize energy performance and economic returns.

Building on this knowledge, the present study addresses the gap in evaluating the techno-economic feasibility of integrating biomethanation with both off-grid and grid-connected bifacial APV systems. APV systems differ significantly from conventional PV systems, requiring distinct modelling approaches to optimize their design and management. Key differences include higher PV array row spacing to allow sunlight for crops, greater height of the mounting system from the ground to accommodate agricultural activities, and the use of bifacial PV modules, which are specifically advantageous in agrivoltaics due to the higher albedo from reflective agricultural soil or vegetation. This study focuses on various mounting configurations of APV systems, including vertical, mono-axial, and biaxial systems, and incorporates additional power sources like biogas CHP units, HP, biogas boilers, Battery Energy Storage Systems (BESS), and the power grid. The objective of this study is to develop an integrated energy model that satisfies the thermal and electrical demands of an AD facility in Piacenza (Italy), while maximizing economic benefits through BioCH_4 sales to the gas grid. Additionally, the study aims to identify the most economically viable energy system configuration over the facility's operational lifespan by systematically evaluating scenarios using a life cycle revenue (LCR) to life cycle cost (LCC) ratio as a decision-making tool.

2.2 METHODOLOGY

This research investigates energy provision strategies by integrating APV systems with a biogas plant characterized by an average capacity of 125 standard cubic meters (Sm^3) of BioCH_4 per hour. Recognizing the limitations of APV systems during night-time and adverse weather, the study models different scenarios to optimize energy performance and ensure system reliability.

To address the stated objective, each system component is optimally sized according to the defined electrical and thermal energy requirements of the facility. The process systematically evaluates and ranks scenarios based on their LCR to LCC ratio to identify the optimal configuration. The schematic presented in Figure 2.2 illustrates the integrated energy system designed to meet the energy demands of an AD facility. It shows the interaction of multiple components, including a biogas boiler, a biogas CHP unit, a heat pump, an APV system, a BESS, and the power grid. The figure demonstrates how heat, electricity, and biogas flow between these components to optimize the facility's operation.

The process starts with biogas production in the AD plant, where organic waste undergoes treatment. This biogas is then upgraded into BioCH4 in an upgrading plant. The upgrading process requires both heat and electricity. Heat can be supplied by the biogas boiler, the heat pump, or the biogas CHP unit, while electricity is provided by the biogas CHP unit, the APV system, the BESS, or the power grid when needed.

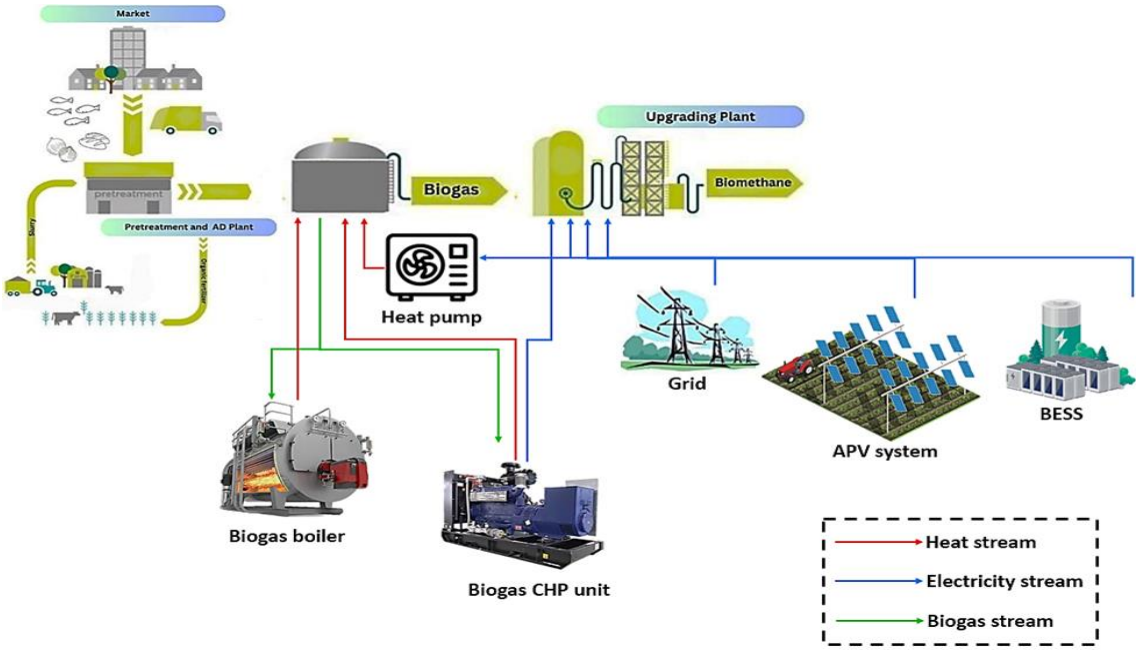

Figure 2-2 Schematic of all involved equipment under investigation in this study.

2.2.1 Description of the site and load profile

The mesophilic AD facility in Piacenza, Italy, operates at a constant temperature of 37°C and incorporates membrane technology for biogas upgrading. Based on site-specific data (CIB - Consorzio Italiano Biogas), the daily biogas production at this facility is approximately 6,789 normal cubic meters (Nm^3), which equates to an annual production of 2,477,985 Nm^3. The biogas produced at this site has a methane content of 54.2%. Consequently, the daily $BioCH_4$ production is calculated to be 3,679.6 Nm^3, resulting in an annual $BioCH_4$ output of 1,343,068 Nm^3. A predominant fraction, constituting 75.95% of the total biogas output, is designated for the $BioCH_4$ conversion process within the upgrading plant. Conversely, the remaining 24.05% is channelled to the CHP unit with a capacity of 150 kW_{el} (1633 Nm^3 biogas/day).

The plant's annual electricity demand is 1,081,422 kWh_{el}, which translates to a daily requirement of 2,963 kWh. This electricity is required for the entire process, from biogas production to $BioCH_4$ upgrading, including components such as biogas compression, upgrading technology, and auxiliary systems. In a 125 Sm^3/h $BioCH_4$ production facility, the fixed electrical requirement is 119 kW, covering the upgrading plant, compression stages, biological processes, and auxiliary systems.

In addition, after sizing, the electricity requirements for the control electronics, motor starter, sensors, and cooling pumps of heat producers, will be incorporated into the overall electrical demand.

The heat demand fluctuates monthly, reflecting the plant's seasonal variations and operational dynamics as shown in Table 1.

Table 1 Monthly heat requirement of a 125 Sm^3/h bioCH4 production plant in Piacenza in 2024.

Month	Thermal power (kW_{th})	Heating hours	Heat demand (MWh_{th})
January	178.6	744	132.9
February	166.2	672	111.7
March	153.7	744	114.3
April	137.1	720	98.7
May	116.3	744	86.5
June	99.7	720	71.8
July	87.2	744	64.9
August	91.4	744	68.1
September	103.9	720	74.8
October	124.6	744	92.7
November	157.9	720	113.7
December	174.5	744	129.9
Total	**1591.1**	**8760**	**1,159.8**

This study utilizes monthly heat demand data, which was similarly reported in other published works and is appropriate for capturing long-term trends and providing a comprehensive analysis of heat requirements (Josimović et al., 2024; Solheim Haugen and Arancibia Holm, 2023).

2.2.2 Description of scenarios

As mentioned before, the thermal and electrical energy requirements for the whole processes are met through eight different scenarios. These scenarios are designed to compare energy provision strategies, including five configurations that incorporate APV and three configurations without APV systems, ensuring a fair assessment. The scenarios are outlined as follows:

S1: Off-grid APVs (APVs + BESS) + biogas boiler
S2: Off-grid APVs + heat pump
S3: Power grid + heat pump
S4: Power grid + biogas boiler
S5: Biogas CHP unit
S6: APVs + Power grid + heat pump
S7: APVs + Power grid + biogas boiler
S8: APVs + Power grid + Biogas CHP unit

Therefore, for clarity all the scenarios are summarized in the Table 2.

Table 2 All combinations assumed of different power sources to meet the energy needs.

Scenarios	*APV systems	BESS	Power Grid	Biogas CHP	Biogas boiler	Heat pump
1	✓	✓	-	-	✓	-
2	✓	✓	-	-	-	✓
3	-	-	✓	-	-	✓
4	-	-	✓	-	✓	-
5	-	-	-	✓	-	-
6	✓	-	✓	-	-	✓
7	✓	-	✓	-	✓	-
8	✓	-	✓	✓	-	-

It should be noted that, in each scenario where APV systems are included, three different mounting configurations are considered: overhead mono-axial, vertical mounting, and overhead bi-axial systems, as illustrated in Figure 2.3. These configurations will be described in detail in the relevant sections.

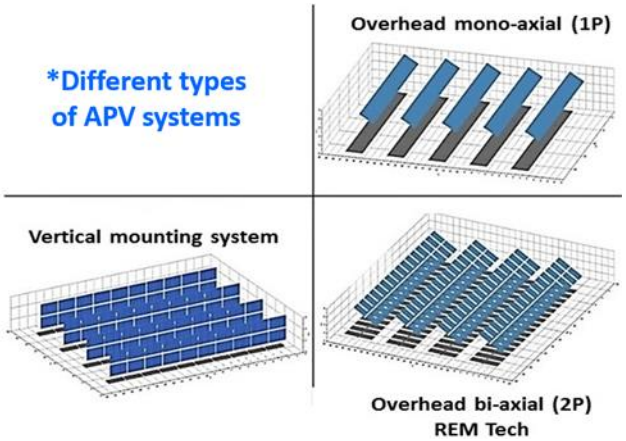

Figure 2-3 Different types of APVs under investigation in this study.

2.2.2.1 Scenario 1: Energy supply by an off-grid APV system and biogas boiler

In this scenario, electricity demand is met by an off-grid APV system, which powers the biogas boiler, upgrading plant, compression stages, and auxiliary systems. Thermal demand is satisfied by a biogas

thermal boiler integrated into the $BioCH_4$ production plant. Figure 2.4 provides an overview of the process in this scenario.

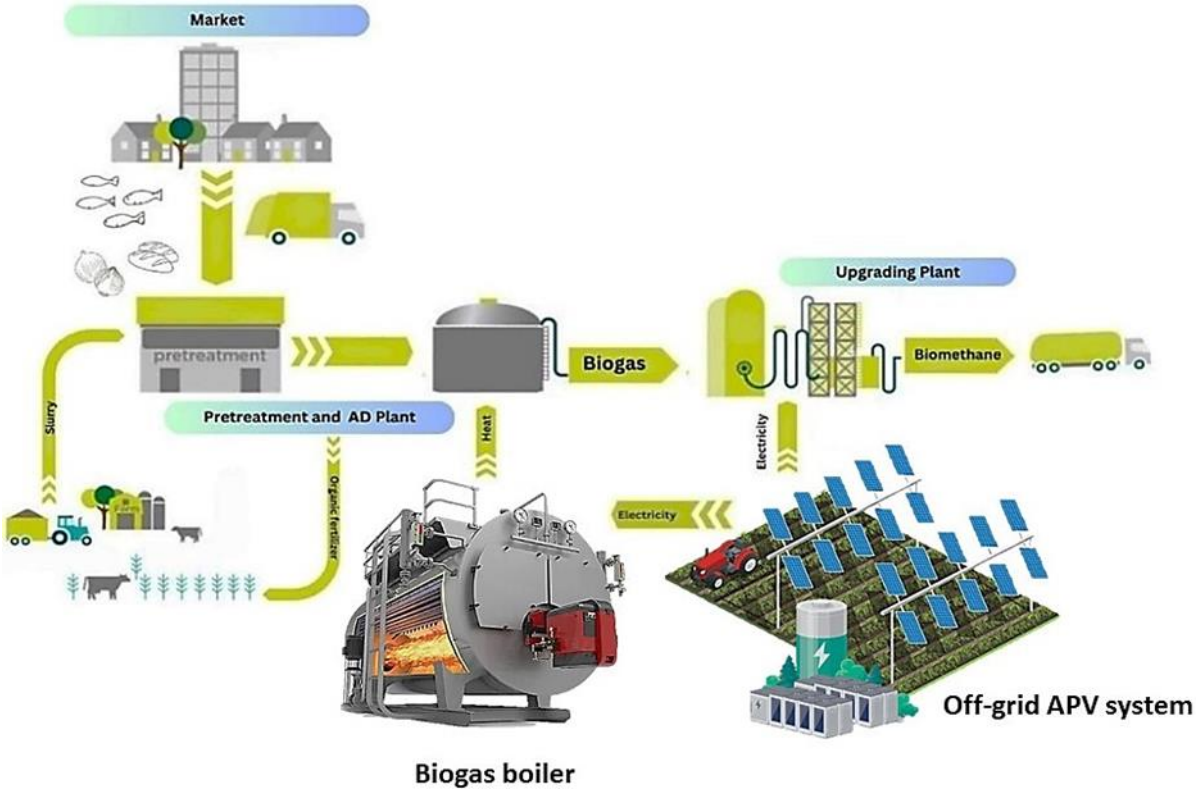

Figure 2-4 S1: Energy needs fully covered by an off-grid APV system and biogas boiler.

2.2.2.2 Scenario 2: Energy supply by an off-grid APV system and heat pump

This scenario operates with a $BioCH_4$ production plant where thermal demand is met by a heat pump. Electricity demand, including the needs of the heat pump, upgrading plant, compression stages, and auxiliary systems, is exclusively supplied by a stand-alone APV system. This APV system is designed to ensure reliable operation during night-time and adverse weather conditions, such as cloudy or rainy days. Figure 2.5 provides an overview of the process in this scenario.

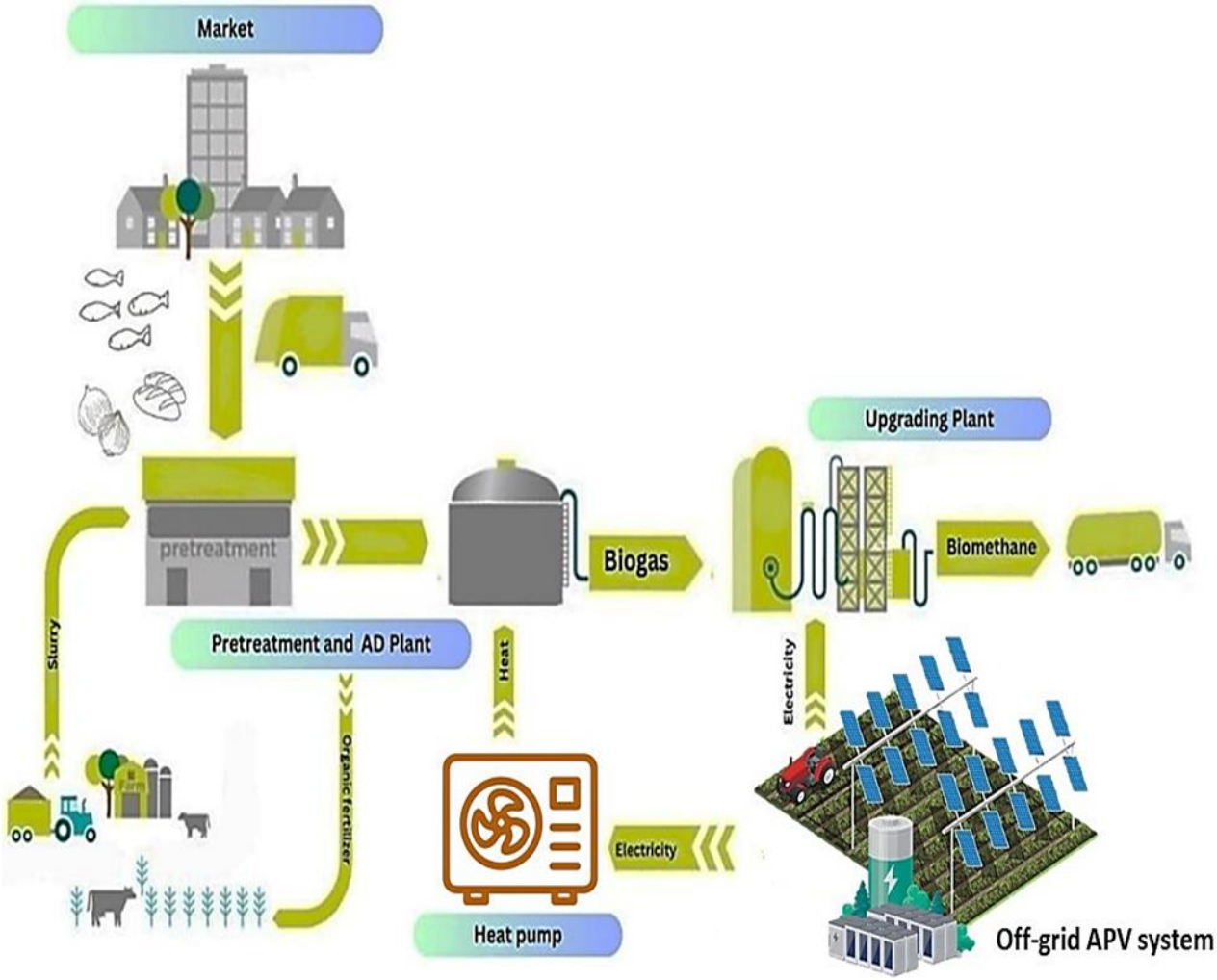

Figure 2-5 S2: Energy needs fully covered by an off-grid APV system and heat pump.

2.2.2.3 Scenario 3: Energy supply by power grid and heat pump

Similar to Scenario 2, thermal demand is met by a heat pump. However, in this scenario, all electricity requirements, including those of the heat pump, upgrading plant, compression stages, and auxiliary systems, are entirely supplied by the Italian national grid. Figure 2.6 provides an overview of the process in this scenario.

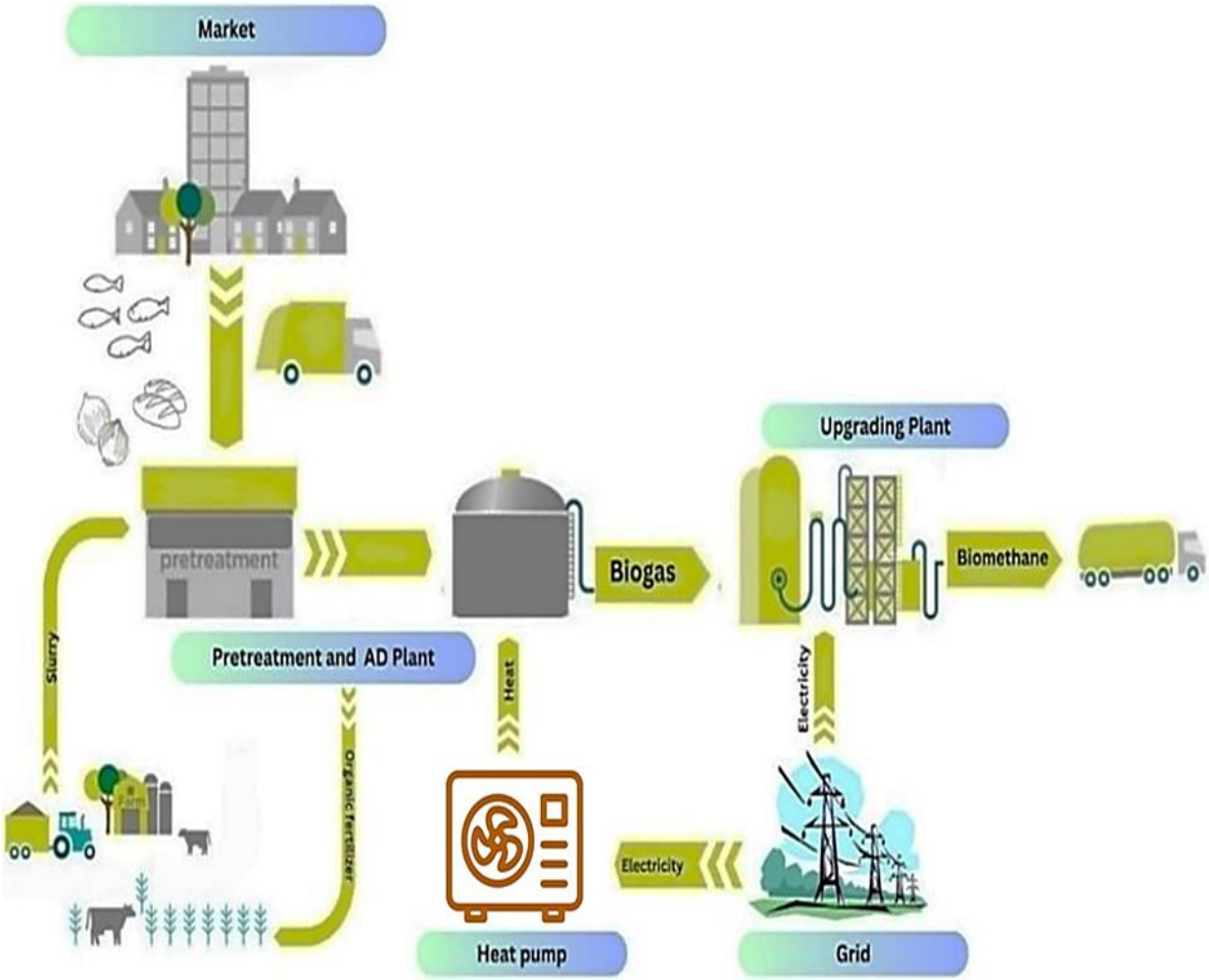

Figure 2-6 S3: Energy needs covered by power grid and heat pump.

2.2.2.4 Scenario 4: Energy supply by power grid and biogas boiler

In contrast to the previous scenario, this scenario employs a biogas boiler to address thermal needs. However, all the electricity required for the operation of the boiler, as well as for the upgrading and compression stages, etc. is fully supplied by the Italian national grid. Figure 2.7 presents an overview of the process in this fourth scenario.

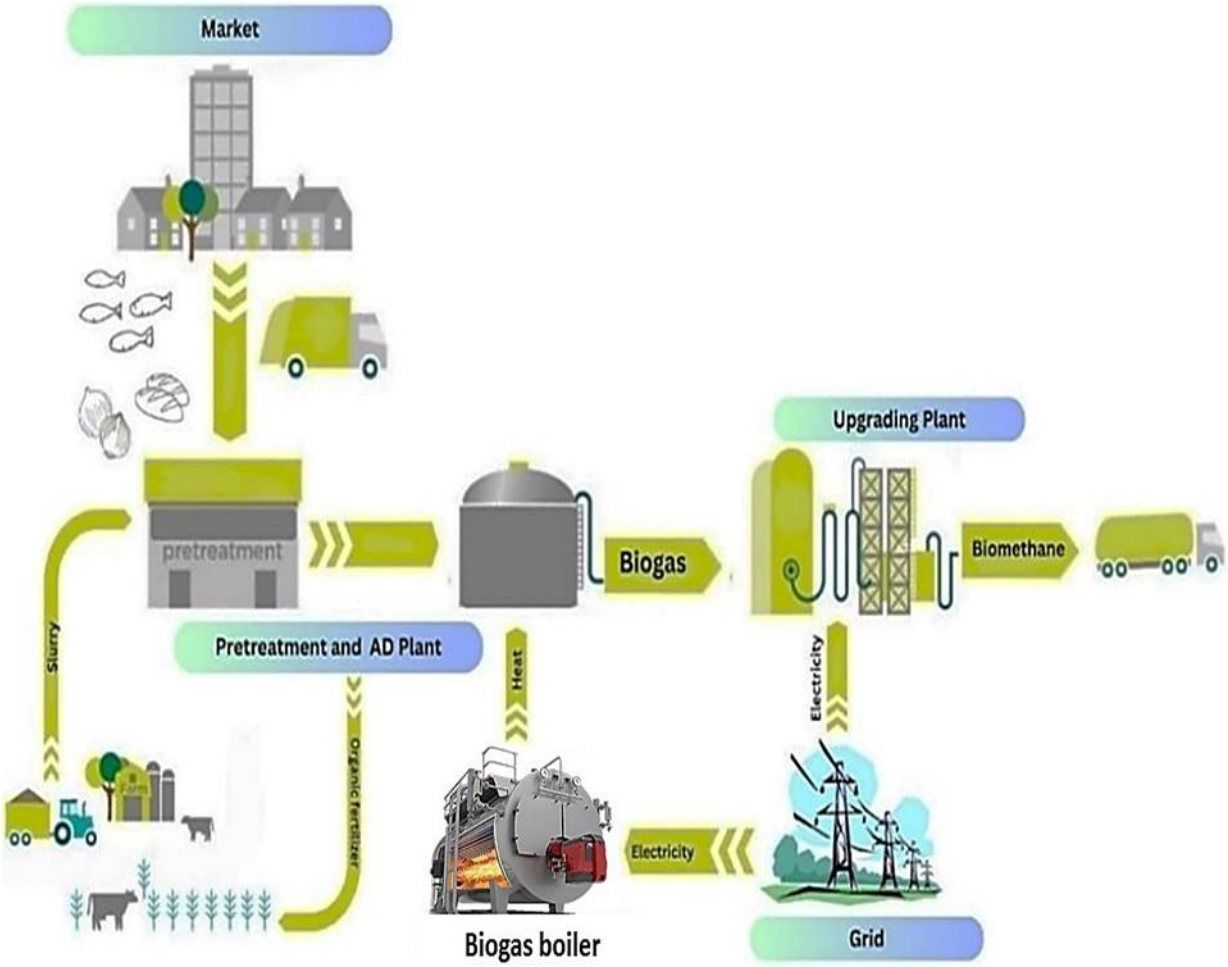

Figure 2-7 S4: Energy needs covered by power grid and biogas boiler.

2.2.2.5 Scenario 5: Energy supply by CHP unit

In this scenario, a biogas-powered CHP system is employed to fulfil all thermal and electrical demands. Importantly, the electrical energy required for the continuous operation of the CHP unit is entirely self-generated by the system. Figure 2.8 provides an illustration of the process in this scenario.

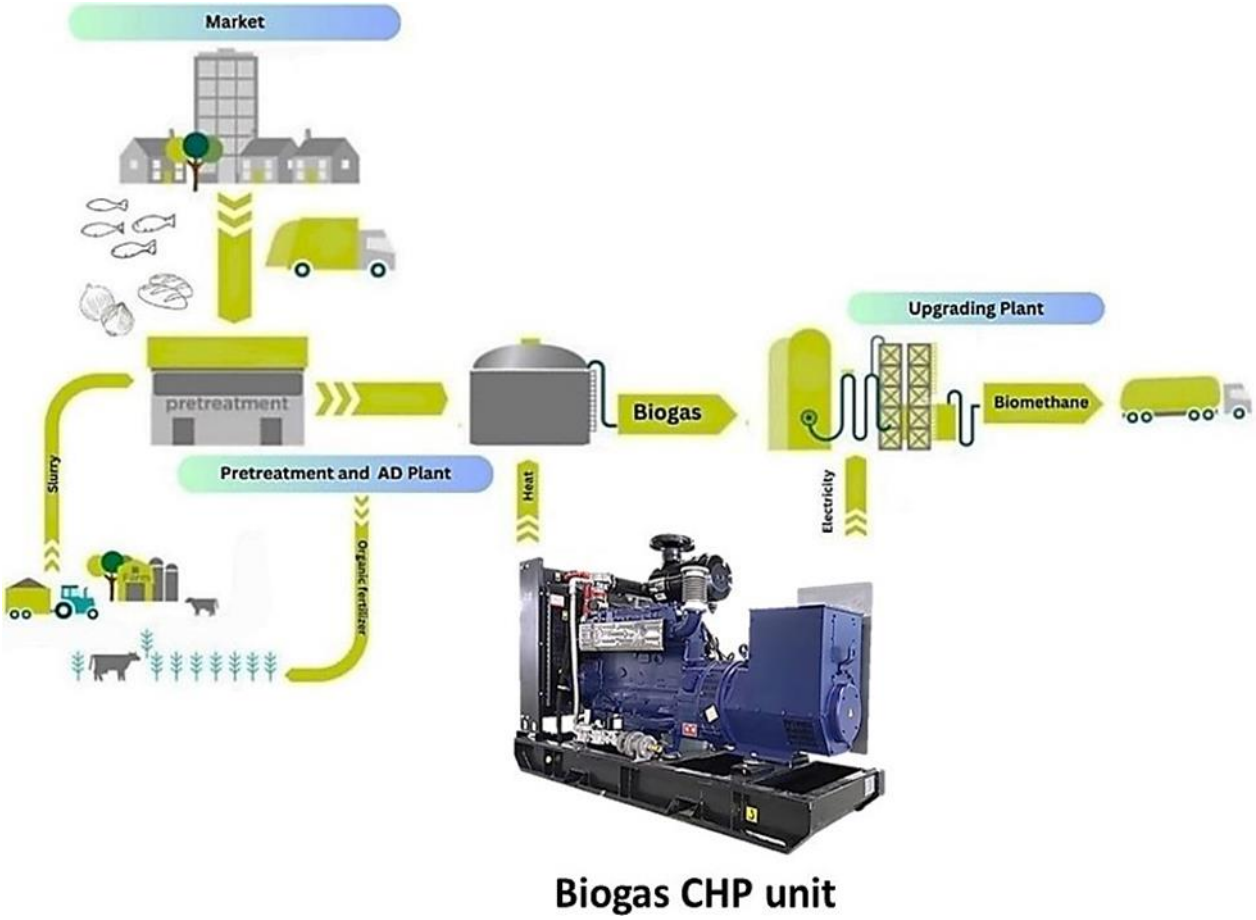

Figure 2-8 S5: Energy needs covered by biogas CHP unit.

2.2.2.6 Scenario 6: Energy supply by an APV system, power grid and heat pump

Electricity demand in this scenario is met by a combination of an APV system and the Italian national grid, with the grid supplying power during insufficient sunny hours. Thermal demand is satisfied by a dedicated heat pump. Figure 2.9 provides an overview of the process in this scenario.

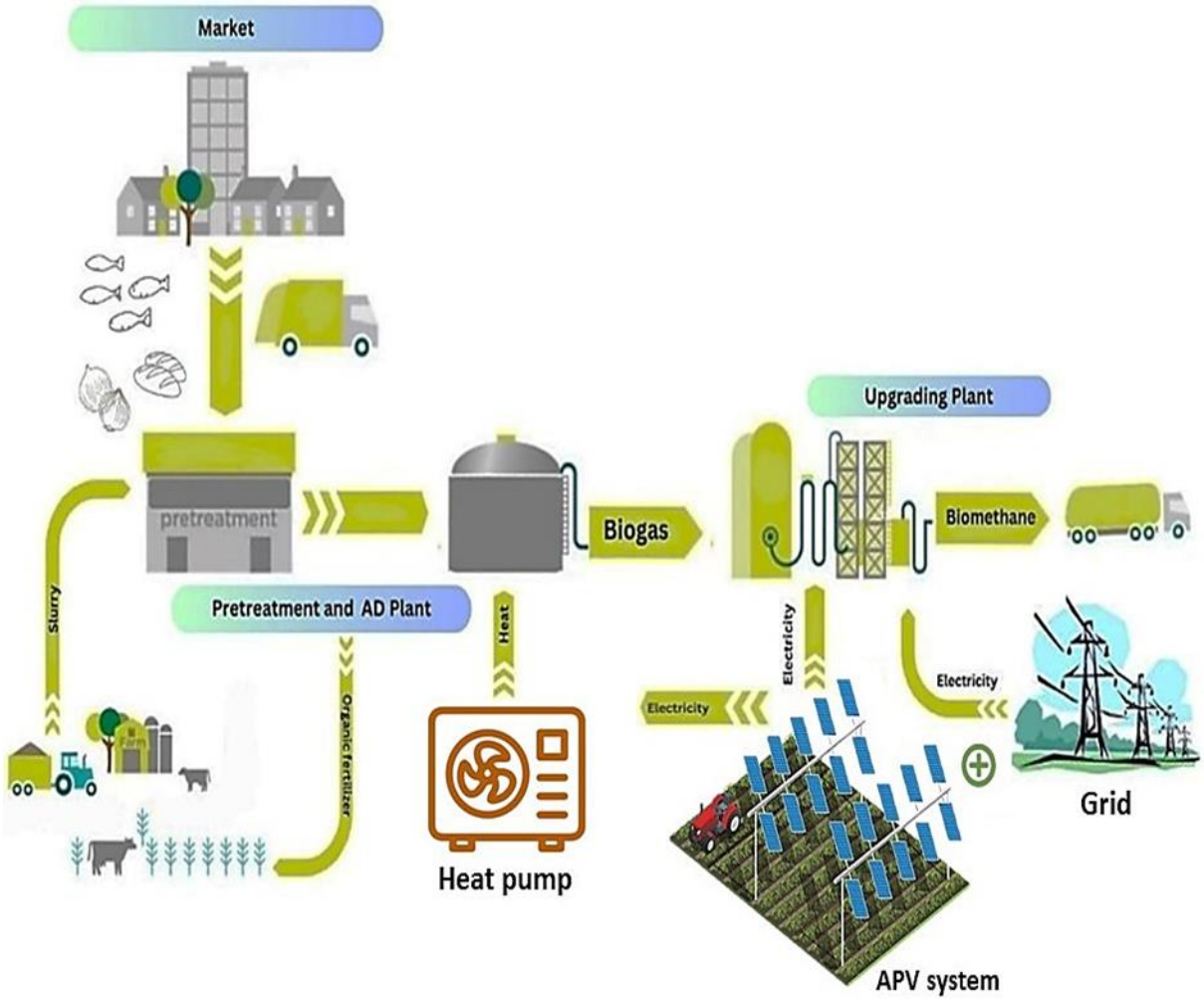

Figure 2-9 S6: Energy needs covered by an APV system, power grid and heat pump.

2.2.2.7 Scenario 7: Energy supply by an APV system, power grid and biogas boiler

Electricity demand in this scenario is met by a combination of an APV system and the Italian national electricity grid, supplying power for the biogas boiler, upgrading plant, compression stages, and auxiliary

systems. Thermal requirements are addressed by a specialized biogas boiler. An overview of this process is depicted in Figure 2.10.

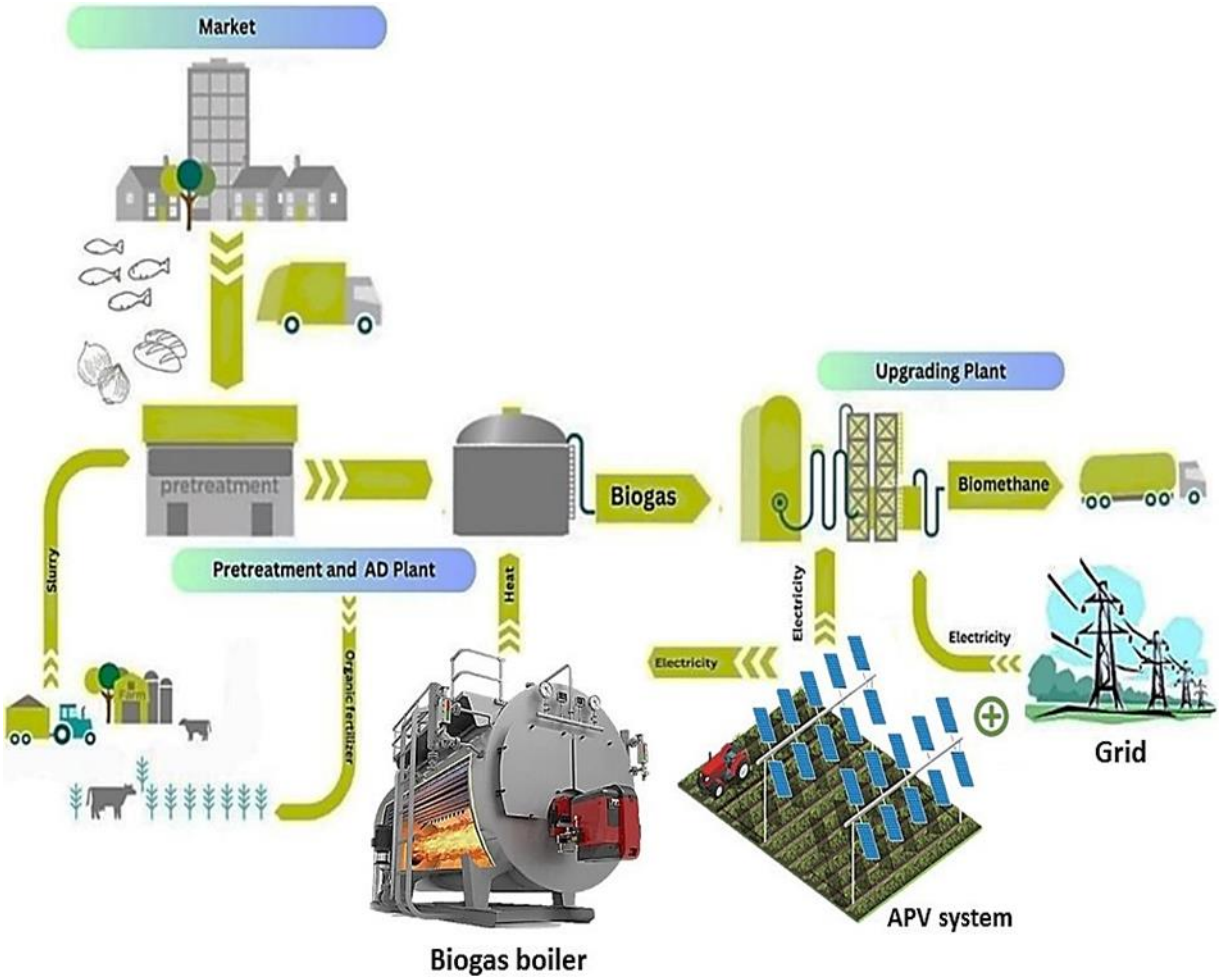

Figure 2-10 S7: Energy needs covered by an APV system, power grid and biogas boiler.

2.2.2.8 Scenario 8: Energy supply by an APV system, power grid and biogas CHP unit

Electricity demand in this scenario is supplied by a combination of APV systems, the power grid, and a biogas CHP unit, meeting the needs of the upgrading plant, compression stages, and related processes. Thermal demands are addressed by the biogas CHP unit. A schematic representation of this process is provided in Figure 2.11.

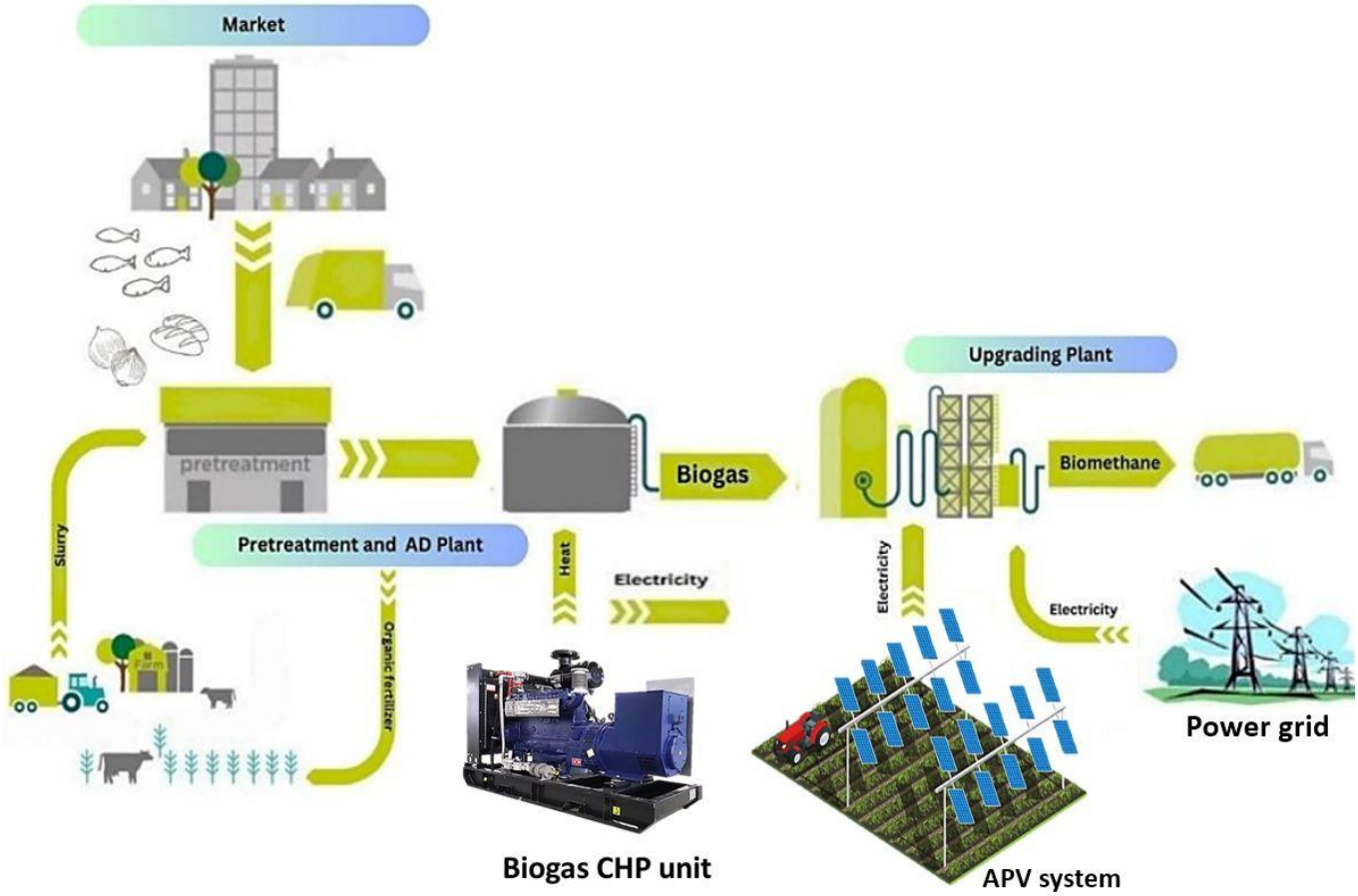

Figure 2-11 S8: Energy needs covered by an APV system, power grid and biogas CHP unit.

It is worth noting that, in all scenarios, any surplus electricity generated by the APV system is fed into the grid to generate financial revenue. If there is an electricity shortage, additional power will be purchased from the grid.

2.2.3 Heat supply

2.2.3.1 Biogas boiler

Biogas boilers burn biogas to generate thermal energy for uses like heating, drying, or preheating digesters. They offer environmental benefits from renewable fuel use but require careful design due to biogas variability and have higher initial costs than conventional boilers.

In this study, the biogas boiler is sized based on the peak heat demand observed in January (see Table 2.1), measured at 178.6 kW_{th}. The LHV of biogas is assumed to be 5.5 kWh/Nm³, with the biogas boiler's efficiency estimated at 85%. Given these parameters, the required biogas input rate can be calculated using Eq. (1) (Petrollese and Cocco, 2020):

$$P_{th,Biogas\ boiler} = Q_{biogas\ boiler} \times LHV_{Biogas} \times \eta_{th,Biogas\ boiler} \quad (1)$$

Where, $P_{th,Biogas}$ boiler represents the thermal output of the biogas boiler (kW_{th}), $Q_{biogas,boiler}$ represents the required biogas input rate (Nm^3), $\eta_{th,BGCHP}$ denotes the biogas boiler efficiency (%), and LHV_{Biogas} signifies the lower heating value of biogas. Finding a biogas boiler that precisely matches the peak thermal load (178.6 kWth in January) poses challenges in the current market. As a result, the ATTSU RL-300 biogas boiler (ATTSU Group Company) with a maximum thermal output of 228 kW_{th} and 85% efficiency, has been identified as the most suitable option.

2.2.3.2 Heat pump

A heat pump is an energy-efficient system that transfers heat from external sources to meet heating demands. A ground-source heat pump (GSHP) is preferred in Northern Italy over an air-source heat pump (ASHP) due to stable ground temperatures, providing higher efficiency and reliability in winter. Despite higher installation costs, GSHPs offer lower operational costs and long-term savings, with reduced environmental impact and maintenance.

In this study, the thermal output of the selected heat pump must meet the peak heat demand of 178.6 kW_{th} in January. Based on the highest heat demand and market availability, the Mitsubishi EW-HT0412 ground-source heat pump (MITSUBISHI ELECTRIC) with a maximum capacity of 181 kW_{th}, has been identified as the most suitable option.

The GSHP unit requires the installation of borehole heat exchangers (BHEs) or wells to facilitate heat exchange with the ground via a closed pipe loop. These loops are typically installed in vertical boreholes specifically drilled for this purpose, commonly referred to as borehole heat exchangers (BHEs). The requisite number of BHEs can be determined using Eq. (2) (Hein et al., 2016):

$$N_{BHE} = \frac{THC_{GSHP}}{HER \times H_{GSHP}} \qquad (2)$$

In this equation, N_{BHE} represents the number of boreholes, THC_{GSHP} denotes the total heating capacity of the GSHP, HER signifies the heat extraction rate per meter (0.05 kW/m (Blum et al., 2011), and H_{GSHP} indicates the depth of each borehole, assumed to be 100 m (Casasso et al., 2019; Ruffino et al., 2022).

2.2.3.3 CHP unit

A biogas CHP unit converts biogas into electricity and heat simultaneously. Equation (3) is utilized to calculate the rated heat capacity of biogas CHP unit (Ennemiri et al., 2024):

$$P_{th,BGCHP} = \frac{Q_{BGCHP} \times LHV_{Biogas} \times \eta_{th,BGCHP}}{OH_{BGCHP}} \qquad (3)$$

Where, $P_{th,BGCHP}$ (kW_{th}) represents the thermal output of the biogas CHP unit. Q_{BGCHP}, the daily biogas availability, is calculated as 24.05% of daily biogas production, and OH_{BGCHP} refers to the daily operating hours, while LHV_{Biogas} is the lower heating value of biogas. These parameters have been obtained through on-site assessments of the proposed biogas plant, as detailed in the Table 3.

Table 3 The technical specifications of biogas plant in this study.

Parameters	Unit	Specification
Q_{BGCHP}	Nm^3	1633
OH_{BGCHP}	hour	24
LHV_{Biogas}	kWh/Nm^3	5.5
Biogas density	Kg/Nm^3	1.28

The thermal conversion efficiency of the biogas CHP unit, denoted as $\eta_{th,BGCHP}$, is assumed to be 50%, for a small-scale biogas plant (Pöschl et al., 2010).

2.2.4 Electrical consumption of heat producers

2.2.4.1 Biogas boiler

The boiler's electrical demand mainly arises from its auxiliary components, such as pumps, fans, and control systems. By examining the catalogues, this consumption is estimated to be 1-2% of the biogas boiler's thermal output, depending on the size of the boilers. In this study, a conservative estimate of 1.5% has been assumed.

2.2.4.2 Heat pump

The required electrical power for operation of the GSHP is calculated using Eq. (4) (Ruffino et al., 2022):

$$E_{GSHP} = \frac{Q_{GSHP}}{COP} \qquad (4)$$

Where, E_{GSHP} represents the electrical power required by the GSHP (kWh_{el}), Q_{GCHP} is the annual thermal energy production by the heat pump (MWh_{th}/y), and the coefficient of performance (COP) is a dimensionless parameter that measures the heat pump's efficiency in converting electrical energy into heating output. In this study, the COP is assumed 4.14, derived from catalogues based on the highest heat demand.

2.2.4.3 Biogas CHP unit

The biogas CHP unit consumes electrical power to operate continuously for its auxiliary systems, including control electronics, sensors, and cooling pumps, which is assumed 3% of its nominal electrical output (Pöschl et al., 2010).

2.2.5 Electricity supply

2.2.5.1 CHP unit

Equation (5) is utilized to calculate the rated electrical capacity of biogas CHP unit (Ennemiri et al., 2024):

$$P_{el,BGCHP} = \frac{Q_{BGCHP} \times LHV_{Biogas} \times \eta_{el,BGCHP}}{OH_{BGCHP}} \qquad (5)$$

Where, $P_{el,BGCHP}$ (kW_{el}) represents the electrical output of the biogas CHP unit. The electrical conversion efficiency of the biogas CHP unit, denoted as $\eta_{el,BGCHP}$ is assumed to be 33%, for a small-scale biogas

plant (Pöschl et al., 2010). Based on equations (3) and (5), the thermal and electrical outputs of the biogas CHP unit are 187.12 kW_{th} and 123.49 kW_{el}, respectively. However, due to market availability, a biogas CHP unit with specifications closely matching the actual energy demand and efficiency requirements has been selected, as presented in Table 4.

Table 4 The technical specifications of TEDOM CENTO-T150 biogas CHP selected in this study (TEDOM Group).

Parameter	Unit	Specification
Max. electrical output @LHV5.5	kW	127.9
Max. heat output @LHV5.5	kW	195.7
Max. electrical consumption	kW	3.84
Max. electrical efficiency	%	34.2
Max. thermal efficiency	%	52.3
Max. overall efficiency	%	86.5

2.2.5.2 Battery energy storage system

The battery pack is essential for storing energy in a hybrid system, particularly in off-grid APV designs, to ensure reliability. This is crucial due to fluctuations in solar radiation and the need for electricity supply during low-sunlight periods, such as cloudy weather or night-time. Surplus solar energy is stored in multiple batteries, and the optimal number can be determined using Eq. (6) (Nikzad et al., 2019):

$$N_{Batt} = \frac{TDL_{el} \times NNSD}{C_n \times V_n \times \eta_{r\text{-}t} \times (1 - \frac{SOC_{min}}{100})} \quad (6)$$

In this equation, N_{batt} represents the number of solar batteries, TDL_{el} is the total daily electrical load (Wh), and NNSD refers to the number of non-sunny days per month (system autonomy days), assumed to be 3. C_n is the nominal capacity of a single storage unit (Ah), $\eta_{r\text{-}t}$ is the roundtrip efficiency (%), and V_n denotes the nominal voltage of a single storage unit (V). The minimum state of charge (SOC_{min}) is set at 20%. The battery details selected for this study are outlined in Table 5.Table 5 The technical specifications of Huawei Luna 2000-15 BESS selected in this study.

Parameters	Specifications
Technology	Lithium-ion phosphate, LFP
Nominal voltage (V)	48
Capacity (Ah)	300
Round-trip efficiency (%)	90

2.2.5.3 Off-grid APV systems

In this section, three different off-grid APV systems are simulated using PVsyst® software, a comprehensive tool for designing, simulating, and analysing PV systems. PVsyst supports various PV installations, including grid-connected and stand-alone, and allows for performance modelling based on meteorological data and component specifications. Recognized for its accuracy in the solar industry, the software's assumptions for modelling the APV configurations are outlined in Table 6.

Table 6 Input data for simulation of energy output from different types of APV systems.

Parameters	Specifications
Location	Piacenza, 44.9744° N, 9.8924° E
Weather data	Year 2019 (measured)
Tracker max/min rotation angle	+55°/-55°
Height at rotation axis for Mono and Biaxial	5 m
Clearance for Vertical mounting system	0.7 m
Axis azimuth angle for Mono and Biaxial	South (0°)
Axis azimuth angle for Vertical	East (-90°)
PV array layout	6-Landscape (Biaxial), 1-Portrait (Mono-axial), 2-Landscape (Vertical)
PV module	Trina solar, TSM-DEG21C-20
PV module nominal capacity	660Wp
Efficiency	21.28%
Bifaciality factor	75%
Nominal operation module temperature	43°C (±2°C)
Temperature co-efficient for P_{max}	- 0.34%/°C
Number of cells	132 (66×2)
PV module dimension	2384mm×1303mm×35mm
Albedo factor	0.25
Pitch between PV strings for biaxial system	15m-18m
Pitch between PV strings for mono-axial system	6m-8m
Pitch between PV strings for vertical system	8m-10m

To determine the total required quantity of PV modules, the following equation is employed (Ebaid et al., 2013):

$$N_{PV,req} = \frac{TDL_{el} \times 1000}{PSH \times P_{PVmax,actual}} \qquad (7)$$

Where, $N_{PV,req}$ represents the total number of PV modules needed, $P_{PVmax,actual}$ represents the maximum output of each PV module (W), factoring in system losses collectively referred to as the derating factor. This includes losses due to soiling, cabling, shading, module aging, and inefficiencies in batteries and inverters. The derating factor typically ranges from 0.7 to 0.8, with an average value of 0.75 assumed in this study (Urs et al., 2024). PSH denotes the peak sun hours, which refer to the duration during which solar irradiation reaches one kWh/m² on the surface of PV module. For the specified location, the PSH values are provided in Table 7.

Table 7 Peak sun hours (PSH) for different types of bifacial APV systems in Piacenza.

Months	PSH@ Vertical APV (kWh/m²)	PSH@ Mono-axial APV (kWh/m²)	PSH@ Biaxial APV (kWh/m²)
January	1.85	2.06	3.26

February	3.50	4.17	5.85
March	5.18	6.31	7.58
April	4.61	5.38	5.64
May	4.88	5.66	5.76
June	7.39	8.93	9.66
July	6.59	7.90	8.14
August	6.07	7.35	7.54
September	4.64	5.51	6.20
October	2.53	2.77	3.31
November	**1.42**	**1.51**	**2.05**
December	1.70	1.94	3.29

In off-grid scenario, a conservative approach is used to size the stand-alone APV systems, considering the worst-case scenario of minimal solar availability. This ensures that the total year-round electrical demand is reliably met, including the fixed load of a 125 Sm^3/h $BioCH_4$ production plant and the variable needs of the biogas boiler or heat pump. The off-grid inverter, essential for converting DC power from batteries to AC, was sized using PVsyst software. This inverter integrates a Maximum Power Point Tracking (MPPT) controller to optimize system efficiency, regulate battery voltage, and prevent overcharging and deep discharging. Technical specifications for the selected off-grid inverter are provided in Table 8.

Table 8 Specifications of the selected solar MPPT off-grid inverter.

Parameters	Specifications
Max. Efficiency (%)	97
Euro. Efficiency (%)	95
AC output	Triple-phase
Grid frequency range (Hz)	50/60
Grid voltage range (V)	230/180-265
Battery voltage range (V)	12/24/36/48 V Auto Select

2.2.5.4 On-grid APV systems

In an on-grid setup, a detailed understanding of the energy exchange dynamics between the APV system and the power grid is crucial. Hourly load data provides a more precise representation of energy production and consumption patterns, facilitating more efficient interactions with the grid and enhancing overall system performance through improved sizing and control strategies. This level of resolution is key to effectively managing the complexity and variability characteristic of on-grid systems.

In this study, a random variability of 10% day-to-day and 20% per time step (Said et al., 2024) is applied to the electrical demand including biomethanation facility (119 kW_{el}) and the electrical consumption of heat producers after sizing to generate hourly electrical and heat demand.

To estimate the hourly heat demand, it is essential to determine the heat needed for both preheating and compensating for thermal losses. The thermal balance of the AD plant, which operates at a constant temperature of 37°C (Mesophilic AD processes), depends on two factors including preheating the feedstock and compensating for heat losses from the biodigester to the external environment, influenced by variations in external temperatures. The hourly heat demand, expressed in kW/h, is the sum of two components: the heat required for preheating (Q_{ph}) and the heat loss to the environment (Q_{loss}). Hourly heat losses Q_{loss} were calculated using the following equation (Casasso et al., 2021):

$$Q_{loss}=[(\pi r^2 \times U_{floor}+2\pi r h_1 \times U_{walls}+(r^2+h^2_2)\times U_{dome})]\times(T_{dig}-T_a) \quad (8)$$

Where, r is the radius of the digester, h_1 is the height of the cylindrical part, and h_2 is the height of the dome. U_{floor} represents the floor's thermal transmittance, U_{walls} represents the transmittance of the lateral walls, and U_{dome} is the dome's transmittance. T_a denotes the ambient temperature in hourly resolution for Piacenza (°C) which is provided in Figure 2.12, and T_{dig} is the digester's internal temperature. These input values are provided in Table 9.

Table 9 Input values of AD plant specifications (Casasso et al., 2021).

Parameters	Value	Unit
r	14	Meter
h_1	6	Meter
h_2	7	Meter
U_{floor}	0.465	$W/m^2 K$
U_{walls}	0.32	$W/m^2.K$
U_{dome}	1	$W/m^2.K$
T_{dig}	37	°C

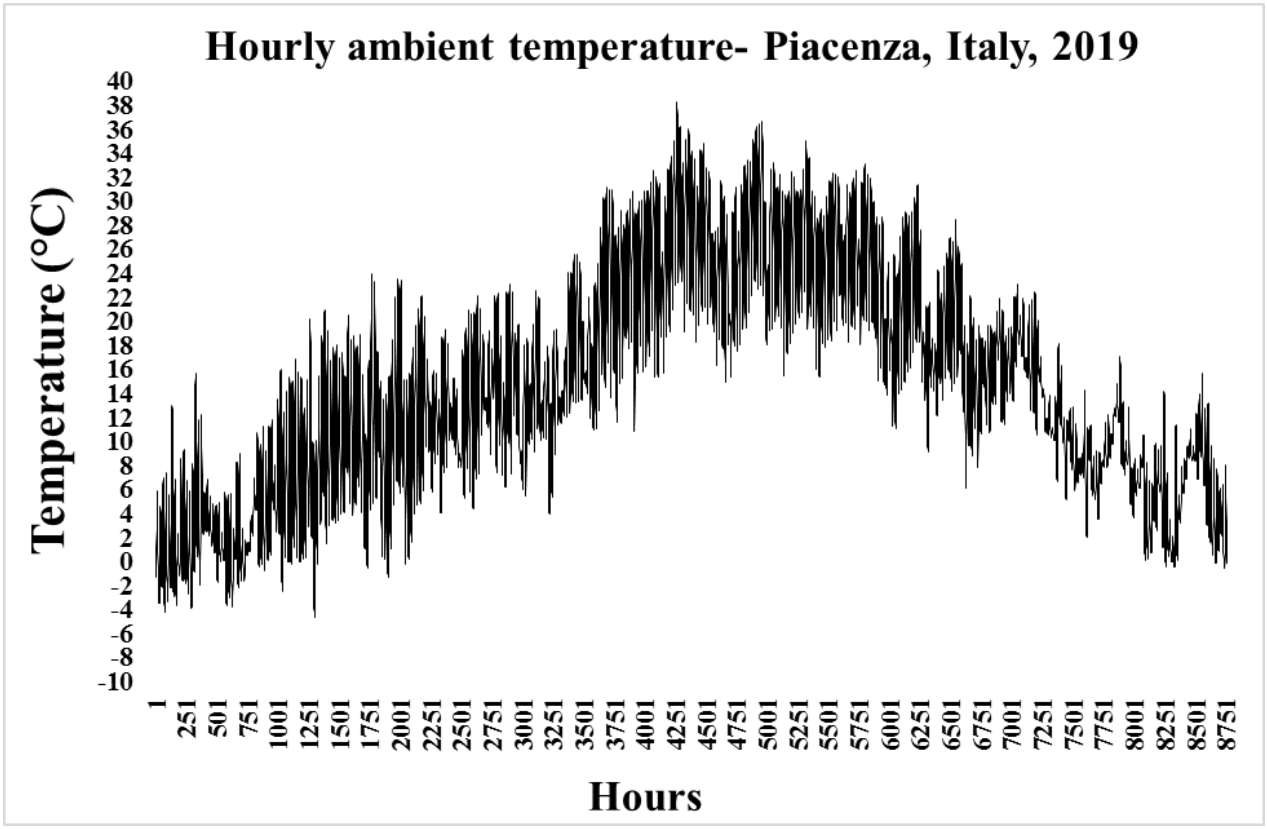

Figure 2-12 Hourly ambient temperature for Piacenza, Italy, in 2019.

The energy required for preheating the biomass is determined using the Eq. (9) (Casasso et al., 2021):

$$Q_{ph}=M_f \times C_f \times (T_{dig}-T_f) \quad (9)$$

Where, T_f is the temperature of feedstock, set at 12 °C, M_f is the feedstock intake (ton/hour) and C_f is the Specific heat of feedstock (J/kg·K). The Table 10 presents the breakdown of feedstock materials in tons per hour, along with their respective specific heat values.

Table 10 The breakdown of feedstock material mass and specific heat values for AD Plant in 2024.

Feedstock material	M_f (ton/hour)	C_f (J/kg·K)
Fresh cattle manure	1.14	3.7
Dairy cattle slurry	1.48	4.0
Corn silage	0.46	3.0
Corn stover silage	0.42	3.2
Dilutants	1.25	4.18

As a result, the hourly feedstock intake is 4.75 tons, with a weighted average specific heat value of approximately 3.81 kJ/kg·°C for the feedstock in the AD plant.

In the on-grid scenarios (6, 7, and 8), the sizing process for heat producers, such as the biogas boiler, heat pump, and biogas CHP, follows the same approach as previously described in the relevant sections. The sizing strategy is based on heat load following, meaning the unit is designed to fully satisfy hourly thermal demands. If an oversized heat producer is identified after sizing due to market availability, it is assumed that a system controller is implemented to modulate its electricity input, ensuring it precisely meets the hourly thermal requirements. Utilizing a system controller helps prevent excess heat generation and reduces waste by ensuring that the system operates efficiently, matching the thermal output to the actual demand. The hourly electrical consumption is combined with the electrical needs of biomethanation facility (119 kW_{el}) to apply the day-to-day variability and time-step variability procedure, as previously described in this section.

In the case of the CHP system, adjusting the electricity input based on hourly heat demand affects the hourly electricity production from the CHP unit. To estimate the hourly electricity generation by CHP unit in this study, the ratio of the CHP's rated electrical output to its rated heat output is applied. These parameters are obtained from the product datasheet after the sizing process. The surplus electricity generated by this unit is directed to the national grid for sale.

The hourly electricity production from the APV systems was simulated using PVsyst software for 1 kW of each technology (bifacial vertical/1-axis/2-axis) paired with an on-grid inverter operating at 97% efficiency.

The difference between the hourly electricity needs and the sum of the electricity produced by the CHP and APV, referred to as "ΔE (Delta Electric)" indicates the amount of electricity that needs to be drawn from the grid or the surplus electricity that can be injected into the grid. This value is crucial for the economic evaluation.

Eventually, to calculate the optimal size of the APV system, for instance in scenario 8, a new term called the Electricity Reliability (ER) is introduced. This term represents how the power sources, including the APV system and CHP unit, contribute to meeting the electrical demands. The Electricity Ratio (ER) is calculated using the following formula:

$$ER=(1-\frac{\sum \text{Electricity drawn from the grid}}{\sum \text{Hourly electrical demand}})\times 100 \qquad (10)$$

The objective function is to maximize the ER using the Excel Solver Tool. The decision variable in this process is the capacity of different types of APV systems. The Solver tool adjusts the APV capacity until a significant change in the ER is observed. Any remaining electricity demand is supplied by the power grid, while any surplus electricity generated is injected back into the grid. In scenarios 6 and 7, an iterative process using the Excel Solver Tool is conducted to determine the optimal size of the APV systems. The iteration is based on the assumption that each APV system must supply at least 25% of the total electrical demand as a lower bound constraint. The upper bound is defined where a significant change in the electricity supply ratio by APV (ER_{APV}) is observed. Any additional electrical demand beyond this upper limit is assumed to be met by the power grid.

2.2.6 Economic modelling

The economic analysis for each scenario is performed by calculating the life cycle cost (LCC), life cycle revenue (LCR), and the revenue-to-cost ratio. The revenue-to-cost ratio is defined as the ratio of life cycle revenue to life cycle cost, expressed in present value worth. A higher ratio signifies greater economic viability of the project.

The life cycle cost represents the total expenses incurred over the lifetime of each component, discounted to present value by accounting for the time value of money. This includes the costs associated with heat and electricity production, such as initial investment, operation and maintenance (O&M), replacement costs, and the cost of purchasing electricity from the power grid. The life cycle cost (LCC) is calculated using the following formula (Ravilla et al., 2024):

$$LCC=C_{cap}+C_{rep}+C_{O\&M}+C_{PPG} \qquad (11)$$

Where, C_{cap} denotes the capital cost of each component along with its installation costs (€), which is calculated using Eq. (12):

$$C_{cap}=C_{APVsystem}+C_{battery\ packages}+C_{CHP\ unit}+C_{Biogas\ boiler}+C_{Heat\ pump} \qquad (12)$$

C_{rep} includes the replacement cost of equipment at the end of its lifetime (€) and is calculated using Eq. (13) (Messenger and Ventre, 2010):

$$C_{rep}=\sum C_0\times PW=\sum C_0\times(\frac{1+i}{1+d})^n \qquad (13)$$

Where, C_0 is the initial cost of each equipment (€) and PW is the present worth factor, which depends on the factors of inflation rate (i) and discount rate (d) and the year of equipment replacement (n).

$C_{O\&M}$ denotes operation and maintenance costs of each component (€) that is calculated as follows (Ravilla et al., 2024):

$$C_{O\&M}=\sum C_0\times(1+i)^n\frac{(1+d)^d-1}{d(1+d)^n} \qquad (14)$$

Where, C_0 represents the first-year operation and maintenance cost of each piece of equipment (€), and n denotes the project lifetime. It is assumed that all biogas fuel for the biogas boiler and CHP unit is supplied by the on-site biogas plant, eliminating the need for fuel price considerations.

C_{PPG} represents the costs associated with purchasing power from the Italian national grid (€) over the project's lifetime, as indicated in Eq. (15) (Ravilla et al., 2024):

$$C_{PPG}=\sum(\text{Annual electricity drawn from the grid}\times\text{cost per unit})\times(1+i)^n\frac{(1+d)^d-1}{d(1+d)^n} \quad (15)$$

The LCR represents the total revenue generated over the project's lifetime from salvage value, surplus electricity production, and the sale of bioCH_4 to the gas grid, expressed in present worth. It is calculated using Eq. (16) (Ravilla et al., 2024):

$$LCR=R_{sal}+R_{SPG}+R_{SBG} \quad (16)$$

The salvage value refers to the estimated residual value of a system component at the end of its useful life, based on the replacement cost rather than the initial capital cost, and includes prorated maintenance costs. The salvage value is calculated using Eq. (17) (Nouadje et al., 2024):

$$R_{sal}=\sum C_{rep}\times\frac{L_{comp}-(L_{proj}-(L_{comp}\times INT(\frac{L_{proj}}{L_{comp}})))}{L_{comp}} \quad (17)$$

Where, R_{sal} refers to the salvage cost of all components (€), calculated based on linear depreciation, where the salvage value is proportional to the component's remaining life. L_{comp} represents the component's lifetime (years), and L_{proj} is the project lifetime, assumed to be 20 years. INT is a function that returns the integer value of a real number.

R_{SPG} and R_{SBG} represent the costs associated with the income from selling power back to the grid (€), and selling bioCH_4 produced to the gas grid (€) over the project's lifetime as indicated in Eq. (18):

$$R_{SPG}=\sum(\text{Annual electricity injected to the grid}\times\text{cost per unit})\times(1+i)^n\frac{(1+d)^d-1}{d(1+d)^n}$$

$$R_{SBG}=\sum(\text{Annual BioCH4 injected to the gas grid}\times\text{cost per unit})\times(1+i)^n\frac{(1+d)^d-1}{d(1+d)^n} \quad (18)$$

Finally, the revenue-to-cost ratio is calculated using Eq. (19) (Ravilla et al., 2024):

$$\frac{\text{Revenue}}{\text{Cost}}\text{ ratio }(\%)=LCR/LCC \quad (19)$$

In this study, the costs per kWh for drawing electricity from the grid and for grid injection were set at 0.2 €/kWh and 0.06 €/kWh, respectively (Calise et al., 2024). To calculate the income from bioCH_4 sales, it is necessary to determine the amount of biogas consumed by both the biogas boiler and the biogas CHP.

To achieve this, the hourly biogas consumption by the biogas boiler is calculated using Eq. (1), where the thermal output of the biogas boiler is set equal to the thermal needs divided by the product of the biogas LHV and the boiler efficiency. Similarly, using Eq. (3), the hourly biogas consumption by the biogas CHP is calculated by setting the thermal output of the biogas CHP equal to the thermal needs divided by the product of the biogas LHV and the CHP's thermal efficiency. Finally, the annual biogas consumed by the biogas boiler and biogas CHP is subtracted from the total yearly biogas produced in the biogas plant. The remaining biogas, considering a methane content of 54.2%, is then upgraded to $BioCh_4$ before being injected into the gas grid for sale. The revenue from $BioCH_4$ sales is 1.1 €/Nm³ (CIB - Consorzio Italiano Biogas). Additionally, an average inflation rate of 2% and a discount rate of 6% were applied, reflecting the economic conditions in Italy (Di Micco et al., 2023). In this study, the PV modules, heat pump, and biogas boiler are assumed to have a lifespan of 20 years (Taramasso et al., 2024), solar batteries 10 years (Calise et al., 2024), the biogas CHP unit 7 years (60K hours), and the solar inverter (DC to AC converter) 15 years (Reher et al., 2024). The other cost items considered in the study are outlined in Table 11. The multipliers for estimating land requirement (m^2/kW_p) for installing each type of APV system were sourced from (Bellone et al., 2024) at the same pitches (distance between PV arrays) and PV layout. For bifacial APV systems, the 1-axis mounting system with a 1-portrait PV layout occupies 14.4 m^2 and 19.1 m^2 for pitches of 6 meters and 8 meters, respectively. The vertical bifacial APV system with a 2-landscape PV layout occupies 19.5 m^2 and 24.2 m^2 for pitches of 8 meters and 10 meters. Lastly, the 2-axis mounting bifacial APV system with a 6-landscape PV layout requires 20.95 m^2 and 24.8 m^2 for pitches of 15 meters and 18 meters, respectively.

Table 11 The CAPEX and OPEX assumed in this study (Bellone et al., 2024; Di Micco et al., 2023; Reher et al., 2024; Taramasso et al., 2024; CIB - Consorzio Italiano Biogas).

Components	CAPEX (€)	OPEX (€)
Overhead Bifacial 2-axis APV (6L layout)		0.025 × CAPEX
PV module	349/kW_p	
Inverters	77/kW_p	
Electric BOS	282/kW_p	
Supporting structure	340/kW_p	
Installation and work	373/kW_p	
Professionals and fees	61/kW_p	
Total	1482/kW_p	
Overhead Bifacial 1-axis APV (1P layout)		0.025 × CAPEX
PV module	305/kW_p	
Inverters	65/kW_p	
Electric BOS	100/kW_p	
Supporting structure	316/kW_p	
Installation and work	354/kW_p	
Professionals and fees	77/kW_p	
Total	1217/kW_p	
Bifacial Vertical APV (2L layout)		0.015 × CAPEX
PV module	291/kW_p	
Inverters	58/kW_p	
Electric BOS	153/kW_p	
Supporting structure	160/kW_p	
Installation and work	267/kW_p	
Professionals and fees	72/kW_p	
Total	1001/kW_p	
Lithium-ion phosphate battery	223/kWh	0.045 × CAPEX
Biogas CHP unit	2600/kW_{el}	6.5€/hour
Biogas boiler	270/kW_{th}	0.063 × CAPEX
Ground-source Heat pump	$(2485 \times P_{th}^{0.6034}) + C_{wells}$	0.01 × CAPEX + 3€/MWh_{th}
Geothermal wells investment cost (C_{wells})	50000	
Land lease cost	-	3000€/ha/year

2.3 RESULTS AND DISCUSSION

2.3.1 Scenario 1: Off-grid APVs (APVs + BESS) + biogas boiler

The required biogas input rate for the boiler, which is the only energy source to satisfy the entire thermal load, was 38.2 Nm³/h (equivalent to 916.8 Nm³/day), which is lower than the biogas requirement of the biogas CHP unit, set at 1633 Nm³/day. This difference indicates a potential for increasing bioCH_4 production.

Given that the boiler is oversized, a system controller is incorporated in this study to modulate the boiler's thermal output based on monthly heat demand. The boiler's electrical consumption, assumed to be 1.5% of its thermal output, is presented in Table 12.

Table 12 The monthly dynamic electrical needs of the biogas boiler.

Month	Electrical needs (kW)	Electrical consumption (MWh)
January	2.68	1.993
February	2.49	1.675
March	2.31	1.715
April	2.06	1.481
May	1.74	1.298
June	1.5	1.077
July	1.31	0.973
August	1.37	1.02
September	1.56	1.122
October	1.87	1.391
November	2.37	1.705
December	2.62	1.947
Year	**1.99**	**17.398**

In this study, the lowest PSH was recorded in November 2019 in Piacenza, with values of 1.42 hour for a vertical, 1.51 for a mono-axial and 2.05 for a biaxial mounting system. After sizing the off-grid APV systems using Equations (6) and (7) to meet the daily electrical demands of Scenario 1, the simulation results for the systems (featuring mono-axial, biaxial, and vertical mounting without tracking, along with two different pitches) are presented in Table 13, based on PVsyst software analysis.

Table 13 Results of different types of bifacial APV systems with varying pitches in Piacenza.

Description	APV mounting system		
	Vertical	Mono-axial	Biaxial
Total PV modules	4155	3908	2878
Total Capacity (MW_p)	2.743	2.580	1.9
Off-grid Inverter Size (MW_p)	2.405	2.260	1.677
Total Batteries		851	
Total energy stored in batteries (MWh)		11.029	
	Pitch 8m/Pitch 10m	Pitch 6m/Pitch 8m	Pitch 15m/Pitch 18m
Land occupation (ha)	5.35/6.64	3.72/4.93	3.98/4.72
Annual surplus electricity (MWh)	2265/2386	2709/2818	2058/2126

The results indicate that the biaxial mounting system, due to its more advanced technology, required up to 26.35% fewer PV modules, capacity, and inverters compared to the mono-axial system. However, the vertically mounted APV system, due to its fixed position and lack of tracking, requires more PV modules to adequately charge the batteries. Despite having more PV panels, the vertical system generates less surplus electricity compared to the mono-axial system, but more than the biaxial system, due to capacity and technology differences among these configurations.

The vertical APV system necessitates the largest land area (5.35 ha for pitch 8m and 6.64 ha for pitch 10m) among the configurations evaluated, as it has the highest photovoltaic capacity, which translates into greater space requirements for installation. In contrast, the biaxial system, despite operating at larger pitches, uses less land than the vertical system due to dual-axis tracking and fewer PV modules, maximizing energy production with fewer rows. The biaxial system's lower land use at the pitch of 18m compared to the mono-axial system's 8m pitch is due to its dynamic module orientation, capturing more energy per module and reducing the need for dense placement. Meanwhile, the mono-axial system, which relies on a single-axis tracking mechanism, requires denser module placement at higher pitches to maintain energy output, leading to increased land use. This makes the biaxial system the most efficient option for minimizing land occupation at higher pitches. However, considerations such as cost and crop production capacity within the facility are also important.

Table 14 shows the economic analysis for Scenario 1, evaluating the life cycle cost (LCC), life cycle revenue (LCR), and the revenue-to-cost ratio for each system configuration throughout the project's duration.

Table 14 The economic analysis results for Scenario 1 (land lease cost included).

	Bifacial Vertical APV system + BESS + biogas boiler	
Scenario 1	**Pitch 8m**	**Pitch 10m**
LCC (M€)	42.8	43.45
LCR (M€)	262.82	264.16
LCR/LCC	**6.14**	**6.08**

	Bifacial 1-axis APV system + BESS + biogas boiler	
Scenario 1	**Pitch 6m**	**Pitch 8m**
LCC (M€)	48.95	49.72
LCR (M€)	267.75	268.96
LCR/LCC	**5.47**	**5.41**

	Bifacial 2-axis APV system + BESS + biogas boiler	
Scenario 1	**Pitch 15m**	**Pitch 18m**
LCC (M€)	47.37	45.85
LCR (M€)	260.52	261.27
LCR/LCC	**5.50**	**5.46**

These outcomes indicate that, on one hand, the vertical APV mounting system has the lowest life cycle cost due to its much lower CAPEX, OPEX, and slightly reduced inverter replacement costs. On the other hand, while the one-axis mounting system, equipped with a tracking system, has generated more income from increased electricity sales to the grid, the difference in income between these mentioned mounting systems is far smaller than the difference in their life cycle costs. As a result, the vertical technology achieves a higher revenue-to-cost ratio over the project's lifetime compared to the mono-axial system. In the case of dual-axis mounting system, its advanced technology leads to higher costs over the project's lifetime compared to the vertical system, but it remains less expensive than the mono-axial system only due to its significantly lower PV capacity (26.3% less PV capacity than the one-axis and 30.7% less than the vertical system). This reduction in capacity decreases income from electricity sales, leading to the lowest life cycle revenue (LCR). However, when land occupation and the associated land lease costs are considered, the dual-axis system achieves a higher revenue-to-cost ratio over the 20-year project lifetime at a 15m pitch compared to the mono-axial system. Conversely, at an 18m pitch, the dual-axis system records a lower revenue-to-cost ratio than the mono-axial system at a 6m pitch, highlighting the impact of land occupation on cost efficiency.

2.3.2 Scenario 2: Off-grid APVs + heat pump

The rated electrical capacity of this heat pump is calculated to be 43.7 kW, as determined by Eq. (4). Since the heat pump is slightly oversized, a system controller is used to modulate its thermal output based on

the monthly heat demand. This system controller also influences the heat pump's electrical consumption, which is calculated and presented in Table 15.

Table 15 The monthly dynamic electrical needs of the heat pump.

Month	Electrical needs (kW)	Electrical consumption (MWh)
January	43.14	32.096
February	40.15	26.978
March	37.13	27.622
April	33.12	23.844
May	28.09	20.900
June	24.08	17.339
July	21.06	15.671
August	22.08	16.426
September	25.10	18.070
October	30.10	22.392
November	38.14	27.461
December	42.15	31.360
Year	**32.03**	**280.558**

The annual electrical power consumption of the GSHP is 280.5 MWh/y. Based on the calculations from Eq. (2), 37 Borehole Heat Exchangers (BHEs) are required. In this scenario, the electrical load is significantly higher than in Scenario 1 due to the increased electricity demands of the heat pump compared to the biogas boiler. This increase in demand necessitates a substantially larger number of PV panels. Following the same sizing procedure using Equations (6) and (7), the simulation results for the different types of APV systems in this study considering two different pitches, are presented in Table 16, based on PVsyst software.

Table 16 Results of different types of bifacial APV systems with varying pitches in Piacenza.

Description	APV mounting system		
	Vertical	Mono-axial	Biaxial
Total PV modules	5537	5207	3835
Total Capacity (MW_p)	3.654	3.437	2.531
Off-grid Inverter Size (MW_p)	3.205	3.000	2.210
Total Batteries		1130	
Total energy stored in batteries (MWh)		14.645	
	Pitch 8m/Pitch 10m	**Pitch 6m/Pitch 8m**	**Pitch 15m/Pitch 18m**
Land occupation (ha)	7.13/8.84	4.95/6.56	5.3/6.28
Annual surplus electricity (MWh)	3135/3292	3681/3827	2724/2814

In this scenario, similar to Scenario 1, the biaxial mounting system required up to 26.35% fewer PV modules, capacity, and inverters than the mono-axial system. In contrast, the vertical mounting system required the most PV modules compared to the other configurations. The specifications for the selected inverter are consistent with those in the previous scenario. This scenario would necessitate 1,130 batteries with a total capacity of 339,000 Ah (14.6 MWh).
The vertical system continues to require the most land, ranging from 7.13 ha (8m pitch) to 8.84 ha (10m pitch), reinforcing its inefficiency in land use. In contrast, the mono-axial system remains more efficient at smaller pitches, with land occupation ranging from 4.95 ha (6m pitch) to 6.56 ha (8m pitch).
The biaxial system, while using larger pitches (15m to 18m), requires 5.3 ha to 6.28 ha, only slightly more than the mono-axial system at tighter configurations. In this scenario, the biaxial system continues to be a strong option for larger pitches, while the mono-axial system remains ideal for tighter configurations.
Table 17 shows the economic analysis for Scenario 2, evaluating the LCC, LCR, and the revenue-to-cost ratio for each system configuration over the project's lifetime.

Table 17 The economic analysis results for Scenario 2 (land lease cost included).

	Bifacial Vertical APV system + BESS + HP	
Scenario 2	**Pitch 8m**	**Pitch 10m**
LCC (M€)	56.85	57.69
LCR (M€)	309.81	311.55
LCR/LCC	**5.45**	**5.40**

	Bifacial 1-axis APV system + BESS + HP	
Scenario 2	**Pitch 6m**	**Pitch 8m**
LCC (M€)	65.13	66.01
LCR (M€)	315.87	317.49
LCR/LCC	**4.85**	**4.81**

	Bifacial 2-axis APV system + BESS + HP	
Scenario 2	**Pitch 15m**	**Pitch 18m**
LCC (M€)	62.81	63.40
LCR (M€)	305.24	306.24
LCR/LCC	**4.86**	**4.83**

The vertical APV mounting system achieves the highest cost-efficiency (LCR/LCC), due to its lower LCC driven by reduced CAPEX, OPEX, and inverter replacement costs than other mounting systems. While

the mono-axial system generates more income from electricity sales than vertical system, the smaller income difference compared to its higher costs results in lower LCR/LCC ratios.
In this scenario, the dual-axis system is less costly than the mono-axial system, primarily due to its significantly smaller PV capacity. Although this results in the lowest LCR due to reduced electricity generation for sale, it still achieves slightly better cost-efficiency at a 15m pitch (4.86 compared to 4.85 for the mono-axial system at a 6m pitch). However, at an 18m pitch, its LCR/LCC decreases to 4.83, falling below the mono-axial system at a 6m pitch, reflecting the influence of land use in its cost-effectiveness.
However, the increased PV capacity across all configurations, combined with the heat pump's operation (which does not require biogas) allows for a larger amount of biogas to be converted into $BioCH_4$ for sale to the gas grid. As a result, this leads to higher life cycle revenue than in Scenario 1.

2.3.3 Scenarios 3 and 4: Power grid + heat pump and Power grid + biogas boiler

In these scenarios, the Italian national power grid supplies the total year-round electrical demand, including both the fixed electrical load of biomethanation and the dynamic electrical needs of the heat pump and biogas boiler. The heat producers and their variable electrical consumption have already been sized in previous scenarios based on monthly heat demand. Table 18 presents the total electrical requirements from the grid for Scenarios 3 and 4, respectively.

Table 18 Total electrical demand required from the grid for Scenarios 3 and 4.

Scenario 3				
Month	**Heat pump electrical consumption (kW)**	**Biomethanation electrical needs (kW)**	**Total electrical demand (kW)**	**Total electrical demand (MWh)**
January	43.14	119	162.14	120.632
February	40.15	119	159.15	106.946
March	37.13	119	156.13	116.158
April	33.12	119	152.12	109.524
May	28.09	119	147.09	109.436
June	24.08	119	143.08	103.019
July	21.06	119	140.06	104.207
August	22.08	119	141.08	104.962
September	25.1	119	144.1	103.750
October	30.1	119	149.1	110.928
November	38.14	119	157.14	113.141
December	42.15	119	161.15	119.896
Year	**32.03**	**119**	**151.03**	**1322.998**
Scenario 4				
Month	**biogas boiler electrical consumption (kW)**	**Biomethanation electrical needs (kW)**	**Total electrical demand (kW)**	**Total electrical demand (MWh)**
January	2.68	119	121.68	90.529
February	2.49	119	121.49	81.643
March	2.31	119	121.31	90.251
April	2.06	119	121.06	87.161
May	1.74	119	120.74	89.834
June	1.5	119	120.5	86.757
July	1.31	119	120.31	89.509
August	1.37	119	120.37	89.556
September	1.56	119	120.56	86.802
October	1.87	119	120.87	89.927
November	2.37	119	121.37	87.385
December	2.62	119	121.62	90.483
Year	**1.99**	**119**	**120.99**	**1059.863**

Consequently, the total electrical demand for scenarios 3 and 4 is 151 kW and 120.9 kW, respectively, requiring an annual supply of 1322.9 MWh and 1059.8 MWh from the grid.

Table 19 shows the economic analysis for Scenarios 3 and 4, evaluating the life cycle cost (LCC), life cycle revenue (LCR), and the revenue-to-cost ratio for each system configuration throughout the project's duration.

Table 19 The economic analysis results for Scenarios 3 and 4.

Scenario 3	Value
LCC (M€)	49.89
LCR (M€)	273.27
LCR/LCC	5.48
Scenario 4	**Value**
LCC (M€)	39.99
LCR (M€)	236.37
LCR/LCC	5.91

In Scenario 3, using the heat pump instead of the biogas boiler increases BioCH_4 production and sales to the gas grid, resulting in a 15.61% higher life cycle revenue (LCR). However, Scenario 4 is more cost-effective. This is because the biogas boiler has lower capital and operating costs (CAPEX and OPEX) and uses significantly less electricity, reducing the life cycle cost (LCC) by 24.75%. Consequently, Scenario 4 has a 7.84% higher LCR/LCC ratio, making it the better economic option.

2.3.4 Scenario 5: Biogas CHP unit

As outlined in the section 2.2.5.1, the CHP unit was carefully sized to address both the peak heat demand of 178.6 kW_{th} in January and the total electrical requirements of 122.8 kW for biomethanation and self-consumption of CHP unit. This section examines the energy output and performance of this component, as detailed in Table 20.

Table 20 Energy output of TEDOM CENTO-T150 biogas CHP.

Month	Total electrical demand (kW)	Total electrical demand (MWh)	CHP electrical output (kW)	CHP electrical output (MWh)	Surplus electricity produced (MWh)
January	122.8	91.4	127.9	95.2	3.8
February	122.8	82.5	127.9	85.9	3.4
March	122.8	91.4	127.9	95.2	3.8
April	122.8	88.4	127.9	92.1	3.6
May	122.8	91.4	127.9	95.2	3.8
June	122.8	88.4	127.9	92.1	3.6
July	122.8	91.4	127.9	95.2	3.8
August	122.8	91.4	127.9	95.2	3.8
September	122.8	88.4	127.9	92.1	3.6
October	122.8	91.4	127.9	95.2	3.8
November	122.8	88.4	127.9	92.1	3.6
December	122.8	91.4	127.9	95.2	3.8
Year	**122.8**	**1076.1**	**127.9**	**1120.4**	**44.3**

Month	Heat demand (kW)	Heat demand (MWh)	CHP thermal output (kW)	CHP thermal output (MWh)	Excess heat produced (MWh)
January	178.6	132.9	195.7	145.6	12.7
February	166.2	111.7	195.7	131.5	19.8
March	153.7	114.4	195.7	145.6	31.2
April	137.1	98.7	195.7	140.9	42.2
May	116.3	86.5	195.7	145.6	59.1
June	99.7	71.8	195.7	140.9	69.1
July	87.2	64.9	195.7	145.6	80.7
August	91.4	68.0	195.7	145.6	77.6
September	103.9	74.8	195.7	140.9	66.1
October	124.6	92.7	195.7	145.6	52.9
November	157.9	113.7	195.7	140.9	27.2
December	174.5	129.8	195.7	145.6	15.8
Year	**132.6**	**1159.8**	**195.7**	**1714.3**	**554.5**

The electrical output of the selected biogas CHP unit slightly exceeds the actual electrical demands of the facility (up to 4.12%). In this scenario, it is not feasible to use a system controller because the CHP unit operates independently. Adjusting the power input of the CHP to modulate its thermal output based on monthly heat demand would also affect its electrical output. Since there is no other electrical generator available in this scenario, using a controller is not a viable option. In this scenario, the excess electricity and heat generated by the selected biogas CHP are 44.3 MWh and 554.5 MWh, respectively.

Table 21 presents the economic analysis for Scenario 5, including CAPEX, OPEX, replacement costs, salvage value, revenue from $BioCH_4$ sales (after deducting biogas consumption by the CHP unit), and revenue from selling excess electricity to the grid. The analysis accounts for inflation and discount rates to evaluate the life cycle cost (LCC), life cycle revenue (LCR), and the overall revenue-to-cost ratio throughout the project's lifetime.

Table 21 The economic analysis results for Scenario 5.

Scenario 5	Value
LCC (M€)	11.31
LCR (M€)	208.06
LCR/LCC	**18.4**

2.3.5 Scenario 6: APVs + Power grid + heat pump

Figure 2.13 illustrates the hourly thermal demand generated using equations 8 and 9, which also applies to scenarios 7 and 8.

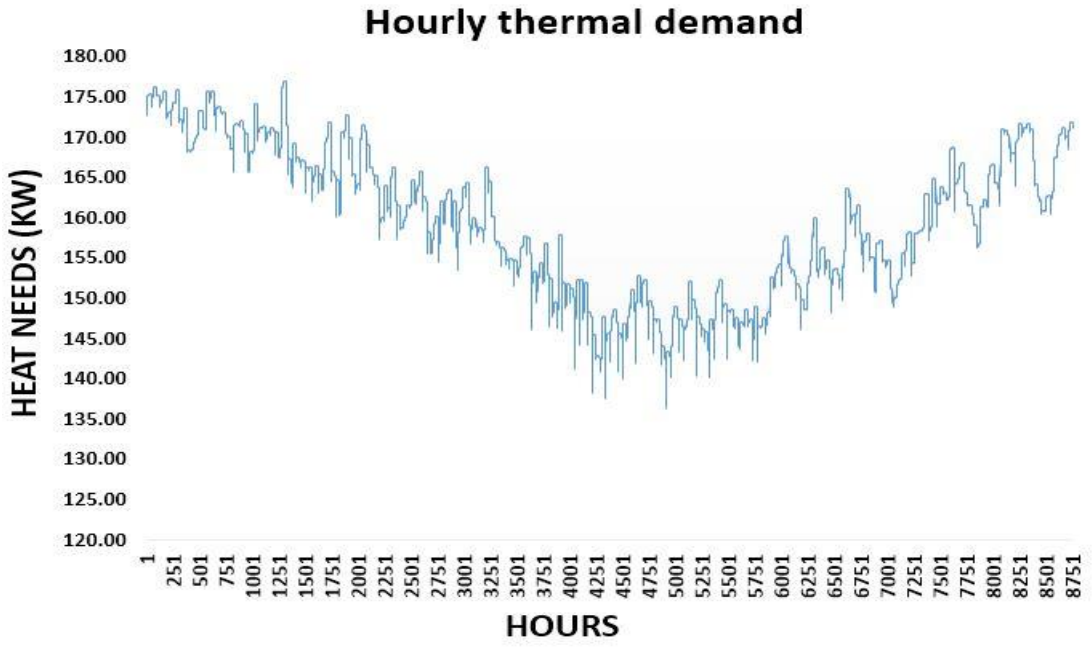

Figure 2-13 Hourly heat requirements of AD plant.

The heat pump sized in scenario 2, equipped with a system controller, can fully meet the hourly heat demands, as illustrated in Figure 2.12. The calculated operational power of the heat pump for this scenario is 43.72 kW. At full capacity, it can produce 181 kW_{th} per hour. However, during months like July when the heat demand is significantly lower, the system controller modulates the input power to match the thermal

output precisely with the hourly heat demand. As a result, the electricity consumption of the heat pump fluctuates on an hourly basis.

This variable hourly consumption, along with the electrical requirements of the upgrading plant, compression stages, biological processes, and auxiliary systems, is used to generate the overall hourly electrical demand for the AD plant in this scenario, incorporating the previously mentioned day-to-day and time-step variability. Figure 2.14 shows the overall hourly electrical demand of the AD plant for the Scenario 6.

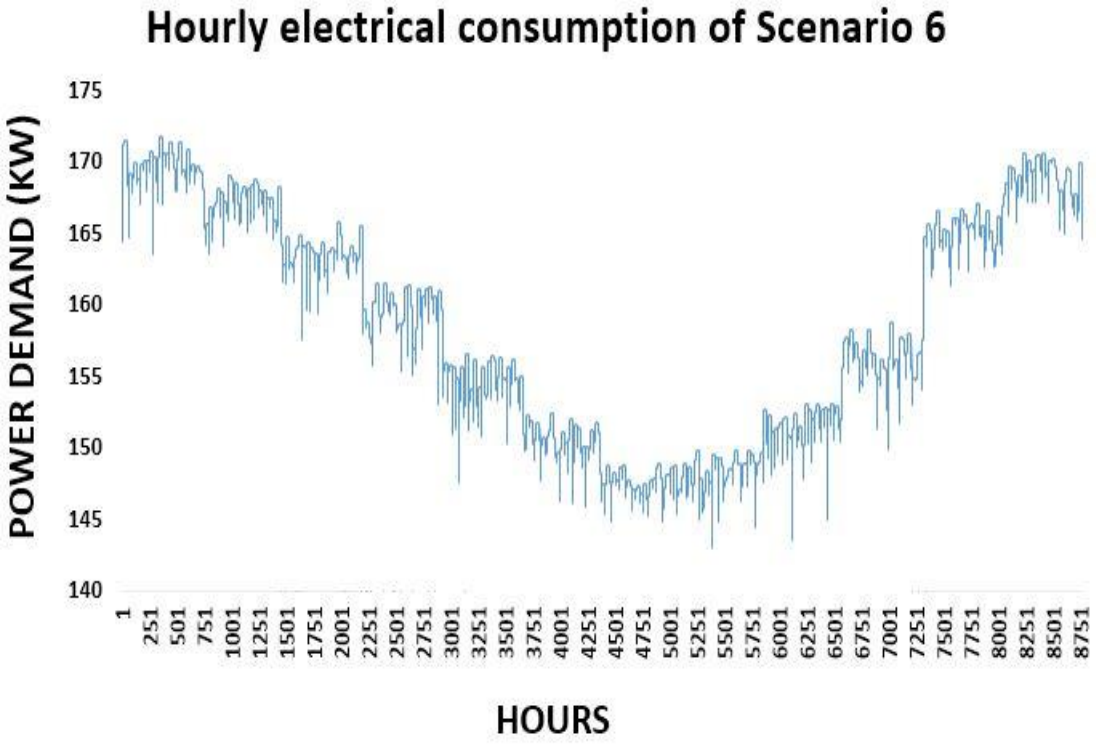

Figure 2-14 Hourly electrical requirements of the Scenario 6.

In this scenario, the overall hourly electrical needs are satisfied by the APV system and the power grid.

Table 22 details the sizing and land use of each APV mounting system, including vertical with an 8m pitch, mono-axial with a 6m pitch, and biaxial with a 15m pitch at various ER levels.

Table 22 The sizing and land occupation results of different APV systems at various ER levels by Excel Solver tool.

ER_{APV}	Bifacial 2-axis APV capacity	Bifacial 1-axis APV capacity	Bifacial vertical APV capacity
25 %	198 kW_p	205 kW_p	267 kW_p
Land use (ha)	0.41	0.3	0.52
30 %	309 kW_p	321 kW_p	420 kW_p
Land use (ha)	0.65	0.46	0.82
35 %	554 kW_p	574 kW_p	753 kW_p
Land use (ha)	1.16	0.83	1.47
40 %	1.32 MW_p	1.37 MW_p	1.8 MW_p
Land use (ha)	2.77	1.97	3.51
45 %	7.42 MW_p	7.7 MW_p	10 MW_p
47 %	45.8 MW_p	47.5 MW_p	62.2 MW_p
48 %	Infinite	Infinite	Infinite

The vertical mounting system, without tracking capabilities, necessitates a larger PV capacity, whereas the advanced tracking features of the dual-axis system allow it to use fewer PV panels to produce the same amount of electricity.

Table 23 presents the total electricity purchased from the grid and total electricity sales to the grid for Scenario 6 at the different ER levels. Higher ER levels have been excluded, as the APV system capacities at those levels reach medium scale, which is not compatible with small-scale APV installations on biogas farms, while offering only a 5% increase in ER.

Table 23 The total electricity purchased and sold of the Scenario 6 at various ER levels.

	BF[1] vertical APV capacity		BF 1-axis APV capacity		BF 2-axis APV capacity	
ER_{APV}	TEP[2] (€)	TES[3] (€)	TEP (€)	TES (€)	TEP (€)	TES (€)
25%	193781	2453	193728	2472	193726	2473
30%	180923	10804	180837	10894	180802	10930
35%	167972	33941	167932	34065	167866	34265
40%	155036	115114	155011	115471	154961	115909

(1) BF: Bifacial, (2) TEP: Total electricity purchased, (3) TES: Total electricity sales

The economic analysis for Scenario 6, shown in Table 24, evaluates the life cycle cost (LCC), life cycle revenue (LCR), and revenue-to-cost ratio for each configuration over the project's lifetime.

Table 24 The economic analysis results for Scenario 6 (land lease cost included).

Scenario 6	BF[(1)] Biaxial APV system			
	ER_{APV} 25%	ER_{APV} 30%	ER_{APV} 35%	ER_{APV} 40%
LCC (M€)	38.77	37.46	37.38	42.29
LCR (M€)	273.74	275.30	279.62	294.75
LCR/LCC	7.06	7.35	7.48	6.97
Scenario 6	**BF Mono-axial APV system**			
	ER_{APV} 25%	ER_{APV} 30%	ER_{APV} 35%	ER_{APV} 40%
LCC (M€)	38.45	36.95	36.55	40.25
LCR (M€)	273.73	275.29	279.58	294.66
LCR/LCC	7.12	7.45	7.65	7.32
Scenario 6	**BF Vertical APV system**			
	ER_{APV} 25%	ER_{APV} 30%	ER_{APV} 35%	ER_{APV} 40%
LCC (M€)	38.23	36.56	35.80	38.56
LCR (M€)	273.72	275.28	279.56	294.60
LCR/LCC	7.16	7.53	7.81	7.64

(1) BF: Bifacial

As observed in both mono-axial and biaxial APV systems, the ratio of total revenue to total cost increases from ER 25% to 35% but declines at ER 40%, indicating that ER 35% (i.e., 35% of total electrical demand met by the APV system, with the remainder supplied by the grid) is the optimal level for both tracking systems.

However, the one-axis system proves more economical due to its higher LCR/LCC ratio, offering approximately 22% lower CAPEX per kW_p and 15.6% lower inverter costs (affecting replacement costs) compared to the dual-axis system (Table 2.11).In this scenario, the small capacity difference between the dual-axis system (554 kW) and the one-axis system (574 kW) at ER 35% (as shown in Table 22) does not enhance the dual-axis system's life cycle cost advantage. On the contrary, the dual-axis system incurs higher life cycle costs due to increased land occupation and corresponding land lease expenses. Additionally, its lower capacity does not significantly contribute to increased electricity generation for sale compared to the one-axis system.

Eventually, the vertical APV system, with the highest LCR to LCC ratio of 7.81 at ER 35%, is the most optimal configuration in Scenario 6. Although this system has a capacity of 753 kW_p at this ER level, 35.9% more than the dual-axis and 31.2% more than the one-axis system, resulting in a larger land area requirement and higher land lease cost, the increased PV capacity enables it to generate approximately the same amount of total annual electricity sales to the grid as the other systems (Table 23). Additionally, the vertical system offers significant cost advantages, with 48.05% and 21.57% lower CAPEX per unit, 40% lower OPEX, and 32.75% and 12.06% lower inverter costs compared to the dual-axis and one-axis systems, respectively. Further details on the economic assessment are available in the Supplementary Materials.

2.3.6 Scenario 7: APVs + Power grid + biogas boiler

In this scenario, as mentioned earlier, the hourly heat demand is the same as in scenario 6. However, after applying the same procedure to generate hourly electrical needs as in the previous scenario, the hourly electrical demand for this scenario is depicted in Figure 2.15.

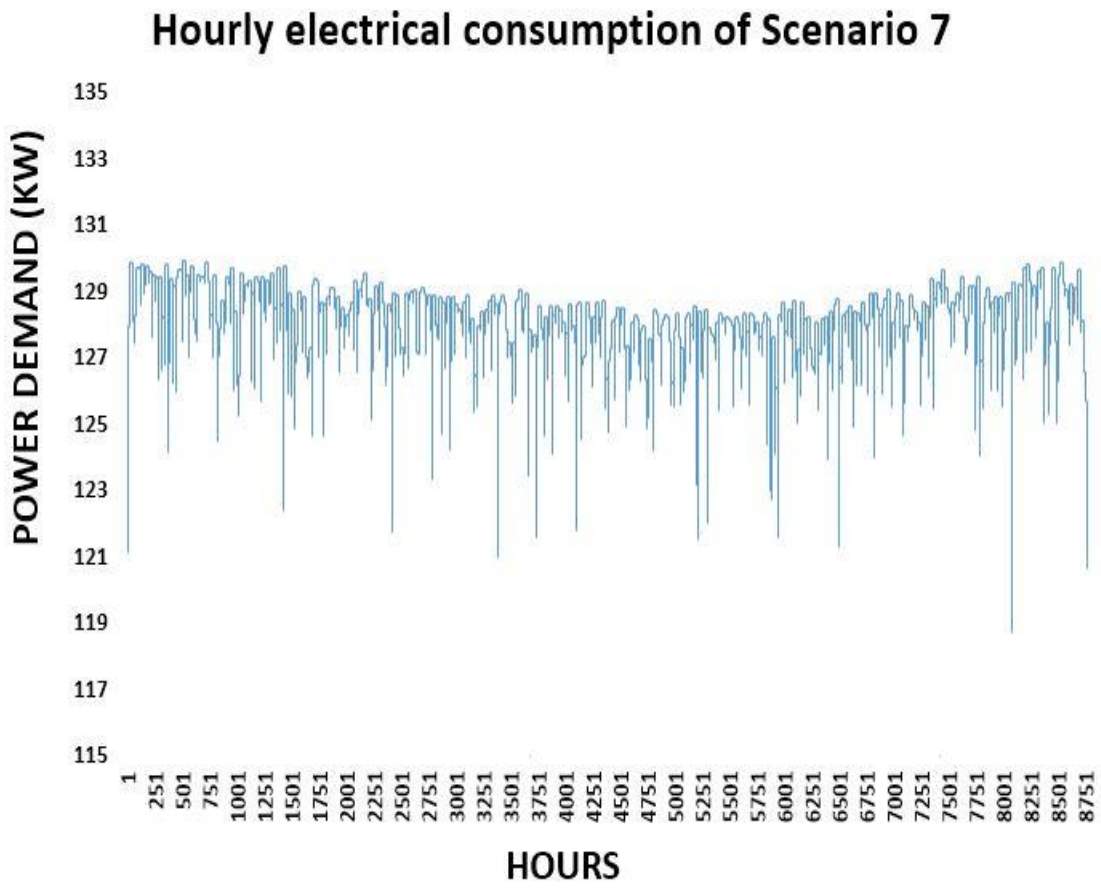

Figure 2-15 Hourly electrical requirements of the Scenario 7.

In this scenario, the overall hourly electrical needs are met by a combination of the APV system and the power grid. The procedure for sizing the APV system is similar to the previous scenario, with the key difference being that, instead of a heat pump, a biogas boiler is used as the heat producer, which results in different hourly electrical requirements. Table 25 outlines the sizing and land use for each APV mounting system (vertical with an 8m pitch, mono-axial with a 6m pitch, and biaxial with a 15m pitch) across different ER levels.

Table 25 The sizing and land occupation results of different APV systems at various ER_{APV} levels by Excel Solver tool.

ER_{APV}	Bifacial 2-axis APV capacity	Bifacial 1-axis APV capacity	Bifacial vertical APV capacity
25%	157 kW_p	163 kW_p	213 kW_p
Land use (ha)	0.33	0.24	0.42
30%	241 kW_p	249 kW_p	327 kW_p
Land use (ha)	0.5	0.36	0.64
35%	419 kW_p	434 kW_p	567 kW_p
Land use (ha)	0.87	0.62	1.11
40%	979 kW_p	1.01 MW_p	1.33 MW_p
Land use (ha)	2.05	1.44	2.6
45%	4.75 MW_p	4.93 MW_p	6.46 MW_p
47%	21.4 MW_p	22.3 MW_p	29.15 MW_p
49%	Infinite	Infinite	Infinite

Since the electrical input of the biogas boiler (3.42 kW at full load) is much lower than that of the heat pump (43.72 kW at full load), this smaller magnitude is negligible compared to the electrical needs of the upgrading plant, compression stages, biological processes, and auxiliary systems (119 kW). As a result, the pattern of hourly electrical demand is less variable. In this scenario, due to lower electrical needs, a smaller APV system capacity is required, and the biaxial mounting system, thanks to its more advanced technology, requires fewer PV panels.

To calculate the hourly biogas consumption by the boiler per unit (kW_{th}), the hourly thermal output from the boiler is divided by the product of the LHV of biogas (5.5 kWh/Nm^3) and the thermal efficiency of the boiler (85%). Figure 2.16 illustrates the hourly biogas consumption by the boiler.

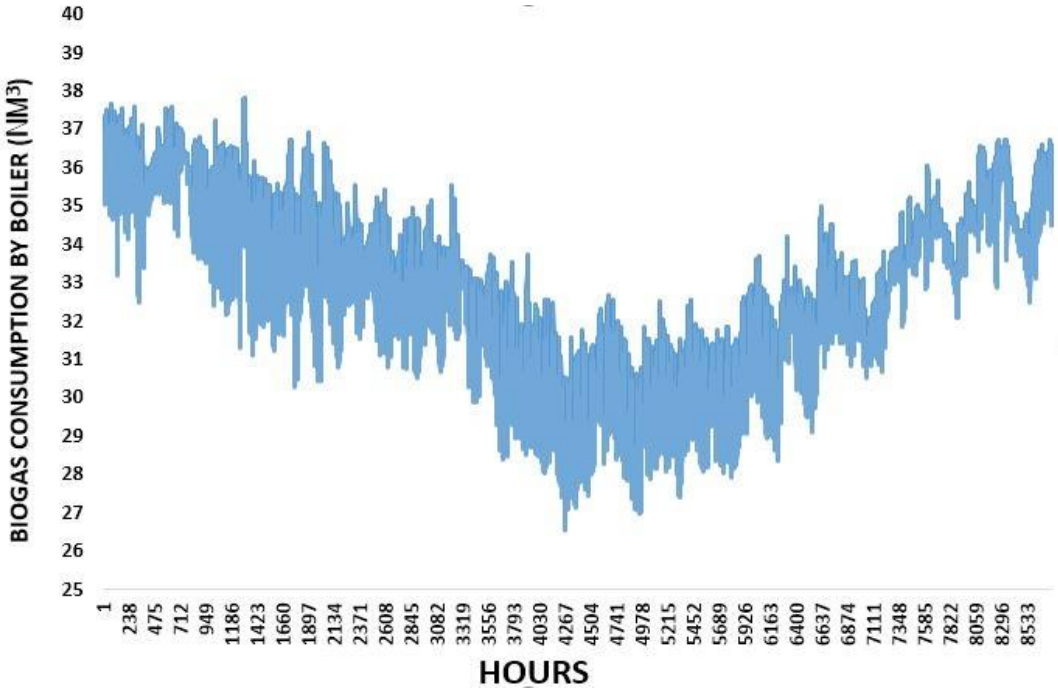

Figure 2-16 The hourly biogas consumption by boiler.

The boiler consumes 286,521 Nm³ of biogas annually. As previously mentioned in Section 2.2.1, the annual biogas production is 2,477,985 Nm³, leaving 2,191,464 Nm³ of biogas available. Considering the methane content of 54.2%, this translates to 1,187,774 Nm³ of bioCH_4 produced in the plant, which is a key figure for the economic analysis.

The total electricity purchased from the grid and the total electricity sold to the grid for Scenario 7 are presented in Table 26, covering ER levels from 25% to 40%.

Table 26 The total electricity purchased and sold of the Scenario 7 at various ER levels.

	BF(1) vertical APV capacity		BF 1-axis APV capacity		BF 2-axis APV capacity	
ER_{APV}	TEP(2) (€)	TES(3) (€)	TEP (€)	TES (€)	TEP (€)	TES (€)
25%	46368	5972	46315	6158	46274	6310
30%	43270	26303	43250	26520	43201	27044
35%	40157	81582	40145	81955	40129	82443
40%	37073	275866	37064	276863	37048	278678

(1) BF: Bifacial, (2) TEP: Total electricity purchased, (3) TES: Total electricity sales

Table 27 shows the economic analysis for Scenario 7, evaluating the life cycle cost (LCC), life cycle revenue (LCR), and the revenue-to-cost ratio for each system configuration throughout the project's

duration. The analysis considers different levels of electricity reliability (ER) rates using various APV system types.

Table 27 The economic analysis results for Scenario 7 (land lease cost included).

Scenario 7	BF Biaxial APV system			
	ER_{APV} 25%	ER_{APV} 30%	ER_{APV} 35%	ER_{APV} 40%
LCC (M€)	10.84	11.06	12.20	16.97
LCR (M€)	237.54	241.37	251.63	287.94
LCR/LCC	21.92	21.82	20.63	16.97
Scenario 7	**BF Mono-axial APV system**			
	ER_{APV} 25%	ER_{APV} 30%	ER_{APV} 35%	ER_{APV} 40%
LCC (M€)	10.60	10.69	11.53	15.32
LCR (M€)	237.51	241.28	251.53	287.60
LCR/LCC	22.41	22.57	21.81	18.77
Scenario 7	**BF Vertical APV system**			
	ER_{APV} 25%	ER_{APV} 30%	ER_{APV} 35%	ER_{APV} 40%
LCC (M€)	10.40	10.38	10.98	14.14
LCR (M€)	237.47	241.24	251.47	287.42
LCR/LCC	22.83	23.24	22.91	20.32

As observed in the mono-axial APV system, the total revenue-to-cost ratio peaks at ER 30% before declining at ER 35%, suggesting that ER 30% is the optimal level for this tracking system. In contrast, the biaxial system achieves its highest LCR/LCC ratio at ER 25%, followed by a decline driven by increasing land lease cost.

However, the one-axis system proves more economical (higher LCR/LCC ratio) due to its lower CAPEX, OPEX and replacement costs compared to the dual-axis system.

Although the dual-axis mounting system can meet the same electricity demands at the same ER levels with a lower PV capacity compared to the mono-axial system, the capacity difference between the two systems in this scenario is only 8 kW_p at ER 30% (Table 25). This slight difference has minimal impact on the LCC advantage of the dual-axis system, particularly when factoring in its higher land use and associated land lease costs, and it does not lead to a significant increase in electricity generation for sale.

The vertical bifacial APV system, with the highest LCR to LCC ratio of 23.24 at ER 30%, is the most optimal configuration in Scenario 7. Despite having 35.7% more capacity than the dual-axis system and 31.3% more than the one-axis system, requiring a larger land area, the increased capacity allows it to generate roughly the same amount of total annual electricity sales to the grid as the other systems (Table 26). Moreover, the vertical system benefits from significantly lower CAPEX, OPEX, and replacement costs compared to the other mounting systems. More details on the economic analysis and sensitivity study can be found in the Supplementary Materials.

2.3.7 Scenario 8: APVs + Power grid + Biogas CHP unit

The hourly heat demand remains unchanged from the previous scenario. The hourly electrical need for this scenario is illustrated in Figure 2.17.

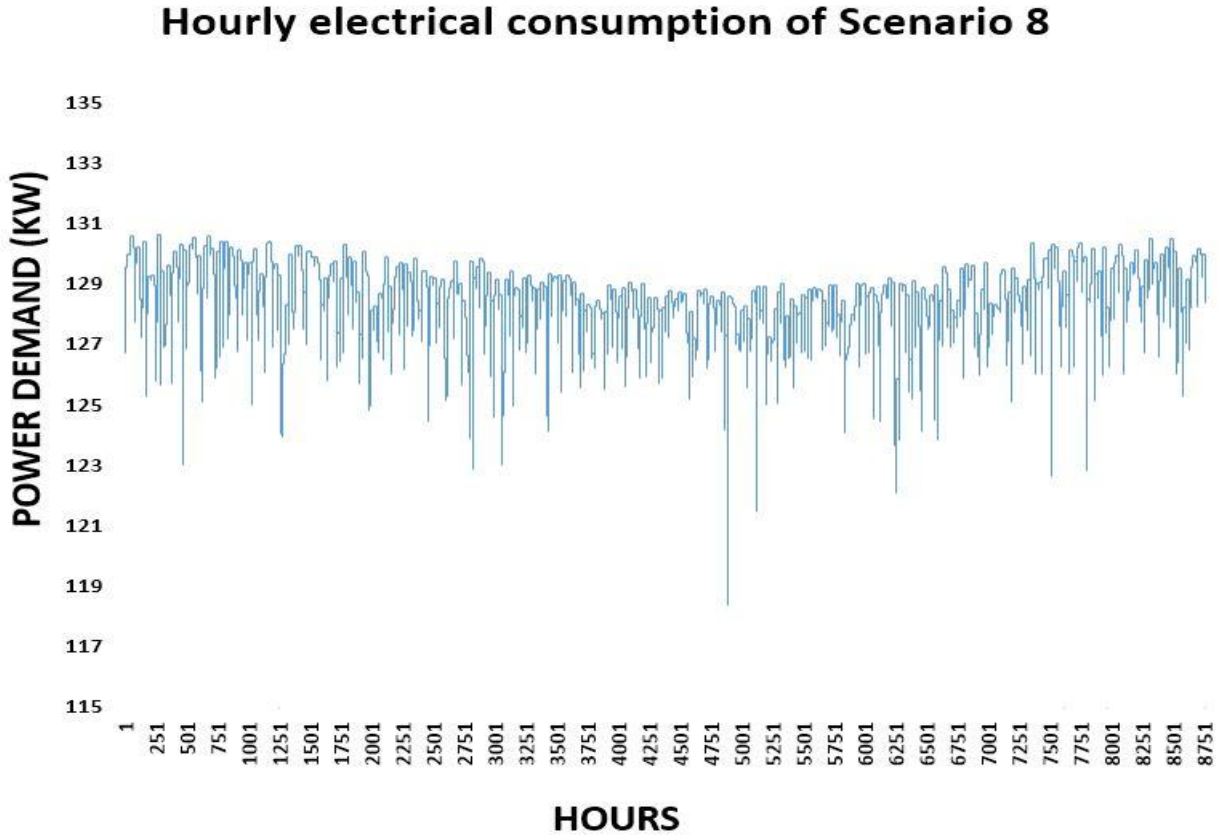

Figure 2-17 Hourly electrical requirements of Scenario 8.

To calculate the hourly electricity production from the CHP unit, the ratio of the rated electrical output to the rated heat output (0.65) was used. This ratio, obtained from the results presented in Section 2.2.5.4 and detailed in Table 4, provided the basis for determining the hourly electricity generation shown in Figure 2.18.

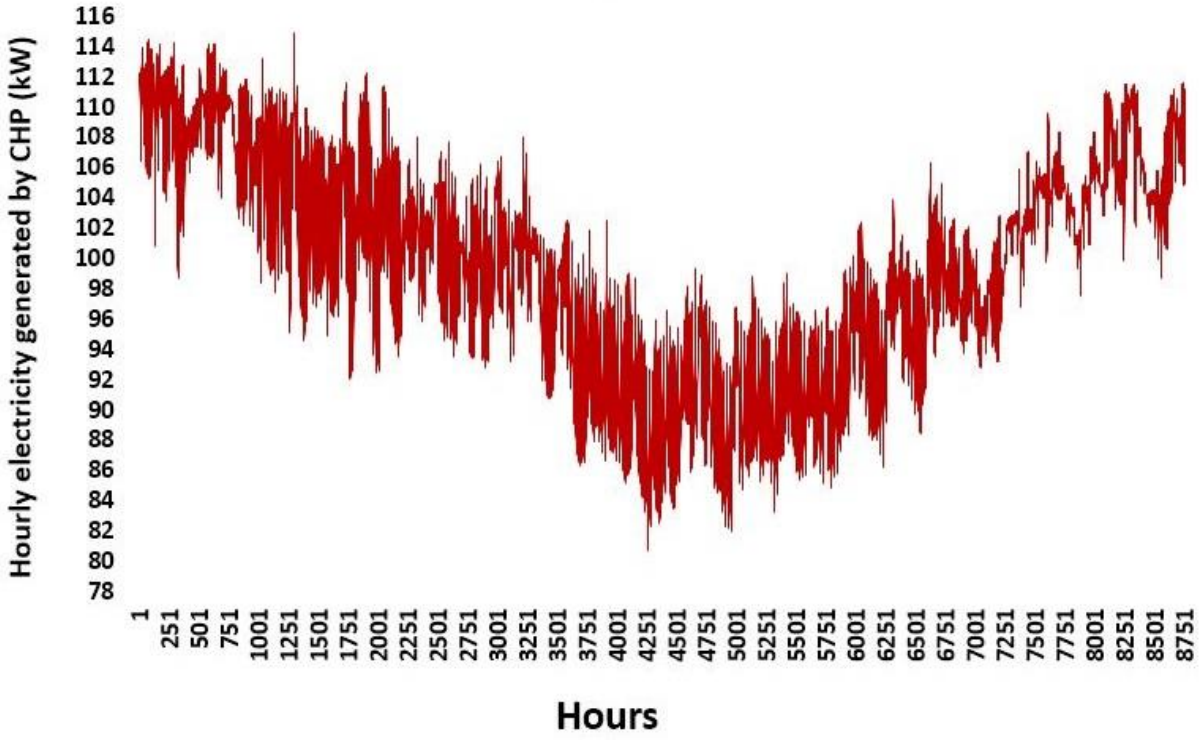

Figure 2-18 The hourly electricity production by CHP.

The total electricity produced by the CHP is 870,665 kWh/year, while the total annual electrical demand is 1,035,302 kWh. This indicates that the biogas CHP satisfies 84.09% of the total electrical needs, with the remaining demand to be covered by the APV system and the power grid. For the rest of electrical demand Table 28 details the sizing and land use of each APV mounting system, for the vertical with an 8m pitch, 1-axis with a 6m pitch, and 2-axis with a 15m pitch at various ER levels.

Table 28 The sizing and land occupation results of different APV systems at various ER_{APV} levels by Excel Solver tool.

$ER_{CHP+APV}$	Bifacial 2-axis APV capacity	Bifacial 1-axis APV capacity	Bifacial vertical APV capacity
86%	11 kW_p	12 kW_p	16 kW_p
Land use (ha)	0.023	0.017	0.031
88%	25 kW_p	26 kW_p	34 kW_p
Land use (ha)	0.052	0.036	0.066
90%	51 kW_p	53 kW_p	70 kW_p
Land use (ha)	0.11	0.08	0.14
91%	90 kW_p	94 kW_p	123 kW_p
Land use (ha)	0.19	0.14	0.24
92%	250 kW_p	261 kW_p	342 kW_p
Land use (ha)	0.52	0.38	0.67
93%	10 MW_p	10.4 MW_p	13.6 MW_p
94%	Infinite	Infinite	Infinite

For example, an ER of 86% means 84.09% is supplied by the CHP and 1.91% by the APV system. The use of dual-axis technology reduces the number of solar panels needed, which becomes more pronounced as ER levels increase.

To estimate the hourly biogas consumption by the CHP per unit (kW_{th}), the hourly thermal output of the CHP is divided by the product of the biogas LHV (5.5 kWh/Nm^3) and the thermal efficiency of the CHP (52.3%). Figure 2.19 illustrates the hourly biogas consumption by the CHP unit.

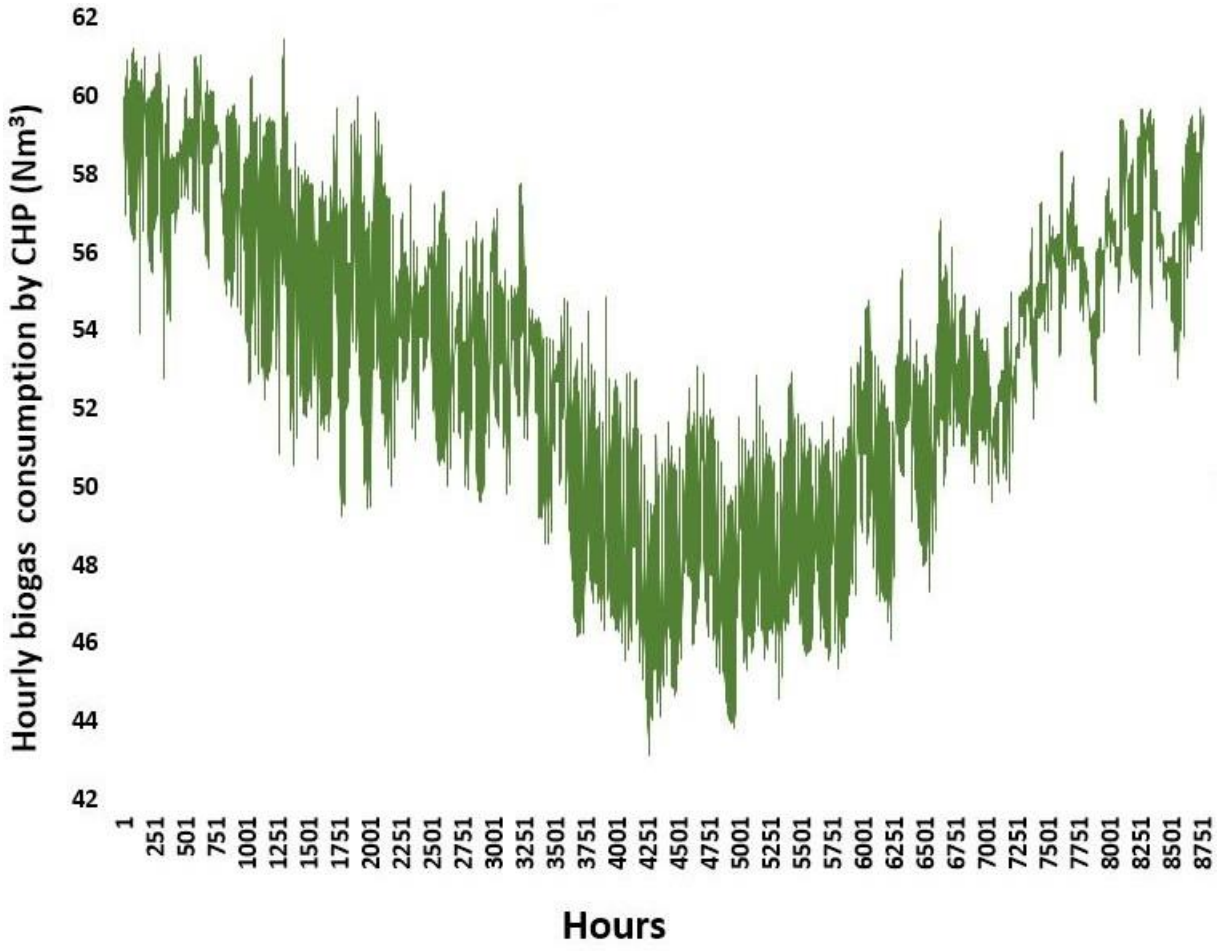

Figure 2-19 The hourly biogas consumption by CHP.

From the total annual biogas production of 2,477,985 Nm³ (283 Nm³/h), 19.08% is consumed by the CHP unit, which amounts to 465,665 Nm³ annually (53 Nm³/h). This percentage is lower than the 24.05% previously estimated in Section 2.2.1 due to the system controller's restriction on the CHP, preventing full-load operation and thereby reducing waste heat generation and biogas consumption. Consequently, 2,012,320 Nm³ of biogas remains available for BioCH_4 conversion. With a methane content of 54.2%, this translates to 1,090,678 Nm³ of BioCH_4.

Table 29 presents the total electricity purchased from the grid and total electricity sales to the grid for the scenario 8.

Table 29 The total electricity purchased and sold of Scenario 8.

	BF(1) vertical APV capacity		BF 1-axis APV capacity		BF 2-axis APV capacity	
$ER_{CHP+APV}$	TEP(2) (€)	TES(3) (€)	TEP (€)	TES (€)	TEP (€)	TES (€)
0.86	8707	165	8701	166	8690	169
0.88	7481	1017	7461	1046	7445	1071
0.90	6240	6322	6224	6489	6201	6735
0.91	5599	18563	5597	18622	5580	19229
0.92	4983	73215	4976	74692	4966	76923

(1) BF: Bifacial, (2) TEP: Total electricity purchased, (3) TES: Total electricity sales

The economic analysis for Scenario 8 evaluates the life cycle cost (LCC), life cycle revenue (LCR), and the revenue-to-cost ratio for each system configuration throughout the project's duration. This analysis considers different levels of electricity reliability (ER) rates across various APV system types, as detailed in Table 30.

Table 30 The economic analysis results for Scenario 8 (land lease cost included).

Scenario 8	BF Biaxial APV system				
	$ER_{CHP+APV\ 86\%}$	$ER_{CHP+APV\ 88\%}$	$ER_{CHP+APV\ 90\%}$	$ER_{CHP+APV\ 91\%}$	$ER_{CHP+APV\ 92\%}$
LCC (M€)	13.03	12.93	12.95	13.20	14.62
LCR (M€)	221.97	222.14	223.19	225.50	236.18
LCR/LCC	**17.04**	**17.18**	**17.24**	**17.08**	**16.16**

Scenario 8	BF Mono-axial APV system				
	$ER_{CHP+APV\ 86\%}$	$ER_{CHP+APV\ 88\%}$	$ER_{CHP+APV\ 90\%}$	$ER_{CHP+APV\ 91\%}$	$ER_{CHP+APV\ 92\%}$
LCC (M€)	13.01	12.89	12.88	13.07	14.41
LCR (M€)	221.97	222.14	223.14	225.39	235.76
LCR/LCC	**17.06**	**17.23**	**17.33**	**17.25**	**16.36**

Scenario 8	BF Vertical APV system				
	$ER_{CHP+APV\ 86\%}$	$ER_{CHP+APV\ 88\%}$	$ER_{CHP+APV\ 90\%}$	$ER_{CHP+APV\ 91\%}$	$ER_{CHP+APV\ 92\%}$
LCC (M€)	13.00	12.86	12.81	12.95	13.91
LCR (M€)	221.97	222.13	223.11	225.38	235.49
LCR/LCC	**17.07**	**17.27**	**17.42**	**17.40**	**16.93**

The analysis of mono-axial and biaxial APV configurations shows that the total revenue-to-cost ratio reaches optimal performance at an ER of 90% (with 84.09% from biogas CHP and 5.91% from APV), followed by a decline at 91% ER, making 90% the ideal operational threshold for both tracking systems. The mono-axial configuration is economically preferable, demonstrated by a higher LCR/LCC ratio due to

lower CAPEX, OPEX, and replacement costs compared to the dual-axis system. Although the biaxial configuration, with its advanced technology, fulfills the same electricity demand at equivalent ER levels with lower PV capacity than the mono-axial system, the capacity difference between them is minor–only 2 kW_p at 90% ER (Table 28). This small difference does not offset the life cycle cost disadvantage or significantly increase electricity generation for sale.

The vertical bifacial APV configuration emerges as the optimal choice in Scenario 8, achieving a LCR to LCC ratio of 17.42 at 90% ER. While requiring 37.2% more capacity than the dual-axis system and 32.1% more than the single-axis system, the increased capacity enables comparable annual electricity sales to the grid (Table 29). Additionally, the vertical configuration benefits from substantially lower CAPEX, OPEX, and replacement costs compared to other mounting options.

Table 31 shows the overall ranking of all scenarios and sub-scenarios.

Table 31 The overall ranking of all scenarios and sub-scenarios of this study.

Rank	Scenario	Configuration	APV type	Description	PV capacity (kW)	LCR (M€)	LCC (M€)	Land occupation (ha)	LCR/LCC (land lease included)
1	Scenario 7	APV + Power grid + biogas boiler	BF Vertical	$ER_{APV\ 30\%\ @pitch8m}$	327	241.24	10.38	0.64	23.24
2		APV + Power grid + biogas boiler	BF Vertical	$ER_{APV\ 35\%\ @pitch8m}$	567	251.47	10.98	1.11	22.91
3		APV + Power grid + biogas boiler	BF Vertical	$ER_{APV\ 25\%\ @pitch8m}$	213	237.47	10.40	0.42	22.83
4		APV + Power grid + biogas boiler	BF Mono-axial	$ER_{APV\ 30\%\ @pitch6m}$	249	241.28	10.69	0.36	22.57
5		APV + Power grid + biogas boiler	BF Mono-axial	$ER_{APV\ 25\%\ @pitch6m}$	163	237.51	10.60	0.24	22.41
6		APV + Power grid + biogas boiler	BF Biaxial	$ER_{APV\ 25\%\ @pitch15m}$	157	237.54	10.84	0.33	21.92
7		APV + Power grid + biogas boiler	BF Biaxial	$ER_{APV\ 30\%\ @pitch15m}$	241	241.37	11.06	0.5	21.82
8		APV + Power grid + biogas boiler	BF Mono-axial	$ER_{APV\ 35\%\ @pitch6m}$	434	251.53	11.53	0.62	21.81
9		APV + Power grid + biogas boiler	BF Biaxial	$ER_{APV\ 35\%\ @pitch15m}$	419	251.63	12.20	0.87	20.63
10		APV + Power grid + biogas boiler	BF Vertical	$ER_{APV\ 40\%\ @pitch8m}$	1330	287.42	14.14	2.6	20.32
11		APV + Power grid + biogas boiler	BF Mono-axial	$ER_{APV\ 40\%\ @pitch6m}$	1001	287.6	15.32	1.44	18.77
12	Scenario 5	Biogas CHP	None	None	None	208.06	11.31	None	18.40
13	Scenario 8	APV + Power grid + Biogas CHP unit	BF Vertical	$ER_{CHP+APV\ 90\%\ @pitch8m}$	70	223.11	12.81	0.14	17.42
14		APV + Power grid + Biogas CHP unit	BF Vertical	$ER_{CHP+APV\ 91\%\ @pitch8m}$	123	225.38	12.95	0.24	17.40
15		APV + Power grid + Biogas CHP unit	BF Mono-axial	$ER_{CHP+APV\ 90\%\ @pitch6m}$	53	223.14	12.88	0.08	17.33
16		APV + Power grid + Biogas CHP unit	BF Vertical	$ER_{CHP+APV\ 88\%\ @pitch8m}$	34	222.13	12.86	0.066	17.27
17		APV + Power grid + Biogas CHP unit	BF Mono-axial	$ER_{CHP+APV\ 91\%\ @pitch6m}$	94	225.39	13.07	0.14	17.25
18		APV + Power grid + Biogas CHP unit	BF Biaxial	$ER_{CHP+APV\ 90\%\ @pitch15m}$	51	223.2	12.95	0.11	17.24

(continued)	Scenario	Configuration	APV type	Description	PV capacity (kW)	LCR (M€)	LCC (M€)	Land occupation (ha)	LCR/LCC (land lease included)
19	Scenario 8	APV + Power grid + Biogas CHP unit	BF Mono-axial	$ER_{CHP+APV\ 88\%\ @pitch6m}$	26	222.14	12.89	0.036	17.23
20		APV + Power grid + Biogas CHP unit	BF Biaxial	$ER_{CHP+APV\ 88\%\ @pitch15m}$	25	222.14	12.93	0.052	17.18
21		APV + Power grid + Biogas CHP unit	BF Biaxial	$ER_{CHP+APV\ 91\%\ @pitch15m}$	90	225.5	13.20	0.19	17.08
22		APV + Power grid + Biogas CHP unit	BF Vertical	$ER_{CHP+APV\ 86\%\ @pitch8m}$	16	221.97	13.00	0.031	17.07
23		APV + Power grid + Biogas CHP unit	BF Mono-axial	$ER_{CHP+APV\ 86\%\ @pitch6m}$	12	221.97	13.01	0.017	17.06
24		APV + Power grid + Biogas CHP unit	BF Biaxial	$ER_{CHP+APV\ 86\%\ @pitch15m}$	11	221.97	13.03	0.023	17.04
25	Scenario 7	APV + Power grid + biogas boiler	BF Biaxial	$ER_{APV\ 40\%\ @pitch15m}$	979	287.94	16.97	2.05	16.97
26	Scenario 8	APV + Power grid + Biogas CHP unit	BF Vertical	$ER_{CHP+APV\ 92\%\ @pitch8m}$	342	235.49	13.91	0.67	16.93
27		APV + Power grid + Biogas CHP unit	BF Mono-axial	$ER_{CHP+APV\ 92\%\ @pitch6m}$	261	235.76	14.41	0.38	16.36
28		APV + Power grid + Biogas CHP unit	BF Biaxial	$ER_{CHP+APV\ 92\%\ @pitch15m}$	250	236.18	14.62	0.52	16.16
29	Scenario 6	APV + Power grid + heat pump	BF Vertical	$ER_{APV\ 35\%\ @pitch8m}$	753	279.56	35.80	1.47	7.81
30		APV + Power grid + heat pump	BF Mono-axial	$ER_{APV\ 35\%\ @pitch6m}$	574	279.58	36.55	0.83	7.65
31		APV + Power grid + heat pump	BF Vertical	$ER_{APV\ 40\%\ @pitch8m}$	1800	294.6	38.56	3.51	7.64
32		APV + Power grid + heat pump	BF Vertical	$ER_{APV\ 30\%\ @pitch8m}$	420	275.28	36.56	0.82	7.53
33		APV + Power grid + heat pump	BF Biaxial	$ER_{APV\ 35\%\ @pitch15m}$	554	279.62	37.38	1.16	7.48
34		APV + Power grid + heat pump	BF Mono-axial	$ER_{APV\ 30\%\ @pitch6m}$	321	275.29	36.95	0.46	7.45
35		APV + Power grid + heat pump	BF Biaxial	$ER_{APV\ 30\%\ @pitch15m}$	309	275.3	37.46	0.65	7.35
36		APV + Power grid + heat pump	BF Mono-axial	$ER_{APV\ 40\%\ @pitch6m}$	1370	294.66	40.25	1.97	7.32

(continued)	Scenario	Configuration	APV type	Description	PV capacity (kW)	LCR (M€)	LCC (M€)	Land occupation (ha)	LCR/LCC (land lease included)
37	Scenario 6	APV + Power grid + heat pump	BF Vertical	$ER_{APV\ 25\%\ @pitch8m}$	267	273.73	38.23	0.52	7.16
38		APV + Power grid + heat pump	BF Mono-axial	$ER_{APV\ 25\%\ @pitch6m}$	205	273.73	38.45	0.3	7.12
39		APV + Power grid + heat pump	BF Biaxial	$ER_{APV\ 25\%\ @pitch15m}$	198	273.73	38.77	0.41	7.06
40		APV + Power grid + heat pump	BF Biaxial	$ER_{APV\ 40\%\ @pitch15m}$	1320	294.75	42.29	2.77	6.97
41	Scenario 1	Off-grid APV + biogas boiler	BF Vertical	Pitch 8m	2743	262.82	42.80	5.53	6.14
42		Off-grid APV + biogas boiler	BF Vertical	Pitch 10m	2743	264.16	43.45	6.64	6.08
43	Scenario 4	Power grid + biogas boiler	None	None	None	236.37	39.99	None	5.91
44	Scenario 1	Off-grid APV + biogas boiler	BF Biaxial	Pitch 15m	1900	260.52	47.37	3.98	5.5
45	Scenario 3	Power grid + Heat pump	None	None	None	273.27	49.87	None	5.48
46	Scenario 1	Off-grid APV + biogas boiler	BF Mono-axial	Pitch 6m	2580	267.75	48.95	3.72	5.47
47		Off-grid APV + biogas boiler	BF Biaxial	Pitch 18m	1900	261.27	47.85	4.72	5.46
48	Scenario 2	Off-grid APV + heat pump	BF Vertical	Pitch 8m	3654	309.81	56.85	7.13	5.45
49	Scenario 1	Off-grid APV + biogas boiler	BF Mono-axial	Pitch 8m	2580	268.96	49.72	4.93	5.41
50	Scenario 2	Off-grid APV + heat pump	BF Vertical	Pitch 10m	3654	311.55	57.69	8.84	5.40
51		Off-grid APV + heat pump	BF Biaxial	Pitch 15m	2531	305.24	62.81	5.3	4.86
52		Off-grid APV + heat pump	BF Mono-axial	Pitch 6m	3437	315.87	65.13	4.95	4.85
53		Off-grid APV + heat pump	BF Biaxial	Pitch 18m	2531	306.24	63.40	6.28	4.83
54		Off-grid APV + heat pump	BF Mono-axial	Pitch 8m	3437	317.49	66.01	6.56	4.81

2.4 Conclusion

The integration of APV and biogas systems was the focus of this study, particularly addressing the energy needs of a BioCH_4 plant in Piacenza, Italy. Scenario 7, integrating a vertical bifacial APV system, the power grid, and a biogas boiler, provides the most economically viable option. In this scenario, 30% of the total electricity demand is fulfilled by a vertically installed bifacial APV system with a capacity of 327 kW_p, occupying 0.64 hectares with an 8-meter PV row spacing. The remaining electricity is sourced from the power grid, while the heat demand is fully met by a biogas boiler.

This configuration yields the highest Life Cycle Revenue (LCR) to Life Cycle Cost (LCC) ratio of 23.24, which is 26.3 % higher than the reference scenario, where only a CHP is used.

Although the vertical APV system requires a larger PV capacity compared to the one-axis and dual-axis configurations, it benefits from significantly lower capital expenditure (CAPEX), operational expenditure (OPEX), and replacement costs per unit. The power grid is preferred over biogas-fuelled CHP unit or battery storage packages due to its more cost-effective approach for balancing energy supply and demand, without the substantial initial investments and ongoing maintenance requirements associated with batteries or CHP system.

The ER level of 30% has shown the optimal balance between reliability and economic efficiency, as higher levels of ER lead to increased costs and diminishing returns. Furthermore, employing a biogas boiler for heat production, rather than a CHP unit or heat pump, results in lower CAPEX, OPEX, and electricity consumption, ultimately minimizing the life cycle cost. The biogas boiler also facilitates increased BioCH_4 production for sale, further enhancing revenue, unlike the CHP system, which consumes a significant portion of biogas for operation.

2.5 References

Akarsu, R. T., & Demir, N. (2024). Techno-economic and environmental analysis of biogas-based hybrid renewable energy systems: A case study for a small-scale livestock farm. Process Safety and Environmental Protection, 191, 1968-1981.

Álvaro, A. G., Palomar, C. R., Torre, R. M., Redondo, D. H., & de Godos Crespo, I. (2023). Hybridization of anaerobic digestion with solar energy: A solution for isolated livestock farms. Energy Conversion and Management: X, 20, 100488.

ATTSU Group Company. https://www.attsu.com/en. (Accessed 15 October 2024).

Bambokela, J. E., Belaid, M., & Muzenda, E. (2020). Preliminary design of a biogas-solar PV hybrid mini-grid system for off-grid agricultural communities.

Bellone, Y., Croci, M., Impollonia, G., Zad, A. N., Colauzzi, M., Campana, P. E., & Amaducci, S. (2024). Simulation-Based Decision Support for Agrivoltaic Systems. Applied Energy, 369, 123490.

Blum, P., Campillo, G., & Kölbel, T. (2011). Techno-economic and spatial analysis of vertical ground source heat pump systems in Germany. Energy, 36(5), 3002-3011.

Calise, F., Cappiello, F. L., Cimmino, L., d'Accadia, M. D., & Vicidomini, M. (2023). Integration of photovoltaic panels and solar collectors into a plant producing biomethane for the transport sector: Dynamic simulation and case study. Heliyon, 9(4).

Calise, F., Cappiello, F. L., Cimmino, L., d'Accadia, M. D., & Vicidomini, M. (2024). Dynamic analysis and thermoeconomic optimization of a Power-to-Gas system driven by renewables. Energy Conversion and Management, 313, 118647.

Casasso, A., Capodaglio, P., Simonetto, F., & Sethi, R. (2019). Environmental and economic benefits from the phase-out of residential oil heating: A study from the Aosta Valley region (Italy). Sustainability, 11(13), 3633.

Casasso, A., Puleo, M., Panepinto, D., & Zanetti, M. (2021). Economic viability and greenhouse gas (GHG) budget of the biomethane retrofit of manure-operated biogas plants: a case study from Piedmont, Italy. Sustainability, 13(14), 7979.

CIB - Consorzio Italiano Biogas. (2024). Biomethane feed-in tariff. https://www.consorziobiogas.it/

Di Micco, S., Romano, F., Jannelli, E., Perna, A., & Minutillo, M. (2023). Techno-economic analysis of a multi-energy system for the co-production of green hydrogen, renewable electricity, and heat. International Journal of Hydrogen Energy, 48(81), 31457-31467.

EBA Statistical Report 2023. https://www.europeanbiogas.eu/eba-statistical-report-2023/ (Accessed 15 October 2024).

Ebaid, M. S., Qandil, H., & Hammad, M. (2013). A unified approach for designing a photovoltaic solar system for the underground water pumping well-34 at Disi aquifer. Energy Conversion and Management, 75, 780-795.

Ennemiri, N., Berrada, A., Emrani, A., Abdelmajid, J., & El Mrabet, R. (2024). Optimization of an off-grid PV/biogas/battery hybrid energy system for electrification: A case study in a commercial platform in Morocco. Energy Conversion and Management: X, 21, 100508.

Fiorentino, G., Zucaro, A., Cerbone, A., Giocoli, A., Motola, V., Rinaldi, C., Scalbi, S., & Ansanelli, G. (2024). The contribution of biogas to the electricity supply chain: an Italian life cycle assessment database. Energies, 17(13), 3264.

Hao, Y., Li, W., Tian, Z., Campana, P. E., Li, H., Jin, H., & Yan, J. (2018). Integration of concentrating PVs in anaerobic digestion for biomethane production. Applied Energy, 231, 80-88.

Hein, P., Kolditz, O., Görke, U. J., Bucher, A., & Shao, H. (2016). A numerical study on the sustainability and efficiency of borehole heat exchanger coupled ground source heat pump systems. Applied Thermal Engineering, 100, 421-433.

Josimović, L., Prvulović, S., Djordjević, L., Bicok, I., Bakator, M., Premčevski, V., Šarenac, U., & Šeljmeši, D. (2024). Enhancing Biogas Plant Efficiency for the Production of Electrical and Thermal Energy. Applied Sciences, 14(13), 5858.

Lowder, S. K., Skoet, J., & Raney, T. (2016). The number, size, and distribution of farms, smallholder farms, and family farms worldwide. World development, 87, 16-29.

Messenger, R. A., & Ventre, J. (2010). Photovoltaic Systems Engineering. CRC Press.

MITSUBISHI ELECTRIC. https://les.mitsubishielectric.co.uk/. (Accessed 15 October 2024).

Nikzad, A., Chahartaghi, M., & Ahmadi, M. H. (2019). Technical, economic, and environmental modeling of solar water pump for irrigation of rice in Mazandaran province in Iran: A case study. Journal of Cleaner Production, 239, 118007.

Nouadje, B. A. M., Kapen, P. T., Chegnimonhan, V., & Tchinda, R. (2024). Techno-economic analysis of an islanded energy system based on geothermal/biogas/wind/PV utilizing battery technologies: A case study of Woulde, Adamawa's region, Cameroon. Energy Strategy Reviews, 54, 101469.

Petrollese, M., & Cocco, D. (2020). Techno-economic assessment of hybrid CSP-biogas power plants. Renewable Energy, 155, 420-431.

Pöschl, M., Ward, S., & Owende, P. (2010). Evaluation of energy efficiency of various biogas production and utilization pathways. Applied Energy, 87(11), 3305-3321.

Ravilla, A., Shirkey, G., Chen, J., Jarchow, M., Stary, O., & Celik, I. (2024). Techno-economic and life cycle assessment of agrivoltaic system (AVS) designs. Science of the Total Environment, 912, 169274.

Reher, T., Lavaert, C., Willockx, B., Huyghe, Y., Bisschop, J., Martens, J. A., Diels, Jan., Cappelle, J., & Van de Poel, B. (2024). Potential of sugar beet (Beta vulgaris) and wheat (Triticum aestivum) production in vertical bifacial, tracked, or elevated agrivoltaic systems in Belgium. Applied Energy, 359, 122679.

Ruffino, E., Piga, B., Casasso, A., & Sethi, R. (2022). Heat pumps, wood biomass, and fossil fuel solutions in the renovation of buildings: A techno-economic analysis applied to Piedmont region (NW Italy). Energies, 15(7), 2375.

Said, T. R., Kichonge, B., & Kivevele, T. (2024). Optimal design and analysis of a grid-connected hybrid renewable energy system using HOMER Pro: A case study of Tumbatu Island, Zanzibar. Energy Science & Engineering, 12(5), 2137-2163.

Sieborg, M. U., Engelbrecht, N., Ottosen, L. D. M., & Kofoed, M. V. W. (2024). Sunshine-to-fuel: Demonstration of coupled photovoltaic-driven biomethanation operation, process, and techno-economical evaluation. Energy Conversion and Management, 299, 117767.

Solheim Haugen, H., & Arancibia Holm, N. (2023). Energy demand and biogas production in rural areas: A case study in the Raqayapampa community in Bolivia.

Su, B., Wang, H., Zhang, X., He, H., & Zheng, J. (2021). Using photovoltaic thermal technology to enhance biomethane generation via biogas upgrading in anaerobic digestion. Energy Conversion and Management, 235, 113965.

Taramasso, M. A., Motaghi, M., & Casasso, A. (2024). A techno-economic feasibility analysis of solutions to cover the thermal and electrical demands of anaerobic digesters. Renewable Energy, 121485.

TEDOM Group. https://www.tedom.com/en/. (Accessed 15 October 2024).

Temiz, M., Sinbuathong, N., & Dincer, I. (2022). Development and assessment of a new agrivoltaic-biogas energy system for sustainable communities. International Journal of Energy Research, 46(13), 18663-18675.

Urs, R. R., Sadiq, M., Jaradat, R., & Mayyas, A. (2024). Harvesting energy horizons: Bifacial PV and reversible fuel cells unite for sustainable building solutions. International Journal of Hydrogen Energy.

Villarroel-Schneider, J., Balderrama, S., Sánchez, C., Cardozo, E., Malmquist, A., & Martin, A. (2023). Open-source model applied for techno-economic optimization of a hybrid solar PV biogas-based polygeneration plant: The case of a dairy farmers' association in central Bolivia. Energy Conversion and Management, 291, 117223.

3 LARGE-SCALE AGRIVOLTAIC INSTALLATION IN BIOGAS FARMS

3.1 INTRODUCTION

Livestock activities have a significant impact on the environment (Battini et al., 2014), with the global dairy sector alone contributing 4.0% of anthropogenic greenhouse gas emissions, which decreases to 2.7% excluding meat production (FAO, 2010). European policies promote the multifunctional role of agriculture to enhance sustainability, recognising that dairy production is a major contributor to global warming, acidification and eutrophication (Ghisellini et al., 2014). Dairy farming is one of the main agro-industries in the Po Valley region of northern Italy. This agro-industry of intensive dairy farms is mainly focused on milk production to produce high-quality cheeses (Ghisellini et al., 2014). In recent years, many Italian dairy farms have been attracted by economic incentives for the installation of biogas plants. Biogas production presents a substantial opportunity for Italian agriculture (Murano et al., 2021), offering not only new revenue streams but also enhanced sustainability in agricultural production (Bortoluzzi et al., 2014). However, achieving sustainable biogas production in Italy necessitates significant investment in advanced equipment and technology, as well as alternative management strategies to mitigate potential environmental impacts (Angelidaki et al., 2018; Bauer et al., 2013; Patrizio & Chinese, 2016). Dale et al. (2016) introduced the *BiogasDoneRight* model, which aims to minimize the environmental footprint of biogas production by integrating non-energy crops in rotation with food/feed crops and utilizing large quantities of "integration biomass" such as livestock manure, hay, and agro-industrial waste. Currently, most Italian biogas plants focus on electricity production, although recent political incentives are shifting the focus towards biomethane production through biogas upgrading (Carfora et al., 2018; Miltner et al., 2017). The conversion of biogas to biomethane, while essential in this energy value chain, is highly energy-intensive, requiring substantial power for processes like compression and refrigeration, as well as specialized equipment such as cryogenic heat exchangers, compressors, and turbines (Baccioli et al., 2018). Therefore, enhancing energy efficiency in biomethane plants is a critical challenge. One promising approach to decarbonize the biomethane production pathway and integrate new renewable energy technologies is the hybridization of biogas plants with agrivoltaics (APV). APV systems combine renewable energy generation with crop cultivation on the same land, creating a synergistic relationship that can reduce carbon emissions and mitigate adverse climatic impacts on crops, such as high temperatures, excessive radiation, and drought (Barron-Gafford et al., 2019; Schweiger & Pataczek, 2023). Recent advancements in APV technology include a variety of PV module designs, layouts, heights, dimensions, and sun-tracking capabilities (Dupraz, 2023). The design of APV systems significantly influences the dynamic shading patterns on the ground, affecting microclimatic conditions such as evapotranspiration, soil temperature, available radiation, crop growth, and yield (Bellone et al., 2024). Numerous studies have explored the impact of APV on key parameters including crop yield (Bellone et al., 2024; Dupraz, 2023) and Water Use Efficiency (WUE) (Barron-Gafford et al., 2019; Bellone et al., 2024; Elamri et al., 2018). System-based models offer a valuable tool for simulating large-scale APV systems, providing critical data on crop performance without the need for actual installation. Simulating APV scenarios involves the integration of radiation models and crop models, and these simulations

provide valuable data on crop performance, making them a useful tool to derive a set of key performance indicators (KPIs) for optimizing APV designs and management in response to specific environmental conditions (Katsikogiannis et al., 2022), offering insights into crop yield potential and constraints (Asseng et al., 2014). Such models can simulate crop responses to APV shading, including yield (Dupraz et al., 2011), water availability (Elamri et al., 2018), and irradiance interception (Trommsdorff et al., 2021). The adaptability of crop models to APV-induced shading has been demonstrated using models like GECROS (Amaducci et al., 2018; Bellone et al., 2024; Potenza et al., 2022), EPIC (Campana et al., 2021), APSIM (Al Mamun et al., 2023), STICS (Dupraz et al., 2011), and DSSAT (Ko et al., 2021). These integrated models thus provide a robust framework for optimizing APV designs and management strategies to enhance the sustainability and productivity of agricultural systems. In this context, the main aim of this work was to develop a case-study in a dairy farm in northern Italy in order to evaluate the use of agricultural land to produce energy carriers for "mobility" (vehicles running on electricity vs biomethane) and to produce food or feed (food/feed vs energy dilemma). A crop model was used to evaluate the response of different *BiogasDoneRight* crop rotations under an APV system. Specifically, various simulation scenarios were analysed to derive a set of KPIs aimed at optimizing APV design parameters (e.g., pitch) and crop management practices (e.g., irrigation).

3.2 MATERIALS AND METHODS

3.2.1 Scenarios description

To assess the trade-off between food/feed production and energy production, four scenarios were examined:

- S1: Milk production only.
- S2: Milk production and biomethane production.
- S3: Milk production and agrivoltaic (APV) energy production.
- S4: Milk production, biomethane production, and APV energy production.

These scenarios were evaluated using different forage/silage crop rotations. The reference crop rotation, labelled R0, includes winter wheat and 2nd harvest maize, which is typical for dairy farms in northern Italy. Additionally, three *BiogasDoneRight* crop rotations were analysed:

- R1A: A rotation involving a cover crop mix, 1st harvest maize, winter wheat, and 2nd harvest soybean.
- R1B: A rotation with a cover crop mix, 1st harvest maize, winter wheat, and 2nd harvest maize.
- R2: A rotation consisting of winter wheat, 2nd harvest maize, forage legume, and 1st harvest sorghum.

In the scenarios involving biomethane production (i.e. S2, and S4), winter wheat, cover crop mix, and 1st harvest sorghum were used for biomethane production, whereas 1st harvest maize, 2nd harvest maize, 2nd harvest soybean, and forage legume were used for milk production. For the optimisation of APV system, several scenarios were simulated using an overhead biaxial APV system in two different configurations,

with pitches of 15 m and 18 m. In addition, two irrigation strategies were evaluated for crop management optimisation: well-irrigated and non-irrigated.

3.2.2 Weather data

The crop simulation analysis was conducted in Piacenza, located in Northern Italy. The simulations covered a ten-year period from 2005 to 2014, utilizing weather data provided by the EU Joint Research Centre's MARS-AGRI4CAST project (Biavetti et al., 2014). The dataset included total global irradiation, daily mean temperature, daily maximum temperature, daily minimum temperature, daily precipitation, and vapor pressure across the entire growing season. The daily data from Agri4cast were converted to hourly data (Yao et al., 2015), and the simulations were performed using hourly time steps. Monthly cumulative precipitation and mean monthly temperature are shown in Table 3.1 and Table 3.2, respectively.

Table 32 Monthly cumulative precipitation data (mm) observed over the 10 years of simulation.

Month	2005	2006	2007	2008	2009	2010	2011	2012	2013	2014
January	4.5	43	24.2	36.8	103.6	55.2	43.2	1.2	94.2	141.2
February	25.9	59.4	14.8	10.4	70.7	138.7	71.2	15.8	52.4	125
March	21.6	14.9	33.4	12	111.2	75	115.7	15.6	188.3	107.1
April	146.1	59.1	5	104.8	195.2	61.2	1	95.8	118.7	97.9
May	85.3	12.3	100.3	114.9	2.1	103.6	35.1	70.6	144.9	30.1
June	21.5	33.5	48.9	121	35.8	110.7	115.4	33.3	22.2	93.1
July	40.8	10.9	14	16.1	17.4	0.1	17.5	46.5	1.6	79.1
August	68.1	86.6	139.7	7.7	8.3	100.1	0.8	43	64.3	43.8
September	47.8	171	95.8	28	81.9	76.3	38.7	109.8	44.5	72
October	139.3	27.7	34.1	59.7	71.2	190.3	60.8	111.4	165.2	55.7
November	111.5	23.4	42.2	164	193.2	258	139.7	129	94	230.9
December	77.7	24.1	3.7	90.4	48.9	87	4.6	19.5	37.5	48.8

Table 33 Mean monthly temperature data (°C) observed over the 10 years of simulation.

Month	2005	2006	2007	2008	2009	2010	2011	2012	2013	2014
January	1.9	-0.1	5.6	4.6	-0.5	1.3	2.5	1.6	2.3	5.5
February	1.7	2.4	5.8	4.9	3.5	3.4	4.4	-0.7	1.9	6.9

March	7.9	7.8	8.5	9.2	8.4	7.5	8.2	10.5	5.5	10.0
April	12.1	12.9	15.1	12.4	13.6	13.3	14.7	12.0	12.5	13.7
May	18.7	18.9	19.3	17.9	20.3	17.9	19.1	17.9	16.1	17.6
June	24.0	23.5	22.9	22.6	23.9	23.1	21.7	23.2	22.2	23.5
July	25.3	27.5	25.4	25.2	25.8	26.6	22.9	25.2	25.9	23.2
August	22.8	22.9	23.9	25.2	26.4	23.7	25.7	25.7	24.0	22.5
September	20.2	20.6	19.1	19.6	21.1	19.0	22.4	19.6	19.9	19.7
October	12.9	15.3	13.2	15.6	13.4	12.0	13.5	14.1	14.3	15.3
November	6.9	8.8	6.8	8.8	8.9	8.9	7.1	9.6	8.4	10.7
December	1.1	4.7	2.4	2.2	2.0	1.9	2.9	1.7	4.1	5.6

3.2.3 Agrivoltaic system configuration

Simulation scenarios were carried out using overhead biaxial APV system. The APV system used the Agrovoltaico® 3D - T2.1 tracker version, characterised by a 10.5 m horizontal tube supporting 4 rows of wings, with a total of 24 panels per tracker. The system has two sectors with different distances between the rows of trackers (i.e. the pitch), set at 15 m and 18 m respectively. The ground coverage ratio (GCR, i.e. the ratio of total module area to land area) for the 15 m and 18 m pitches was 35% and 30% respectively. The height of the system, at 5 m above the ground, allows conventional agricultural machinery to be operated underneath. The permitted rotation ranges are ±50° from the horizontal and ±60° from the vertical.

3.2.4 Radiation and crop models description

Radiation simulations were carried out using a model developed in SciLab (Dassault Systèmes, France), as described in (Amaducci et al., 2018). This model simulates the hourly irradiation distribution at ground level under an APV plant. The solar irradiance distribution under the APV system was simulated separately for both direct and diffuse irradiance components of the global irradiance, from which the photosynthetically active radiation (PAR) can be calculated. Using a ten-year weather dataset obtained from Agri4Cast, both shading and ground-level irradiation were computed for each pitch scenario of the APV plant at an hourly time step. To account for variations in daily PAR due to module shading, the model calculates data for an area equal to the pitch spacing (in metres). This area is divided into pixels with a resolution of 0.6 m. The number of pixels involved in each simulation was determined by the spacing of the simulated APV system, with 25 pixels for the 15-metres pitch scenario and 30 pixels for the 18-metres pitch scenario. For each pixel, the crop model independently computes outputs based on the micrometeorological conditions at that specific location within the APV system. For these two pitch configurations, the global radiation reduction in percentage was calculated by comparing the global radiation in APV simulated by the radiation model and the global radiation under full light conditions. This

information is crucial because the shade pattern varies significantly based on factors such as spacing pitch, panel height, orientation, tilting, and season. Therefore, it is essential for optimizing the APV plant design. Figure 3.1 shows the mean variation (± the standard deviation based on the ten-year simulation period) of global radiation reduction (%) according to the position across the pitch, from the axis of one PV array to the axis of the next one, for both the 15 m and 18 m pitches. As expected, the values decreased as the distance between the PV arrays increases. Overall, the APV plant with a pitch of 15 m had a mean global radiation reduction of 40%, while the plant with a pitch of 18 m had a mean global radiation reduction of 33%.

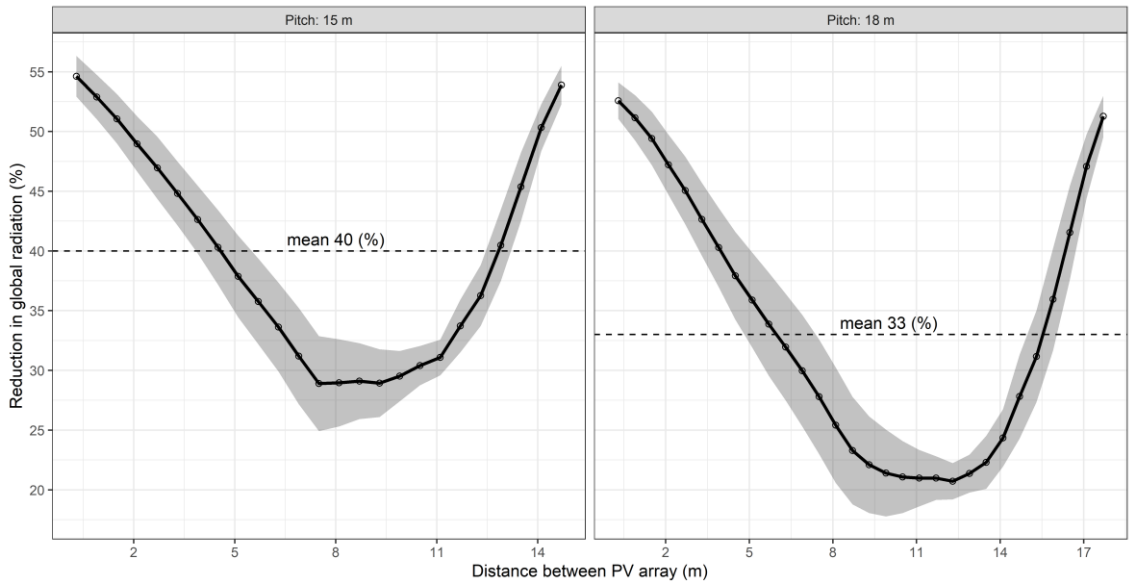

Figure 3-1 Global radiation reduction (%) in APV compared to full light conditions for both 15 m and 18 m pitch configurations.

The crop simulations were carried-out using the DAISY model (Abrahamsen & Hansen, 2000), a dynamic agro-ecosystem model that integrates several sub-models: hydrological, mineral nitrogen, soil organic matter, and crop models. It simulates key processes such as water dynamics (including evapotranspiration, soil water transport, and soil temperature), nitrogen transformation and transport, nitrogen immobilization and mineralization, and carbon cycling. The crop model focuses on plant growth and development, covering dry matter and nitrogen accumulation, leaf-area index development, and root density distribution, with a detailed phenology module for different growth phases. Additionally, DAISY includes a management module for simulating various agricultural practices like soil tillage, sowing, fertilization, irrigation, and harvesting. Comprehensive details of the DAISY model are available in these papers (Hansen & Abrahamsen, 2009; S. Hansen et al., 2012). The data collected during the field experiments in Italy, as part of Task 3.3 Demonstrations of the Value4Farm project, will enable future calibration of the DAISY model. However, since the trials are either incomplete or yet to be conducted, the

model has only been partially calibrated to simulate these scenarios. The forage/silage crop rotations were simulated in DAISY model using the ten-year weather dataset in APV scenario. To simulate the crop response over the ten-year evaluation period, the initial crop in the rotation was iteratively changed according to the number of crops in the evaluated rotation.

3.2.5 Key Performance Indicators (KPIs)

Radiation and crop simulation outputs were used to derive a set of Key Performance Indicators (KPIs) for evaluating scenarios in the food/feed vs energy dilemma and for optimising both the pitch of the APV system and crop irrigation management. Crop yield, water use efficiency (WUE), and water stress (WS) days were calculated as KPIs. Crop yield, measured in tons per hectare (t ha^{-1}), represents the biomass production of forage and silage crops. In the APV scenarios, land losses were considered in order to simulate the realistic conditions, taking into account the necessary safety margin for agricultural mechanisation and APV infrastructure. A safety margin of 0.6 m on each side of the APV support structures was used, as suggested by Bellone et al., to prevent damage to the modules and structures during mechanised agricultural operations. The safety margin has implications for yield losses, particularly when comparing APV systems to full light (FL) conditions. The proportion of non-cropped surface area is highest for APV systems with narrow pitches. To accurately reflect these assumed land losses, raster pixel stripes within the safety margin of the APVs were excluded from the crop yield calculations. This approach ensures that the impact of the safety margin on available cropping area and yield is properly accounted for in the performance assessment of the APV systems. WUE, expressed in kilograms per cubic meter (kg m^{-3}), was calculated as the ratio of crop biomass yield to the total volume of water consumed, which was determined as the cumulative total of crop evapotranspiration. Water Stress (WS), measured in days, is the number of days during which crops experienced water stress and provides an indication of the frequency with which crops are exposed to insufficient water availability, which can affect their growth and yield. WUE and WS KPIs are critical in assessing the capability of APV systems to mitigate climate-related challenges, such as drought. By evaluating WUE and WS, the study aims to understand how effectively APV systems use water resources and mitigate drought stress compared to full light conditions, especially under different climatic conditions and crop irrigation strategies (i.e. well-irrigated and non-irrigated). Regarding the APV KPI, the energy production per hectare (MWh ha^{-1}) was calculated using PVsyst® software. The energy production per hectare indicates the power density of an APV system, measuring the annual energy produced per hectare of land. In addition to the primary KPIs, derived KPIs were calculated based on APV energy production and crop yield across different scenarios (i.e. S1, S2, S3, and S4). For crop biomass yield, conversions were made into both milk and biomethane. For milk conversion, the crop biomass yield was first converted into milk fodder units (UFL). The UFL values used were 800 UFL per ton for winter wheat and cover crop mix, 850 UFL per ton for forage legume and 2nd harvest soybean, and 900 UFL per ton for 1st harvest maize, 2nd harvest maize and 1st harvest sorghum. These UFL values were converted into an estimated milk yield, assuming that 0.44 UFL is required to produce one liter of milk. For biomethane conversion, the crop biomass yield was first converted into biomethane, with 1 ton of dry biomass yielding 250 cubic meters (m^3) of biomethane Sánchez Nocete & Pérez Rodríguez, 2022). This biomethane volume was then converted into kilograms, where 1 cubic meter

equals 0.671 kilograms. Finally, the biomass in kilograms was converted into distance, with 1 kilogram of biomethane corresponding to 57 kilometres. The energy produced by the APV system was also converted into kilometers using the average energy consumption of an electric car, which is 0.15 kWh per kilometer. These conversions enable the evaluation of both energy production and crop yield in terms of kilometers, providing a comprehensive metric for comparing the efficiency of different APV systems.

3.3 RESULTS AND DISCUSSION

3.3.1 KPIs evaluation for APV plant optimisation

The crop simulation results, detailed in Table 3.3, include crop yield, water use efficiency (WUE), and water stress days. These KPIs values were used to evaluate the effects of different pitch configurations in the agrivoltaic (APV) system and different crop irrigation management strategies (well-irrigated vs. non-irrigated) across four crop rotations. For summer crops under well-irrigated conditions, the most significant yield reduction between full light (FL) and APV conditions was observed in soybean, with a decrease of 40-50% (see Ratio values in Table 3.3). This reduction is consistent with findings from previous studies, which indicated that reduced global radiation in APV systems negatively impacts soybean yield (Egli & Bruening, 2005; Potenza et al., 2022). Maize and sorghum showed smaller yield reductions, with approximately 30% for the 18 m pitch and around 36% for the 15 m pitch, corroborating other research on the effects of reduced radiation (Laub et al., 2022; Ramos-Fuentes et al., 2023). The impact of shading stress on yield is influenced by its severity, duration, and the crop's developmental stage during exposure, particularly during critical phenological stages like VT (tasselling) and R1 (silking), which are sensitive periods for grain yield formation (Early et al., 1967; Loomis & Connor, 1992; Otegui & Bonhomme, 1998). Under non-irrigated conditions, soybean yields increased by approximately 55% in APV systems compared to FL, and maize yields increased by 5-10%, aligning with findings by Amaducci et al. (2018), who reported higher maize yields under APV conditions in water-limited scenarios. In contrast, sorghum experienced a yield decrease of 5-10% in APV systems under non-irrigated conditions. However, sorghum exhibited higher WUE in APV systems under both irrigation conditions, and water stress days in non-irrigated sorghum decreased from 17 to 2-4 days. These results highlight sorghum's ability to maintain biomass yield under drought stress, underscoring its drought-tolerant characteristics (Bhattarai et al., 2020). In non-irrigated conditions, winter wheat yields decreased by approximately 21% with an 18 m pitch and 27% with a 15 m pitch in APV systems compared to FL conditions. These results are in line with previous reports on shaded wheat (Estrada-Campuzano et al., 2008; Mu et al., 2010) and are consistent with results from APV studies conducted in northern Italy (Dal Prà et al., 2024), southwestern Germany (Weselek et al., 2021) and India(Prakash et al., 2023). The reduction in winter wheat yield under shading conditions may be attributed to extended vegetative growth due to high shading intensity, which shortens the flowering period (Healey et al., 1998). Except for cover crop mix and forage legume, which showed very low biomass yields in APV systems, WUE was generally higher under APV compared to FL conditions. Additionally, the number of water stress days was significantly reduced under APV, with a decrease of approximately 80%. This reduction suggests that APV systems may enhance crop resilience to climate change, particularly under drought stress conditions. For optimising APV pitch configurations,

the KPIs generally indicated that an 18 m pitch is more favourable for agricultural production compared to a 15 m pitch, resulting in a 6% increase in crop yield. In addition, the yield reduction due to the application of a safety margin is more significant in APV configurations with narrower pitches. These configurations have more PV arrays, which results in a larger area of land being left uncultivated compared to APV systems with wider pitches (Bellone et al., 2024). This is significant as it highlights the potential to reduce yield losses in APV systems, which is crucial for meeting certain threshold values, such as those in the UNI/PdR 148:2013[1] standard for APVs in Italy. However, for summer crops under non-irrigated conditions, there was no substantial difference in yield between the 15 m and 18 m pitch configurations. These results suggest that in regions where irrigation is not feasible, APV systems can be an important technology for maintaining satisfactory crop yields while also supporting energy production.

Table 34 Mean and standard deviation of ten-year simulations for three Key Performance Indicators (KPIs): yield, water use efficiency (WUE), and water stress, across different crop rotations, pitch configurations, and irrigation crop management. Each KPI is shown in three columns: FL (Full Light), APV (Agrivoltaic), and Ratio. The FL column displays the KPI values under full light conditions, while the APV column shows the values under agrivoltaic conditions. The Ratio column indicates the percentage change between FL and APV values, where positive values indicate an increase under APV conditions, and negative values indicate a decrease.

	Crop rotation	Irrigation	Pitch (m)	Yield (t ha^{-1})			WUE (kg m^{-3})			Water Stress (days)		
				FL	APV	Ratio (%)	FL	APV	Ratio (%)	FL	APV	Ratio (%)
R0	Winter Wheat	non-irrigated	15	9.4 ± 1.7	6.6 ± 0.4	-27 ± 13	2.4 ± 0.4	2.5 ± 0.2	4 ± 15	4.4 ± 4.8	0.2 ± 0.5	-89 ± 26
			18		7.2 ± 0.5	-21 ± 13		2.5 ± 0.2	5 ± 13		0.3 ± 0.7	-86 ± 29
	2nd harvest Maize	well-irrigated	15	16.3 ± 0.7	10.4 ± 0.4	-36 ± 1	3.4 ± 0.1	3.4 ± 0.1	0 ± 2			
			18		11.4 ± 0.5	-31 ± 1		3.5 ± 0.1	0 ± 2			
		non-irrigated	15	7.9 ± 2.7	7.9 ± 1.8	5 ± 18	3.4 ± 0.6	3.4 ± 0.4	2 ± 12	42.4 ± 14.9	18.9 ± 15.1	-63 ± 27
			18		8 ± 2.1	4 ± 14		3.4 ± 0.5	2 ± 9		23.4 ± 16.3	-53 ± 27
	Cover crop mix	non-irrigated	15	2.2 ± 1.3	0.8 ± 0.7	-73 ± 17	0.6 ± 0.3	0.3 ± 0.3	-63 ± 24	0.9 ± 1.2	0.5 ± 0.9	-67 ± 39
			18		0.9 ± 0.9	-65 ± 19		0.3 ± 0.3	-54 ± 26		0.5 ± 1	-61 ± 40
R1A	1st harvest Maize	well-irrigated	15	19.6 ± 0.8	12.3 ± 0.4	-37 ± 1	3.8 ± 0.2	3.8 ± 0.2	1 ± 1			
			18		13.5 ± 0.4	-31 ± 1		3.8 ± 0.2	1 ± 1			
		non-irrigated	15	10.1 ± 3.1	10 ± 1.9	5 ± 25	3 ± 0.5	3.6 ± 0.5	21 ± 16	32.9 ± 15.1	9.2 ± 8.6	-77 ± 18
			18		10.1 ± 2.3	5 ± 22		3.5 ± 0.5	17 ± 14		12.5 ± 9.8	-68 ± 20
	Winter Wheat	non-irrigated	15	9.4 ± 1.9	6.7 ± 0.4	-26 ± 15	2.4 ± 0.4	2.5 ± 0.2	5 ± 16	4 ± 5.1	0 ± 0	-100 ± 0
			18		7.3 ± 0.5	-20 ± 15		2.5 ± 0.2	6 ± 15		0.2 ± 0.4	-97 ± 4
	2nd harvest Soybean	well-irrigated	15	7 ± 0.3	3.2 ± 0.2	-53 ± 4	1.9 ± 0.1	1.5 ± 0.1	-20 ± 5			
			18		3.9 ± 0.2	-43 ± 4		1.7 ± 0.1	-13 ± 4			
		non-irrigated	15	2 ± 1.9	2 ± 0.9	66 ± 108	1.1 ± 0.8	1.3 ± 0.4	49 ± 78	31.4 ± 11	10.2 ± 8.9	-73 ± 21
			18		2.1 ± 1.3	52 ± 78		1.3 ± 0.5	38 ± 54		13.8 ± 10.2	-62 ± 23
	Cover crop mix	non-irrigated	15	2 ± 1.2	0.7 ± 0.7	-70 ± 19	0.5 ± 0.3	0.3 ± 0.3	-59 ± 25	1.9 ± 2.1	0.8 ± 1.3	-68 ± 36
			18		0.9 ± 0.8	-62 ± 20		0.3 ± 0.3	-51 ± 27		0.8 ± 1.3	-65 ± 36
R1B	1st harvest Maize	well-irrigated	15	19.6 ± 0.8	12.3 ± 0.4	-37 ± 1	3.8 ± 0.2	3.8 ± 0.2	1 ± 1			
			18		13.5 ± 0.4	-31 ± 1		3.8 ± 0.2	1 ± 1			
		non-irrigated	15	9.9 ± 2.9	9.9 ± 2	5 ± 25	3 ± 0.5	3.5 ± 0.5	21 ± 16	34 ± 15.5	9.9 ± 9.1	-76 ± 18

[1] UNI/PdR 148:2013 is an Italian standard that provides guidelines for the design and implementation of agrivoltaic systems. It outlines the best practices for integrating photovoltaic systems with agricultural activities, ensuring that both energy production and agricultural productivity are optimized. The standard aims to support the sustainable development of agrivoltaics, considering factors such as land use, crop selection, and system configuration to maximize both renewable energy generation and agricultural output.

			18		9.9 ± 2.3	5 ± 22		3.4 ± 0.5	17 ± 14		13.6 ± 10.2	-66 ± 19
	Winter Wheat	non-irrigated	15	9.6 ± 1.8	6.8 ± 0.4	-27 ± 14	2.5 ± 0.4	2.5 ± 0.2	3 ± 14	4.1 ± 5.1	0 ± 0	-100 ± 0
			18		7.4 ± 0.5	-21 ± 14		2.5 ± 0.2	4 ± 13		0.2 ± 0.4	-97 ± 4
	2nd harvest Maize	well-irrigated	15	15.9 ± 0.8	10 ± 0.4	-37 ± 1	3.4 ± 0.1	3.4 ± 0.1	-1 ± 2			
			18		10.9 ± 0.5	-31 ± 1		3.4 ± 0.1	-1 ± 1			
		non-irrigated	15	7.6 ± 3	7.8 ± 1.7	14 ± 43	3.3 ± 0.6	3.4 ± 0.3	5 ± 16	38.7 ± 14	15.9 ± 14.1	-66 ± 27
			18		7.9 ± 2	14 ± 40		3.4 ± 0.4	5 ± 15		20 ± 15.2	-56 ± 28
	Winter Wheat	non-irrigated	15	9.8 ± 1.5	6.7 ± 0.4	-30 ± 11	2.5 ± 0.4	2.5 ± 0.2	0 ± 11	4.6 ± 5.2	0 ± 0.1	-98 ± 5
			18		7.3 ± 0.5	-24 ± 11		2.5 ± 0.2	2 ± 10		0.2 ± 0.4	-94 ± 10
	2nd harvest Maize	well-irrigated	15	16.5 ± 0.8	10.4 ± 0.4	-37 ± 1	3.5 ± 0.1	3.4 ± 0.1	-1 ± 1			
			18		11.4 ± 0.5	-31 ± 1		3.5 ± 0.1	-1 ± 1			
		non-irrigated	15	7.8 ± 2.7	7.9 ± 1.7	6 ± 20	3.3 ± 0.6	3.4 ± 0.4	2 ± 12	42.4 ± 14.8	18.3 ± 14.9	-64 ± 26
			18		8 ± 2	6 ± 16		3.4 ± 0.5	2 ± 10		23 ± 16.1	-53 ± 27
R2	Forage legume	non-irrigated	15	2.7 ± 1	1.4 ± 0.9	-54 ± 21	1.4 ± 0.4	1.1 ± 0.6	-30 ± 32	2 ± 2.1	1 ± 1.5	-53 ± 35
			18		1.6 ± 0.9	-47 ± 21		1.1 ± 0.6	-25 ± 30		1.1 ± 1.6	-47 ± 37
	1st harvest Sorghum	well-irrigated	15	18 ± 0.8	11.5 ± 0.3	-36 ± 2	3.8 ± 0.2	4 ± 0.2	4 ± 1			
			18		12.5 ± 0.4	-30 ± 1		4 ± 0.2	4 ± 1			
		non-irrigated	15	12.6 ± 2.9	11 ± 0.7	-9 ± 18	3.7 ± 0.4	4 ± 0.3	10 ± 8	17.5 ± 11.8	2.2 ± 3.7	-93 ± 11
			18		11.5 ± 1.1	-6 ± 15		4 ± 0.3	9 ± 8		4.1 ± 5.2	-86 ± 16

3.3.2 Spatial and temporal variability of KPIs

The shade patterns created by APV systems result in areas with varying levels of shading, which influence crop responses differently. These patterns can fluctuate annually, especially due to varying weather conditions, impacting crop performance. Figures 3.2, 3.3, and 3.4 show the spatial and temporal variability of KPIs for summer crops, including crop yield, WUE, and water stress days. The data are reported as reduction (i.e. negative values) or increase (i.e. positive values) in APV compared to FL conditions. In particular, the figures illustrate how the KPIs vary according to the position across the pitch, from the axis of one PV array to the axis of the next one. The analysis considers how these KPIs are affected by the heterogeneous shading provided by the APV system, highlighting areas of the field that may benefit from a specific management practice. Understanding this variability is crucial for optimising both agricultural productivity and APV system layout. The spatial and temporal variability in crop yield (Figure 3.2) illustrates the impact of different pitch configurations (15 m and 18 m) and irrigation strategies (well-irrigated and non-irrigated) on agricultural performance under APV systems. In well-irrigated conditions, yield ratio (%) generally increased with the distance between PV arrays, peaking at the centre of the pitch where shading is minimal and declining near the PV arrays where shading is most intense. The 15 m pitch configuration revealed two distinct management zones with varying yield potentials, while the 18 m pitch configuration exhibited three zones. These results suggest that the integration of precision agriculture practices could optimise crop management across different zones by applying site-specific inputs, such as irrigation, tailored to the variability in crop requirements within the field. In well-irrigated conditions, year-to-year yield variability was minimal. However, under non-irrigated conditions, the yield ratio in Figure 3.2 shows reduced variability related to the distance between PV arrays but a significant increase in inter-annual variability, highlighting the influence of weather conditions. Notably, an increase in WUE ratio was observed under non-irrigated conditions (Figure 3.3), suggesting that APV systems may improve water resource use in water-limited environments. Figure 3.4, which details water stress days under non-irrigated conditions, shows the greatest reduction in water stress near the PV arrays and the least reduction at the pitch's centre. This pattern underscores the potential of APV systems to mitigate drought stress, with sorghum showing greater drought tolerance compared to maize, as evidenced by the more significant reduction in water stress days for sorghum. These results emphasize the role of APV systems

in improving crop resilience to water stress and optimising resource use through site-specific management strategies. The analysis of winter crops revealed significant insights into the spatial and temporal variability of KPIs such as crop yield ratio, WUE ratio, and the number of water stress days. These KPIs, depicted in Figures 3.5, 3.6, and 3.7 respectively, were examined across different pitch configurations of 15 m and 18 m. Overall, the temporal variability of these KPIs across different years was generally low, indicating consistency in performance over time. However, notable exceptions were observed. In 2011, there was a significant deviation in both the crop yield ratio and WUE ratio from the average values observed in other years. Similarly, 2009 and 2012 exhibited considerable differences in the number of water stress days compared to the average, suggesting unusual climatic or environmental conditions during these periods. These anomalies suggest that specific years experienced unique conditions that impacted crop performance differently compared to the general trend. Spatial variability was also analysed, particularly in relation to the proximity of crops to PV arrays. The greatest reduction in yield was observed in areas close to the PV arrays, with this effect being more pronounced in crop cover mix and forage legume compared to winter wheat. The shading and microclimatic changes induced by the PV arrays likely contributed to this reduction. In contrast, no significant spatial variability was observed in the WUE ratio and the number of water stress days, especially for winter wheat. This indicates that WUE and water stress responses were relatively uniform across the different spatial locations, regardless of their distance from the PV arrays. These findings highlight the importance of considering both temporal and spatial factors when assessing the impacts of PV arrays on agricultural productivity, particularly in the context of integrated agricultural and renewable energy systems. The observed spatial reduction in yield near the PV arrays suggests a potential trade-off between energy production and agricultural output, which needs to be balanced in system design and management.

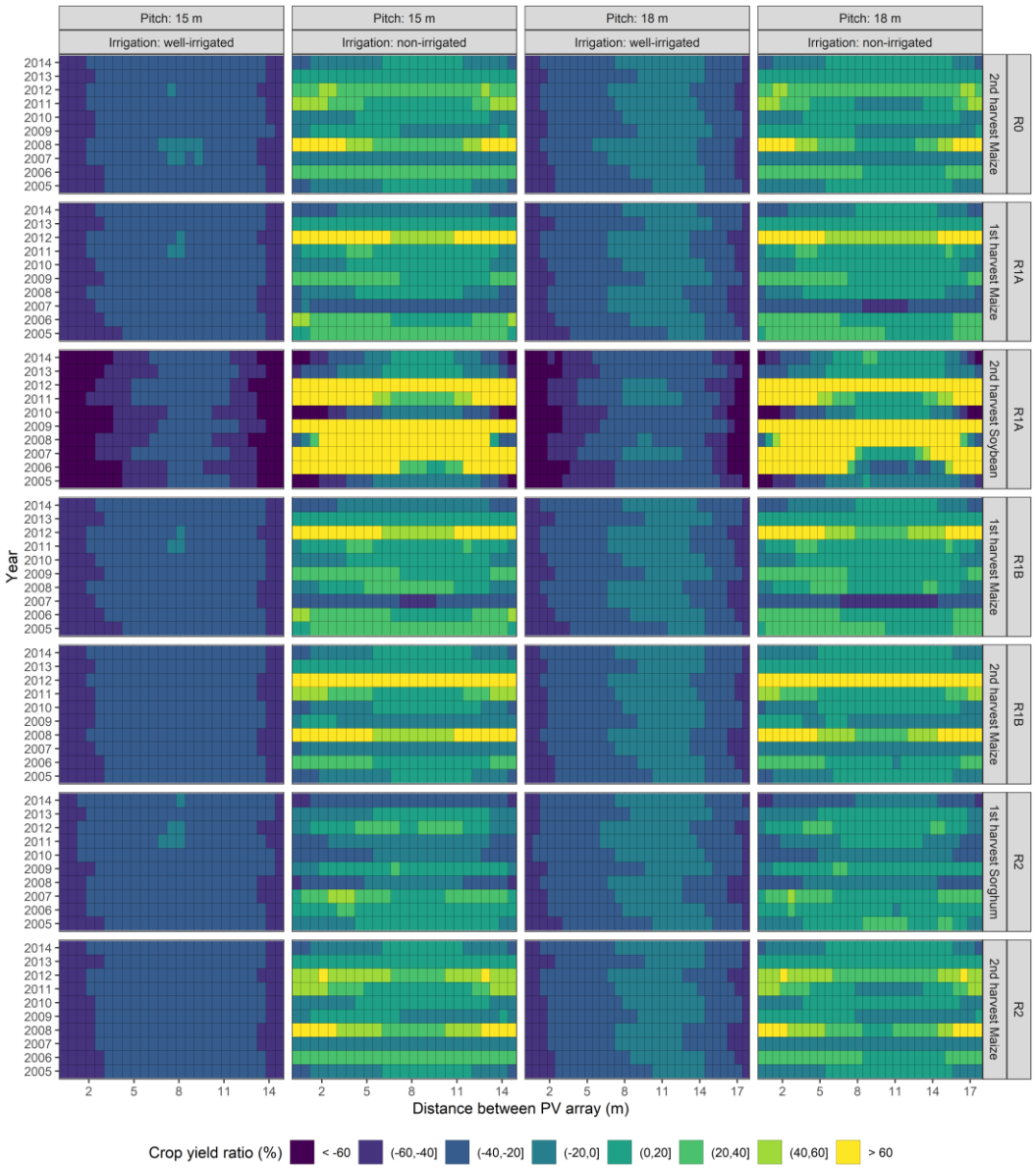

Figure 3-2 Crop yield ratio (%) variability of the summer crops between different years (2005-2014, y-axis) and position in the APV field (x-axis) according to the different crop rotations, pitch configurations, and irrigation management strategies. Crop yield ratio in percentage was calculated as the decrease (negative values) or increase (positive values) in the APV condition compared to full light conditions.

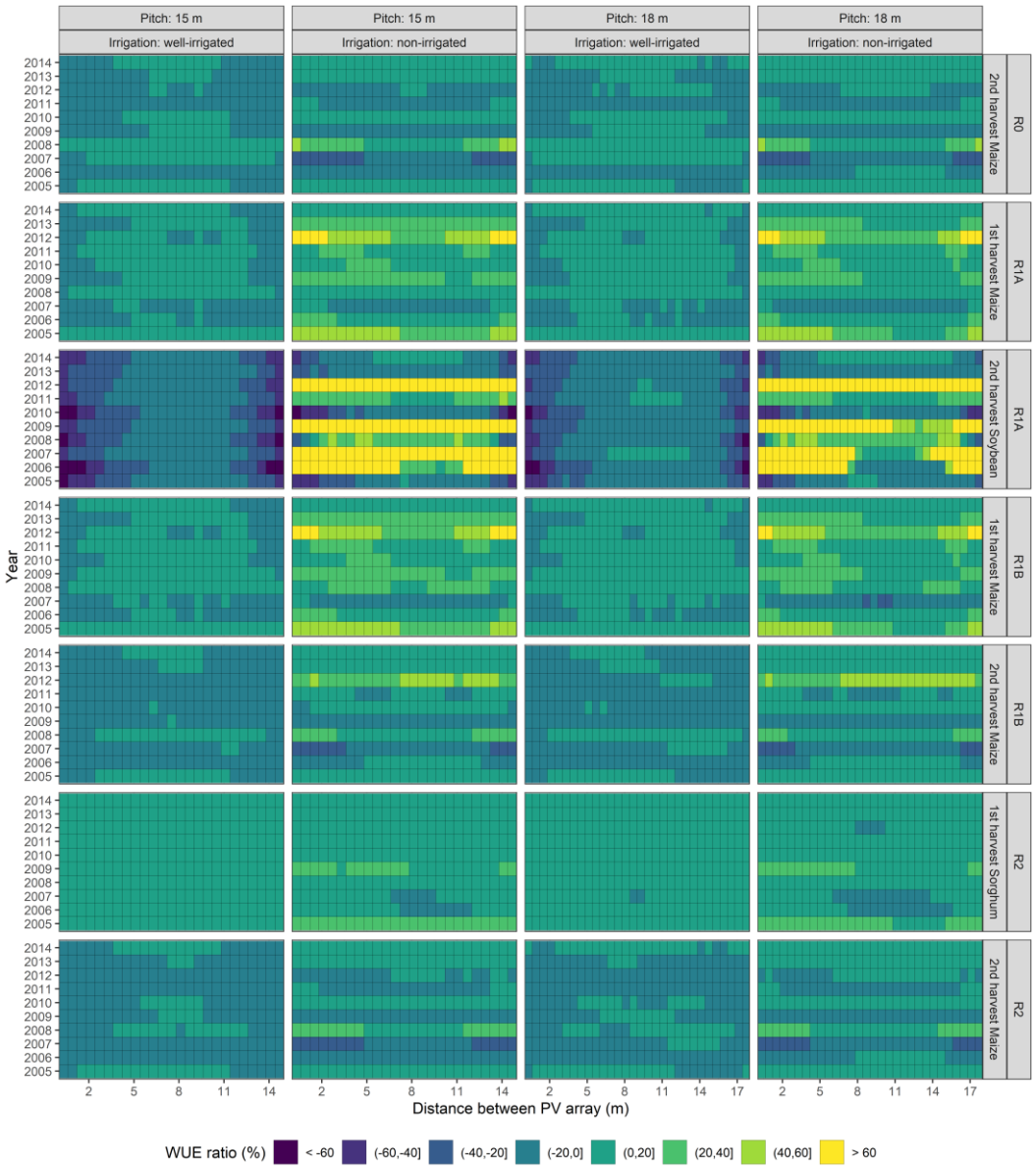

Figure 3-3 Water use efficiency (WUE) ratio (%) variability of the summer crops between different years (2005-2014, y-axis) and position in the APV field (x-axis) according to the different crop rotations, pitch configurations, and irrigation management strategies. WUE ratio in percentage was calculated as the decrease (negative values) or increase (positive values) in the APV condition compared to full light conditions.

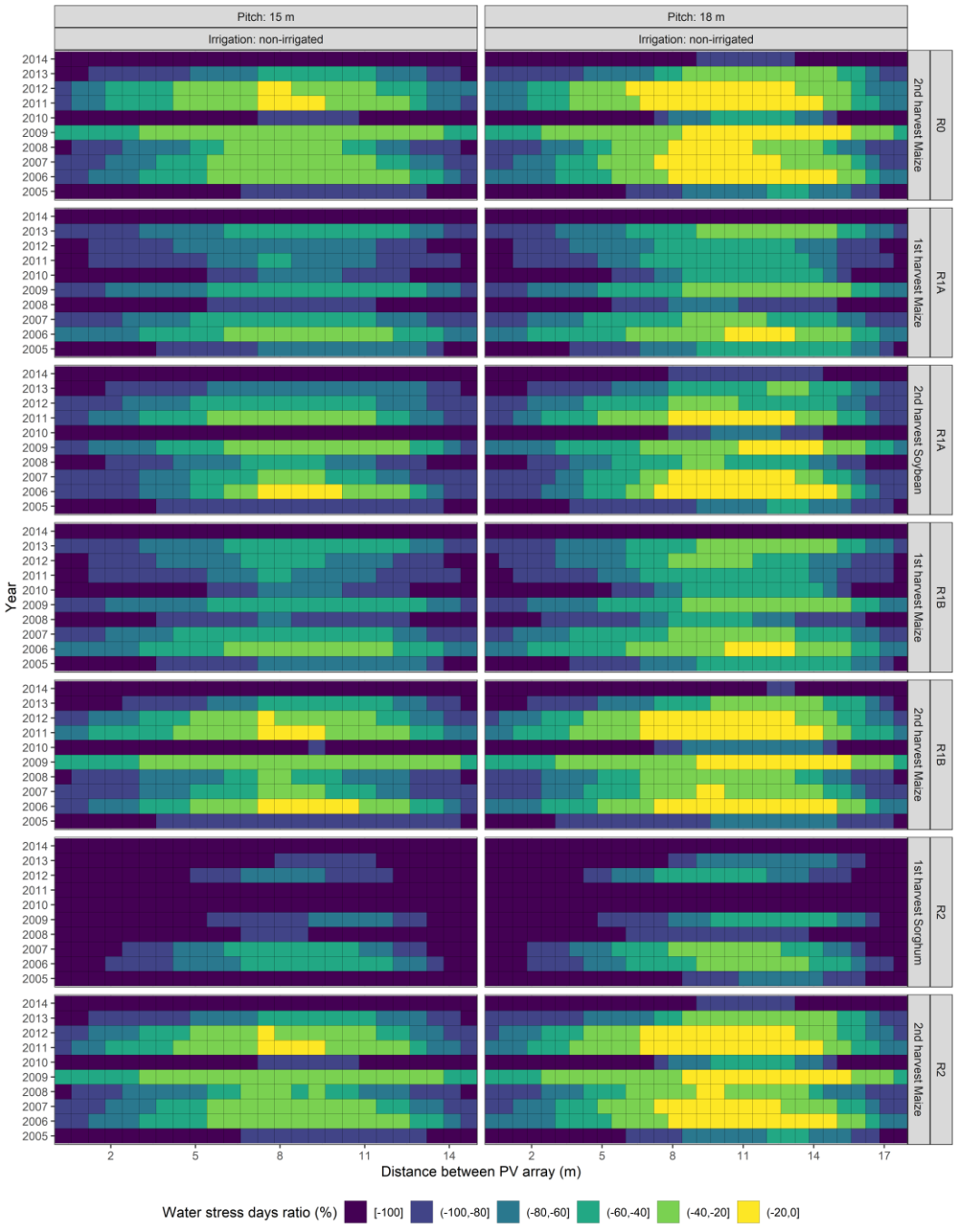

Figure 3-4 Water stress days ratio (%) variability of the summer crops between different years (2005-2014, y-axis) and position in the APV field (x-axis) according to the different crop rotations, pitch configurations, and irrigation management strategies. Water stress days in percentage was calculated as the decrease (negative values) or increase (positive values) in the APV condition compared to full light conditions.

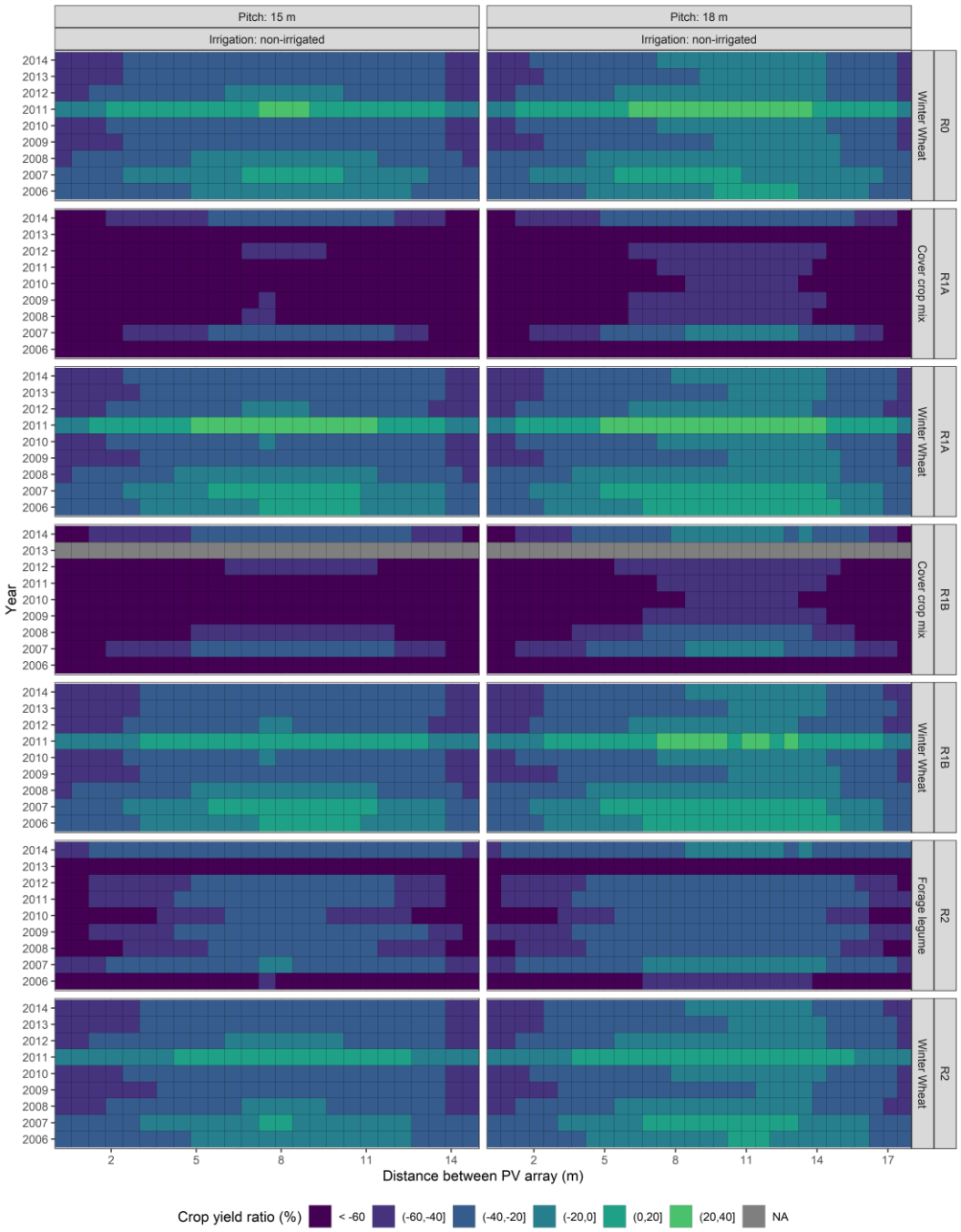

Figure 3-5 Crop yield ratio (%) variability of the winter crops between different years (2005-2014, y-axis) and position in the APV field (x-axis) according to the different crop rotations, pitch configurations, and irrigation management strategies. Crop yield ratio in percentage was calculated as the decrease (negative values) or increase (positive values) in the APV condition compared to full light conditions.

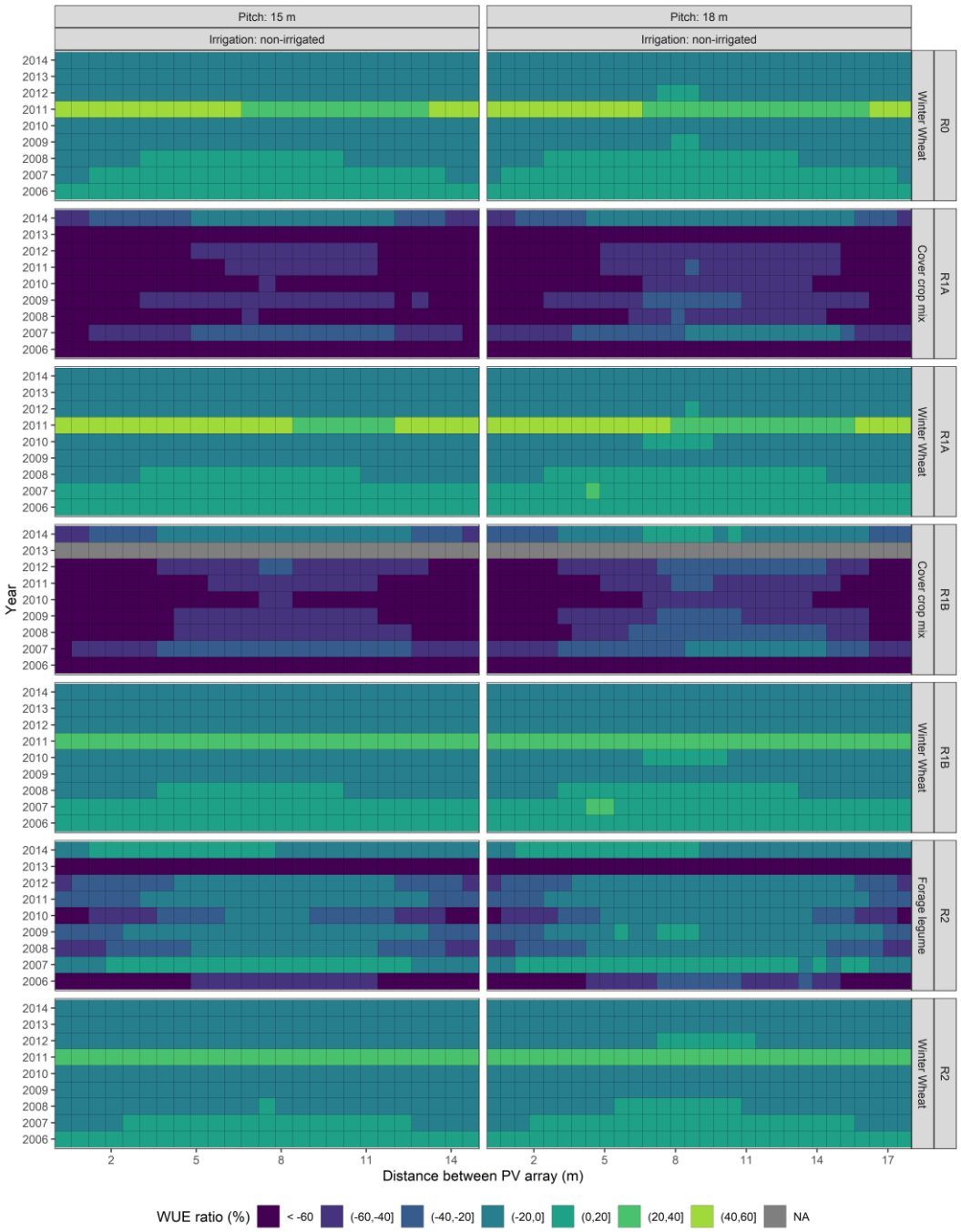

Figure 3-6 Water use efficiency (WUE) ratio (%) variability of the winter crops between different years (2005-2014, y-axis) and position in the APV field (x-axis) according to the different crop rotations, pitch configurations, and irrigation management strategies. WUE ratio in percentage was calculated as the decrease (negative values) or increase (positive values) in the APV condition compared to full light conditions.

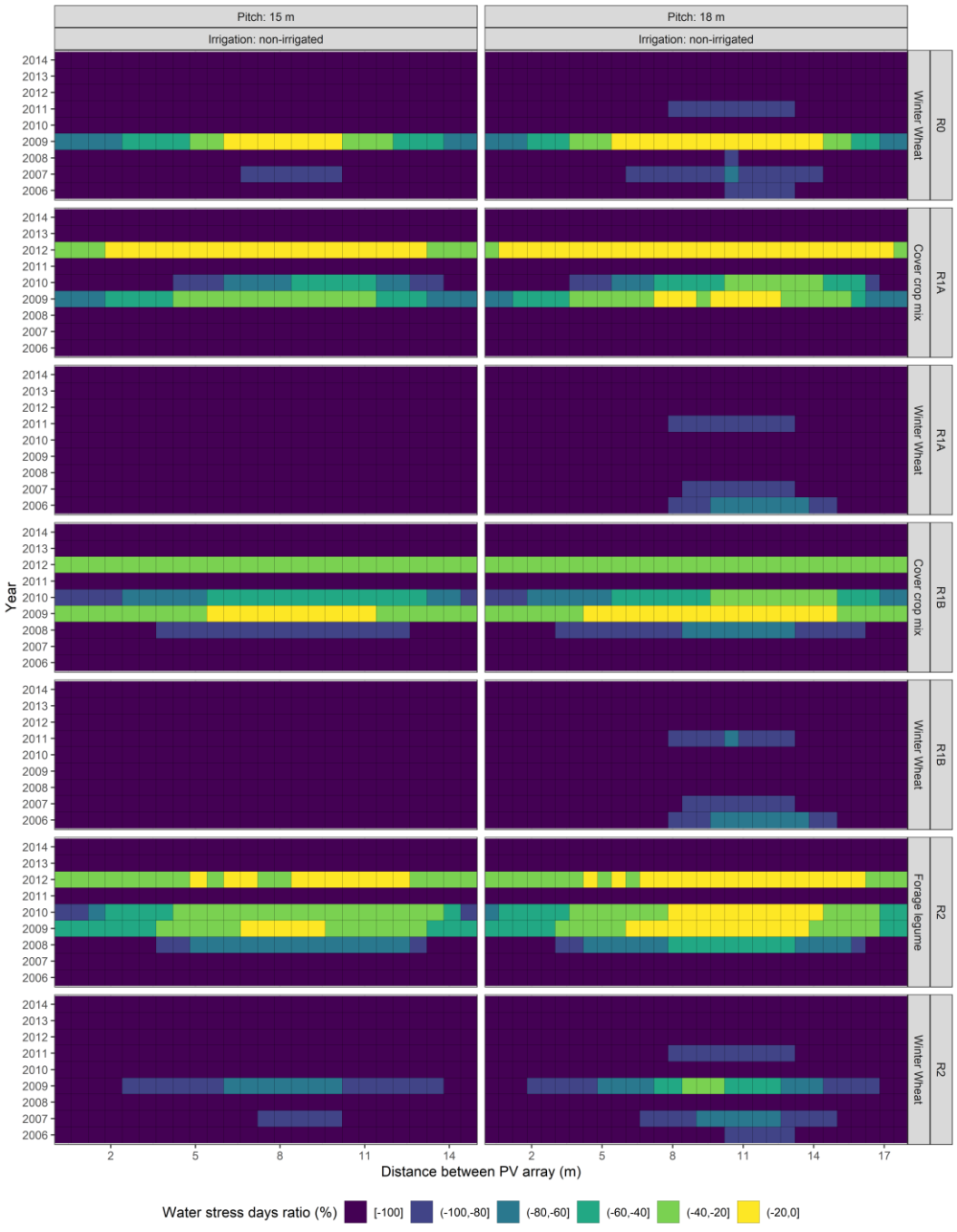

Figure 3-7 Water stress days ratio (%) variability of the winter crops between different years (2005-2014, y-axis) and position in the APV field (x-axis) according to the different crop rotations, pitch configurations, and irrigation management strategies. Water stress days in percentage was calculated as the decrease (negative values) or increase (positive values) in the APV condition compared to full light conditions.

3.3.3 Evaluation of food/feed vs energy dilemma scenarios

To evaluate the food/feed versus energy dilemma, the crop yield biomass was converted into both milk and biomethane production. These conversions were analysed across four scenarios: milk production only (S1), milk and biomethane production (S2), milk and photovoltaic (PV) energy production (S3), and a combination of milk, biomethane, and PV energy production (S4). The outcomes of these scenarios are detailed in Table 3.4. Milk production was measured in liters, while biomethane production was quantified by the equivalent number of kilometers an electric car could travel using the energy produced by a biomethane plant. PV energy production was also expressed in terms of kilometers. PV energy production only with the pitch configurations of the PV arrays. In contrast, the variations in milk and biomethane production were influenced by different crop rotations (R0, R1A, R1B, and R2). These rotations affected the total biomass yield, which in turn determined the potential outputs for both milk and biomethane. In addition, the inclusion of APV system also impacted these outputs. The S1 scenario represented the maximum potential for milk production, serving as a baseline for comparison. The S2 scenario, which includes both milk and biomethane production, was used as a reference to evaluate the food/feed vs energy dilemma, highlighting the trade-offs when crop biomass is allocated to both outputs. Comparing the S2 and S3 scenarios, which include APV systems, the results indicated that the energy produced by the PV plant far exceeded that produced by the biomethane plant. For instance, when comparing S2 to S3 with pitch configurations of 15 m and 18 m, the number of kilometers produced increased in S3 by 14 to 33-fold and 12 to 28-fold, respectively. Additionally, in non-irrigated conditions, milk production was significantly higher in S3 than in S2, due to the beneficial effects of the APV system on crops, such as reduced water stress and improved soil moisture retention. However, in well-irrigated conditions (i.e. when irrigation water was non a limiting factor in the crop model simulation), milk production was higher in S2 than in S3 for crop rotations R1A and R1B. When comparing S2 with S4, the results showed generally higher milk production in S2 under well-irrigated conditions, while similar levels of milk production were observed in non-irrigated conditions. Moreover, the biomethane production in S4 resulted in significantly lower kilometers compared to S2, with an average difference of 111,229 km for a 15 m pitch and 89,461 km for an 18 m pitch. However, PV energy production in S4 was drastically higher, with figures reaching 8,046,666 km for a 15 m pitch and 6,973,333 km for an 18 m pitch. This demonstrates a remarkable increase in resource efficiency and land use, as 1 hectare of APV system can convert the same amount of energy needed to drive the same number of kilometers than approximately 20 hectares dedicated to biomethane production. The comprehensive analysis presented in this study underscores the intricate relationship between agricultural practices and renewable energy integration, particularly in the context of APV systems. The findings highlight the necessity of strategic planning to optimize the balance between food/feed production and energy generation, addressing the critical food versus energy dilemma. The significant differences observed in energy output between biomethane and PV systems point to a marked advantage of PV technology in terms of energy efficiency. Under APV configurations, PV systems demonstrated a substantially higher energy yield compared to biomethane production, with energy outputs expressed in kilometers traveled by an electric car. In contrast, the energy output from biomethane was markedly lower, even when considering the same crop biomass inputs. This discrepancy underscores the potential of APV systems to enhance land use efficiency. By combining agricultural activities with solar energy production, APV systems can generate significant amounts of renewable energy while maintaining agricultural output. The ability to produce energy equivalent to what would be generated from 20 hectares dedicated to biomethane with just 1 hectare of APV installation highlights the efficiency and sustainability of this integrated approach. The results emphasize the need for strategic planning and policy support to maximize the benefits of integrating agriculture with renewable energy systems. Policymakers and

stakeholders should consider the unique advantages of APV systems, including increased land use efficiency, enhanced crop performance, and significant renewable energy production. Policies encouraging the adoption of APV systems could support both sustainable energy goals and agricultural productivity, thereby addressing multiple sustainability targets simultaneously.

Table 35 Estimated production of milk (l), biomethane (km), and PV (km) for the four scenarios (S1-S4) according to the different pitch (m), irrigation strategies (well-irrigated, non-irrigated), and crop rotations (R0, R1A, R1B, and R2). The four scenarios were: S1) Milk production only, S2) Milk production and biomethane production, S3) Milk production and photovoltaic (PV) energy production, S4) Milk production, biomethane production, and PV energy production.

Scenario	Pitch (m)	Product	R0		R1A		R1B		R2	
			well-irrigated	non-irrigated	well-irrigated	non-irrigated	well-irrigated	non-irrigated	well-irrigated	non-irrigated
S1		milk (l)	100,864	66,500	74,705	45,614	93,705	56,886	93,602	64,762
S2		milk (l)	66,682	32,318	53,614	24,523	72,614	35,795	38,966	21,171
		biomethane (km)	399,255	399,255	246,349	246,349	246,349	246,349	590,387	475,708
S3	15	milk (l)	66,546	56,318	44,978	37,956	59,251	49,842	59,683	53,546
		PV (km)	8,046,666	8,046,666	8,046,666	8,046,666	8,046,666	8,046,666	8,046,666	8,046,666
	18	milk (l)	72,818	58,910	50,057	39,625	65,000	51,500	65,250	56,251
		PV (km)	6,973,333	6,973,333	6,973,333	6,973,333	6,973,333	6,973,333	6,973,333	6,973,333
S4	15	milk (l)	42,546	32,318	31,341	24,319	45,614	36,205	23,978	18,864
		biomethane (km)	280,328	280,328	159,277	159,277	159,277	159,277	386,513	375,894
		PV (km)	8,046,666	8,046,666	8,046,666	8,046,666	8,046,666	8,046,666	8,046,666	8,046,666
	18	milk (l)	46,636	32,728	35,148	24,716	49,909	36,409	26,409	19,455
		biomethane (km)	305,812	305,812	174,143	176,267	176,267	176,267	420,492	399,255
		PV (km)	6,973,333	6,973,333	6,973,333	6,973,333	6,973,333	6,973,333	6,973,333	6,973,333

3.4 Conclusion

This study provides a comprehensive evaluation of the interplay between agricultural productivity and renewable energy generation within agrivoltaic (APV) systems, focusing on key performance indicators (KPIs) such as crop yield, water use efficiency (WUE), and water stress days. The findings reveal significant variations in agricultural output under different pitch configurations and irrigation strategies, emphasizing the influence of shading on crop performance. Notably, APV systems demonstrated a substantial potential to enhance land use efficiency by producing both food/feed and energy on the same land area, with PV systems significantly outperforming biomethane production in terms of energy yield. The analysis of crop yield under well-irrigated and non-irrigated conditions indicated that while certain crops like soybeans experienced reduced yields under APV conditions, others such as maize and sorghum showed resilience, particularly in water-limited scenarios. This variability underscores the importance of selecting appropriate crops and management practices to maximize the benefits of APV systems. Additionally, the study highlighted the critical role of strategic planning in optimizing APV layouts to balance agricultural output with renewable energy production, especially given the observed differences in performance across different crop rotations and irrigation levels. In terms of the food/feed versus energy

dilemma, the study found that integrating PV systems with agriculture (scenarios S3 and S4) provided a markedly higher energy output compared to biomethane production alone (scenario S2). This finding suggests that PV technology, particularly when implemented in APV configurations, offers a more efficient and sustainable solution for meeting energy demands without significantly compromising agricultural productivity. The potential to generate renewable energy equivalent to what would be produced on a much larger area dedicated solely to biomethane production further underscores the land use efficiency of APV systems. The results of this study have important implications for policy and decision-making. The demonstrated benefits of APV systems, including increased resource efficiency, enhanced crop resilience to water stress, and significant renewable energy generation, make a strong case for the promotion of such integrated systems. Policymakers and stakeholders are encouraged to consider the adoption of APV technologies as a strategy to simultaneously achieve food security, sustainable agriculture, and renewable energy goals. This integrated approach not only addresses multiple sustainability targets but also offers a pathway toward more resilient and efficient land use practices in the face of growing environmental and resource challenges.

3.5 References

Abrahamsen, P., & Hansen, S. (2000). Daisy: an open soil-crop-atmosphere system model. *Environmental Modelling and Software*, *15*(3), 313-330. https://doi.org/10.1016/S1364-8152(00)00003-7

Al Mamun, M. A., Garba, I. I., Campbell, S., Dargusch, P., deVoil, P., & Aziz, A. A. (2023). Biomass production of a sub-tropical grass under different photovoltaic installations using different grazing strategies. *Agricultural Systems*, *208*, 103662. https://doi.org/10.1016/j.agsy.2023.103662

Amaducci, S., Yin, X., & Colauzzi, M. (2018). Agrivoltaic systems to optimise land use for electric energy production. *Applied Energy*, *220*, 545-561. https://doi.org/10.1016/j.apenergy.2018.03.081

Angelidaki, I., Treu, L., Tsapekos, P., Luo, G., Campanaro, S., Wenzel, H., & Kougias, P. G. (2018). Biogas upgrading and utilization: Current status and perspectives. *Biotechnology Advances*, *36*(2), 452-466. https://doi.org/10.1016/j.biotechadv.2018.01.011

Asseng, S., Zhu, Y., Basso, B., Wilson, T., & Cammarano, D. (2014). Simulation Modeling: Applications in Cropping Systems. In *Encyclopedia of Agriculture and Food Systems* (pp. 102-112). Elsevier. https://doi.org/10.1016/B978-0-444-52512-3.00233-3

Baccioli, A., Antonelli, M., Frigo, S., Desideri, U., & Pasini, G. (2018). Small scale bio-LNG plant: Comparison of different biogas upgrading techniques. *Applied Energy*, *217*, 328-335. https://doi.org/10.1016/j.apenergy.2018.02.149

Barron-Gafford, G. A., Pavao-Zuckerman, M. A., Minor, R. L., Sutter, L. F., Barnett-Moreno, I., Blackett, D. T., Thompson, M., Dimond, K., Gerlak, A. K., Nabhan, G. P., & Macknick, J. E. (2019). Agrivoltaics provide mutual benefits across the food-energy-water nexus in drylands. *Nature Sustainability*, *2*(9), 848-855. https://doi.org/10.1038/s41893-019-0364-5

Battini, F., Agostini, A., Boulamanti, A. K., Giuntoli, J., & Amaducci, S. (2014). Mitigating the environmental impacts of milk production via anaerobic digestion of manure: Case study of a dairy farm in the Po Valley. *Science of The Total Environment*, *481*, 196-208. https://doi.org/10.1016/j.scitotenv.2014.02.038

Bauer, F., Persson, T., Hulteberg, C., & Tamm, D. (2013). Biogas upgrading – technology overview, comparison and perspectives for the future. *Biofuels, Bioproducts and Biorefining*, *7*(5), 499-511. https://doi.org/10.1002/bbb.1423

Bellone, Y., Croci, M., Impollonia, G., Nik Zad, A., Colauzzi, M., Campana, P. E., & Amaducci, S. (2024). Simulation-Based Decision Support for Agrivoltaic Systems. *Applied Energy*, *369*, 123490. https://doi.org/10.1016/j.apenergy.2024.123490

Bhattarai, B., Singh, S., West, C. P., Ritchie, G. L., & Trostle, C. L. (2020). Effect of deficit irrigation on physiology and forage yield of forage sorghum, pearl millet, and corn. *Crop Science*, *60*(4), 2167–2179. https://doi.org/10.1002/csc2.20171

Biavetti, I., Karetsos, S., Ceglar, A., Toreti, A., & Panagos, P. (2014). *European meteorological data: contribution to research, development, and policy support* (D. G. Hadjimitsis, K. Themistocleous, S. Michaelides, & G. Papadavid, Eds.; p. 922907). https://doi.org/10.1117/12.2066286

Bortoluzzi, G., Gatti, M., Sogni, A., & Consonni, S. (2014). Biomethane production from agricultural resources in the Italian scenario: techno-economic analysis of water wash. *CHEMICAL ENGINEERING TRANSACTIONS*, *37*.

Campana, P. E., Stridh, B., Amaducci, S., & Colauzzi, M. (2021). Optimisation of vertically mounted agrivoltaic systems. *Journal of Cleaner Production*, *325*, 129091. https://doi.org/10.1016/j.jclepro.2021.129091

Carfora, A., Pansini, R. V., Romano, A. A., & Scandurra, G. (2018). Renewable energy development and green public policies complementarities: The case of developed and developing countries. *Renewable Energy*, *115*, 741–749. https://doi.org/10.1016/j.renene.2017.09.008

Dal Prà, A., Miglietta, F., Genesio, L., Lanini, G. M., Bozzi, R., Morè, N., Greco, A., & Fabbri, M. C. (2024). Determination of feed yield and quality parameters of whole crop durum wheat (Triticum durum Desf.) biomass under agrivoltaic system. *Agroforestry Systems*. https://doi.org/10.1007/s10457-024-00979-8

Dale, B. E., Sibilla, F., Fabbri, C., Pezzaglia, M., Pecorino, B., Veggia, E., Baronchelli, A., Gattoni, P., & Bozzetto, S. (2016). Biogasdoneright™: An innovative new system is commercialized in Italy. *Biofuels, Bioproducts and Biorefining*, *10*(4), 341–345. https://doi.org/10.1002/bbb.1671

Dupraz, C. (2023). Assessment of the ground coverage ratio of agrivoltaic systems as a proxy for potential crop productivity. *Agroforestry Systems*. https://doi.org/10.1007/s10457-023-00906-3

Dupraz, C., Marrou, H., Talbot, G., Dufour, L., Nogier, A., & Ferard, Y. (2011). Combining solar photovoltaic panels and food crops for optimising land use: Towards new agrivoltaic schemes. *Renewable Energy*, *36*(10), 2725–2732. https://doi.org/10.1016/j.renene.2011.03.005

Early, E. B., McIlrath, W. O., Seif, R. D., & Hageman, R. H. (1967). Effects of Shade Applied at Different Stages of Plant Development on Corn (*Zea mays* L.) Production [1]. *Crop Science*, *7*(2), 151–156. https://doi.org/10.2135/cropsci1967.0011183X000700020018x

Egli, D. B., & Bruening, W. P. (2005). Shade and Temporal Distribution of Pod Production and Pod Set in Soybean. *Crop Science*, *45*(5), 1764–1769. https://doi.org/10.2135/cropsci2004.0557

Elamri, Y., Cheviron, B., Lopez, J.-M., Dejean, C., & Belaud, G. (2018). Water budget and crop modelling for agrivoltaic systems: Application to irrigated lettuces. *Agricultural Water Management*, *208*, 440–453. https://doi.org/10.1016/j.agwat.2018.07.001

Estrada-Campuzano, G., Miralles, D. J., & Slafer, G. A. (2008). Yield determination in triticale as affected by radiation in different development phases. *European Journal of Agronomy*, *28*(4), 597–605. https://doi.org/10.1016/j.eja.2008.01.003

FAO. (2010). *Greenhouse Gas Emissions from the Dairy Sector A Life Cycle Assessment*. http://www.foodsec.org/docs/GAUL_DISCLAIMER.pdf

Ghisellini, P., Protano, G., Viglia, S., Gaworski, M., Setti, M., & Ulgiati, S. (2014). Journal of Environmental Accounting and Management Integrated Agricultural and Dairy Production within a Circular Economy Framework. A Comparison of Italian and Polish Farming Systems. *Journal of*

Environmental Accounting and Management, *2*(4), 372-391. https://doi.org/10.5890/JEAM.2014.10.007

Hansen, S., & Abrahamsen, P. (2009). Modeling Water and Nitrogen Uptake Using a Single-Root Concept: Exemplified by the Use in the Daisy Model. In *Quantifying and Understanding Plant Nitrogen Uptake for Systems Modeling*.

Healey, K. D., Hammer, G. L., Rickert, K. G., & Bange, M. P. (1998). Radiation use efficiency increases when the diffuse component of incident radiation is enhanced under shade. *Australian Journal of Agricultural Research*, *49*(4), 665. https://doi.org/10.1071/A97100

Katsikogiannis, O. A., Ziar, H., & Isabella, O. (2022). Integration of bifacial photovoltaics in agrivoltaic systems: A synergistic design approach. *Applied Energy*, *309*, 118475. https://doi.org/10.1016/j.apenergy.2021.118475

Ko, J., Cho, J., Choi, J., Yoon, C.-Y., An, K.-N., Ban, J.-O., & Kim, D.-K. (2021). Simulation of Crop Yields Grown under Agro-Photovoltaic Panels: A Case Study in Chonnam Province, South Korea. *Energies*, *14*(24), 8463. https://doi.org/10.3390/en14248463

Laub, M., Pataczek, L., Feuerbacher, A., Zikeli, S., & Högy, P. (2022). Contrasting yield responses at varying levels of shade suggest different suitability of crops for dual land-use systems: a meta-analysis. *Agronomy for Sustainable Development*, *42*(3), 51. https://doi.org/10.1007/s13593-022-00783-7

Loomis, R. S., & Connor, D. J. (1992). *Crop Ecology*. Cambridge University Press. https://doi.org/10.1017/CBO9781139170161

Miltner, M., Makaruk, A., & Harasek, M. (2017). Review on available biogas upgrading technologies and innovations towards advanced solutions. *Journal of Cleaner Production*, *161*, 1329-1337. https://doi.org/10.1016/j.jclepro.2017.06.045

Mu, H., Jiang, D., Wollenweber, B., Dai, T., Jing, Q., & Cao, W. (2010). Long-term Low Radiation Decreases Leaf Photosynthesis, Photochemical Efficiency and Grain Yield in Winter Wheat. *Journal of Agronomy and Crop Science*, *196*(1), 38-47. https://doi.org/10.1111/j.1439-037X.2009.00394.x

Murano, R., Maisano, N., Selvaggi, R., Pappalardo, G., & Pecorino, B. (2021). Critical Issues and Opportunities for Producing Biomethane in Italy. *Energies*, *14*(9), 2431. https://doi.org/10.3390/en14092431

Otegui, M. E., & Bonhomme, R. (1998). Grain yield components in maize. *Field Crops Research*, *56*(3), 247-256. https://doi.org/10.1016/S0378-4290(97)00093-2

Patrizio, P., & Chinese, D. (2016). The impact of regional factors and new bio-methane incentive schemes on the structure, profitability and CO2 balance of biogas plants in Italy. *Renewable Energy*, *99*, 573-583. https://doi.org/10.1016/j.renene.2016.07.047

Potenza, E., Croci, M., Colauzzi, M., & Amaducci, S. (2022). Agrivoltaic System and Modelling Simulation: A Case Study of Soybean (Glycine max L.) in Italy. *Horticulturae*, *8*(12), 1160. https://doi.org/10.3390/horticulturae8121160

Prakash, V., Lunagaria, M. M., Trivedi, A. P., Upadhyaya, A., Kumar, R., Das, A., Kumar Gupta, A., & Kumar, Y. (2023). Shading and PAR under different density agrivoltaic systems, their simulation and effect on wheat productivity. *European Journal of Agronomy*, *149*, 126922. https://doi.org/10.1016/j.eja.2023.126922

Ramos-Fuentes, I. A., Elamri, Y., Cheviron, B., Dejean, C., Belaud, G., & Fumey, D. (2023). Effects of shade and deficit irrigation on maize growth and development in fixed and dynamic AgriVoltaic systems. *Agricultural Water Management*, *280*, 108187. https://doi.org/10.1016/j.agwat.2023.108187

Sánchez Nocete, E., & Pérez Rodríguez, J. (2022). A Simple Methodology for Estimating the Potential Biomethane Production in a Region: Application in a Case Study. In Sustainability (Vol. 14, Issue 23, p. 15978). MDPI AG. https://doi.org/10.3390/su142315978

S. Hansen, P. Abrahamsen, C. T. Petersen, & M. Styczen. (2012). Daisy: Model Use, Calibration, and Validation. *Transactions of the ASABE*, *55*(4), 1317-1335. https://doi.org/10.13031/2013.42244

Schweiger, A. H., & Pataczek, L. (2023). How to reconcile renewable energy and agricultural production in a drying world. *PLANTS, PEOPLE, PLANET*, *5*(5), 650-661. https://doi.org/10.1002/ppp3.10371

Trommsdorff, M., Kang, J., Reise, C., Schindele, S., Bopp, G., Ehmann, A., Weselek, A., Högy, P., & Obergfell, T. (2021). Combining food and energy production: Design of an agrivoltaic system applied in arable and vegetable farming in Germany. *Renewable and Sustainable Energy Reviews*, *140*, 110694. https://doi.org/10.1016/j.rser.2020.110694

Weselek, A., Bauerle, A., Hartung, J., Zikeli, S., Lewandowski, I., & Högy, P. (2021). Agrivoltaic system impacts on microclimate and yield of different crops within an organic crop rotation in a temperate climate. *Agronomy for Sustainable Development*, *41*(5), 59. https://doi.org/10.1007/s13593-021-00714-y

Yao, W., Li, Z., Xiu, T., Lu, Y., & Li, X. (2015). New decomposition models to estimate hourly global solar radiation from the daily value. *Solar Energy*, *120*, 87-99. https://doi.org/10.1016/j.solener.2015.05.038

4 SIMULATION IN DENMARK

In our previous study conducted in Italy, the integration of a vertical bifacial APV system, the power grid, and a biogas boiler (Scenario 7) was identified as the optimal configuration. This system achieved the highest LCR-to-LCC ratio, minimizing costs while maximizing revenue from $BioCH_4$ production. This study applies the optimal Italian scenario to Denmark, evaluating its technical and economic feasibility under Danish conditions. However, the performance of integrated APV-biogas systems depends heavily on region-specific conditions such as solar availability, energy costs, and plant size.

4.1.1 *Description of the site and load profile*

The thermophilic AD plant on the Aarhus University (AU) campus in Foulum, Denmark, maintains a steady operating temperature of 51°C. Utilizing site-specific data, the facility produces approximately 4,246 Nm^3 of biogas daily, amounting to an annual output of 1,550,000 Nm^3. The methane content of the biogas is 53%, resulting in a daily production of 2,250.7 Nm^3 of $BioCH_4$ and an annual $BioCH_4$ yield of 821,500 Nm^3.

The facility's annual heat demand is 960,350 kWh_{th} in 2023. Monthly heat demand values are provided in Table 36, while Figure 4.1 presents the data with hourly resolution.

Table 36 Monthly heat requirement of the bioCH4 production plant in Foulum in 2023.

Month	Thermal power (kW_{th})	Heat demand (MWh_{th})
January	147.88	110023
February	137.61	92476
March	127.26	94684
April	113.52	81733
May	96.30	71644
June	82.55	59437
July	72.20	53718
August	75.68	56305
September	86.03	61941
October	103.17	76757
November	130.74	94133
December	144.49	107497
Total	**1317.43**	**960350**

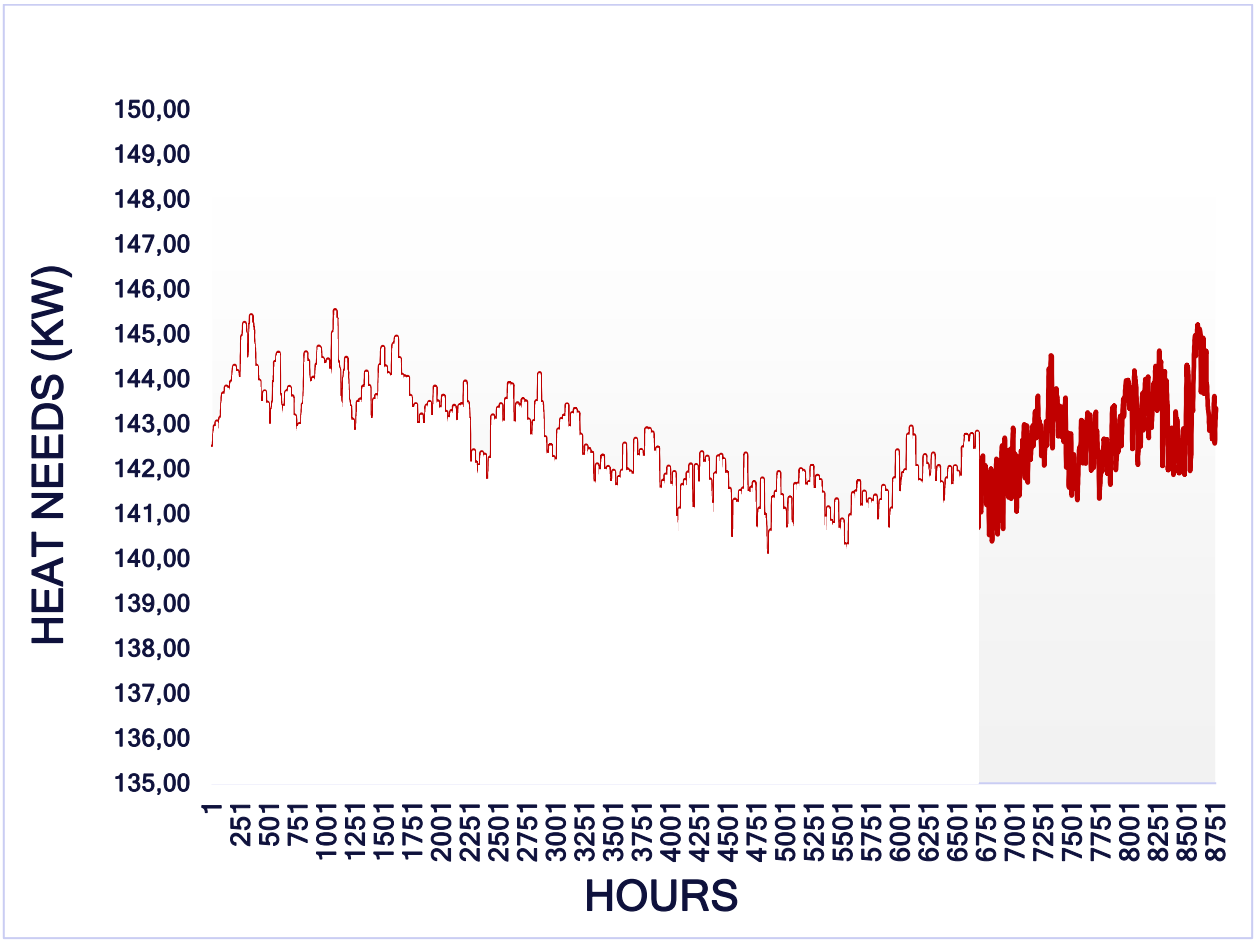

Figure 4-1 Hourly heat requirements of Danish case study AD plant.

The plant's annual electricity consumption is 877,703 kWh_{el}, equivalent to a daily usage of 2,404 kWh in 2023. On average, the facility has a fixed electrical demand of 100.2 kW_{el}, which supports the upgrading plant, compression stages, biological processes, and auxiliary equipment. Additionally, the electricity requirements for the biogas boiler's control electronics, motor starter, and sensors, based on heat demand and system controller usage, have been calculated. These values, detailed in Table 37, are integrated into the plant's overall electrical demand.

Table 37 The monthly dynamic electrical needs of the biogas boiler for Danish case study.

Month	Electrical needs (kW)	Electrical consumption (MWh)
January	2.22	1.65
February	2.06	1.38
March	1.91	1.42
April	1.7	1.22
May	1.44	1.07
June	1.24	0.89
July	1.08	0.80
August	1.14	0.85
September	1.29	0.93
October	1.55	1.15
November	1.96	1.41
December	2.17	1.61
Year	**1.65**	**14.4**

Figure 4.2 illustrates the hourly electrical requirements of the Danish BioCH_4 production facility case study, incorporating both fixed and variable (i.e. biogas boiler) electrical loads.

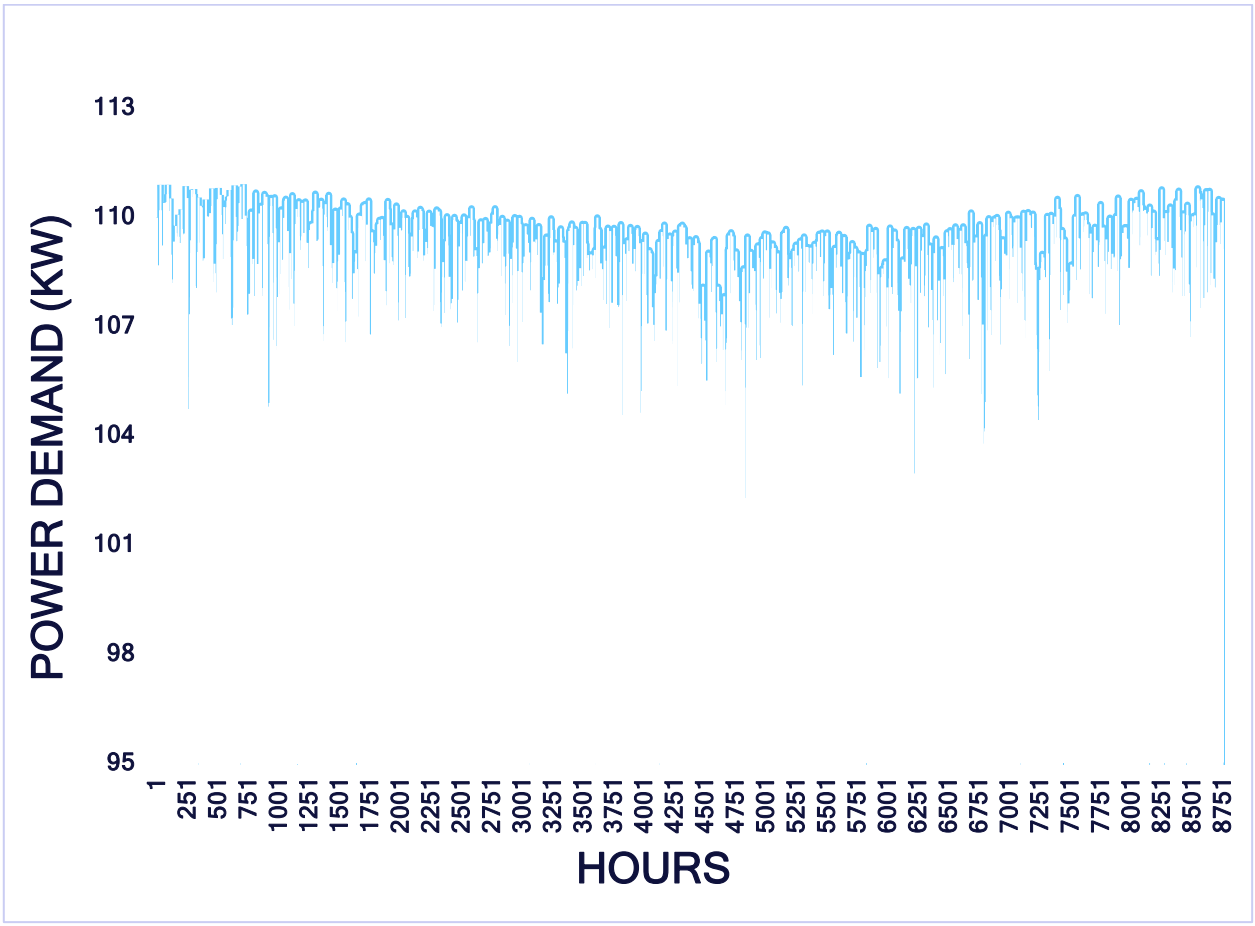

Figure 4-2 Hourly electrical requirements of Danish case study.

4.1.2 *Biogas consumption of heat producer*

It should be noted that, considering the boiler's 85% efficiency, a lower heating value of 5.3 kWh/Nm³ for biogas in this case study, and the plant's hourly heat demand, the boiler requires 213,227 Nm³ of biogas per year to fulfil the total heat demand. The hourly biogas consumption by the boiler is illustrated in Figure 4.3.

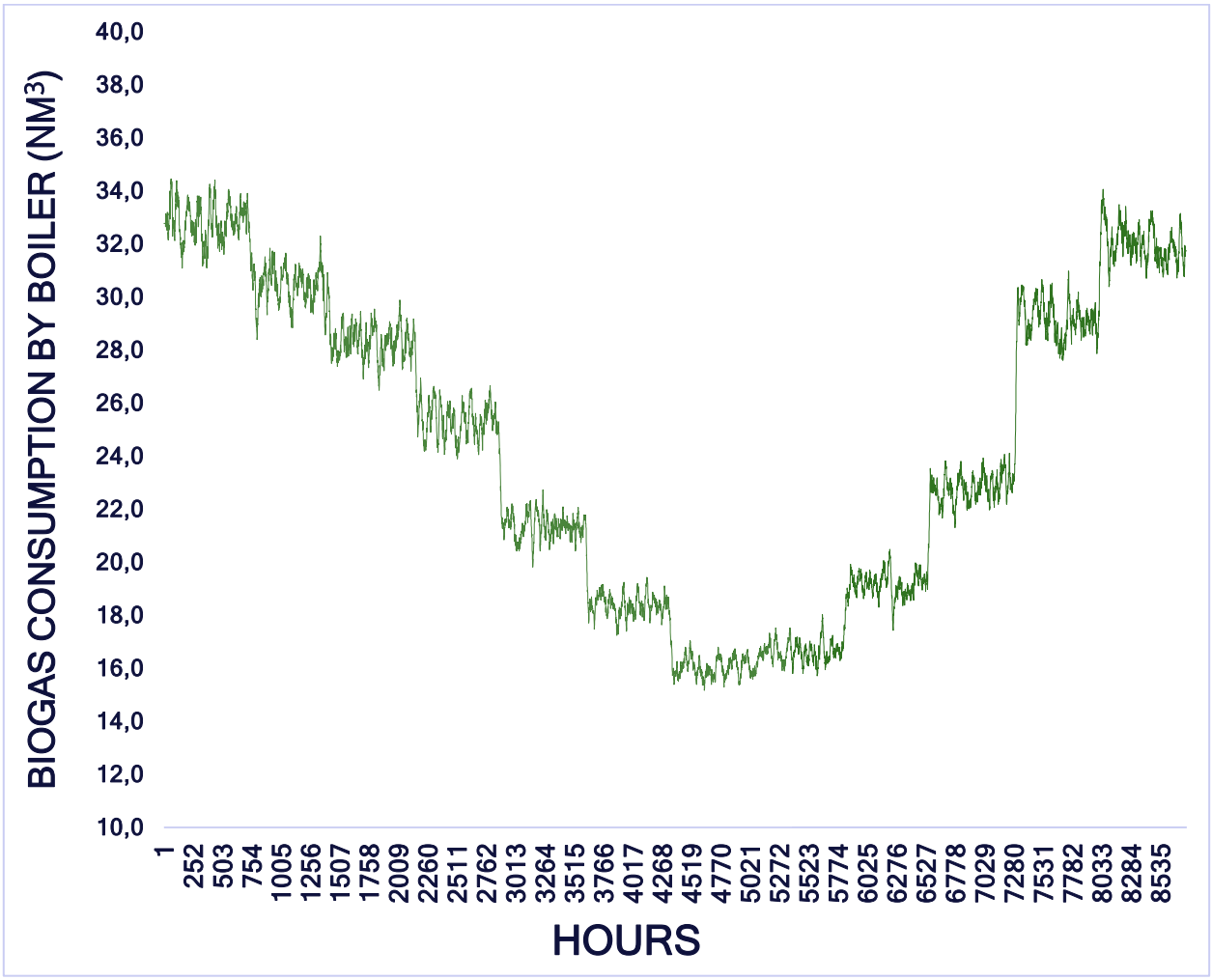

Figure 4-3 The hourly biogas consumption by boiler for Danish case study.

While the annual biogas production is 1,550,000 Nm³, leaving 1,336,773 Nm³ of biogas available. Considering the methane content of 53%, this translates to 708,490 Nm³ of bioCH_4 produced in the plant, which is a key figure for the economic analysis.

4.1.3 Electricity production by APV system

A vertical bifacial APV system with a capacity of 44.4 kW_p is installed at the Aarhus University (AU) campus in Foulum, as illustrated in Figure 4.4.

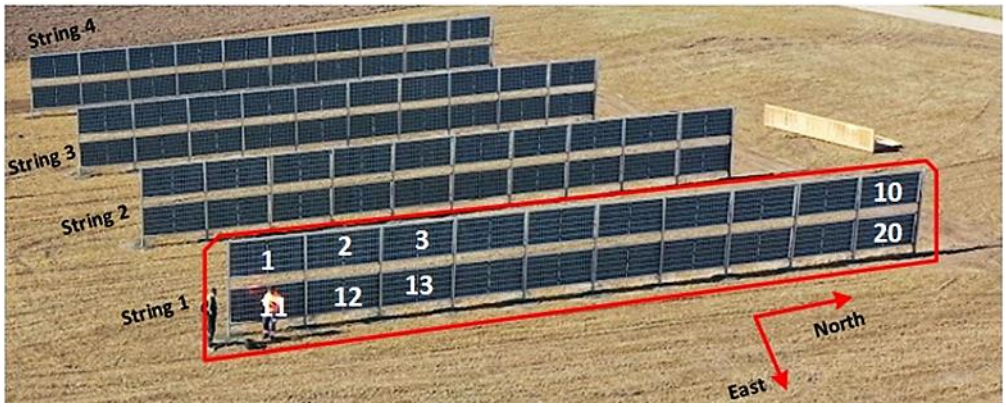

Figure 4-4 The bifacial vertical APV system setup on Arhus University (AU) campus in Foulum.

The system features PV panels arranged with the backside facing east and the front side facing west. It comprises four PV strings, each with a pitch of 11 meters, containing 20 series-connected PV panels in a landscape orientation. Detailed technical specifications for this system are provided in Table 38.

Table 38 Input data for simulation of energy output from vertical bifacial APV system for Danish case study.

Parameters	Specifications
Location	Foulum, Denmark (56.4966° N, 9.5843° E)
Meteorological data	Year 2023 (TMY)
Albedo factor	0.25
Clearance for Vertical mounting system	0.7 m
Orientation and tilt angle	West/90°
PV array layout	2-Landscape (Vertical)
PV module	Jolywood, JW-HD144N
PV module nominal capacity	555Wp
PV Efficiency	21.42%
Bifaciality factor	75%
Nominal operation module temperature	42°C (±2°C)
Temperature co-efficient for P_{max}	- 0.32%/°C
Number of cells	144 (12×12)
PV module dimension	2285mm×1134mm×30mm
Number of PV panels per string	20
Number of PV panels per inverter	80
Inverter	SUN2000-40KTL
Inverter Euro.Efficiency	97.5 %
Pitch between PV strings for vertical system	11m

Since hourly electricity production data per unit (per kW) for this system is not available, the APV system was modelled using PVsyst® software. The simulation utilized the specifications in Table 38 and satellite-based meteorological data for the Foulum location in 2023, generating results on an hourly scale. Similar to Italian case study APV sizing procedure, in Danish case study, an iterative process using the Excel Solver Tool is conducted to determine the optimal size of the APV systems. The iteration is based on the assumption that each APV system must supply at least 25% of the total electrical demand as a lower bound constraint. The upper bound is defined where a significant change in the electricity supply ratio by APV (ER_{APV}) is observed. Any additional electrical demand beyond this upper limit is assumed to be met by the power grid while any surplus electricity generated is injected back into the grid. The calculation procedure follows the same approach as previously described in Section 2.2.5.4.

4.1.4 Economic modelling Inputs

Economic assessments are highly sensitive to regional factors, such as energy prices, CAPEX costs, and market conditions. In the Danish case study, these variations, along with $BioCH_4$ market prices, play a pivotal role in shaping the outcomes of the LCR-to-LCC analysis. In Denmark, the costs per kWh for drawing electricity from the grid and feed-in-tariff in Denmark were set at 0.1944 €/kWh and 0.04 €/kWh, respectively (European Commission, 2022; Martín et al., 2021). The average revenue from $BioCH_4$ sales in Denmark is estimated at 0.725 €/Nm³ (Lawson et al., 2021). Additionally, an average inflation rate of 1.2% and a discount rate of 4% were applied, reflecting the economic conditions in Denmark (Micheli et al., 2024). In this case study, the project lifetime, as well as the lifespan of the PV modules, solar inverter, and biogas boiler, are assumed to be identical to those in the Italian case study. Details of the other cost items considered are presented in Table 39.

Table 39 The CAPEX and OPEX assumed for Danish case study (Campana et al., 2024; Taramasso et al., 2024; European Commission, 2022).

Components	CAPEX (€)	OPEX (€)
Bifacial Vertical APV (2L layout)	940/kW_p	0.01 × CAPEX
Inverter replacement costs	-	55/kW_p
Biogas boiler	270/kW_{th}	0.063 × CAPEX
Land lease cost in 2022	-	561€/ha/year

Additionally, the vertical bifacial APV system, featuring a two-landscape PV panel layout, occupies 26.2 m² per 11-meter pitch, as reported by Bellone et al. (2024).

4.1.5 Results and discussion

In this section, the various sizes of the vertical bifacial APV system with an 11-meter pitch, determined based on different ER levels using the Excel Solver Tool which previously described, along with the corresponding land occupation for each size, are presented in Table 40.

Table 40 The sizing and land occupation results of vertical bifacial APV system at various ER levels by Excel Solver tool for Danish case study.

ER_{APV}	Bifacial vertical APV capacity
25%	217 kW_p
Land use (ha)	0.57
30%	304 kW_p
Land use (ha)	0.80
35%	506 kW_p
Land use (ha)	1.33
40%	1.24 MW_p
Land use (ha)	3.25
45%	10.07 MW_p
50%	Infinite

The total electricity purchased from the grid and the total electricity sold to the grid for Danish case study are presented in Table 41, covering ER levels from 25% to 40%.

Table 41 The total electricity purchased and sold of the Danish case study at various ER levels.

	BF(1) vertical APV capacity	
ER_{APV}	TEP(2) (€)	TES(3) (€)
25%	26320	3734
30%	24565	13812
35%	22814	48497
40%	21060	196961

(1) BF: Bifacial, (2) TEP: Total electricity purchased, (3) TES: Total electricity sales

Table 42 shows the economic outcomes for Danish case study, evaluating the life cycle cost (LCC), life cycle revenue (LCR), and the revenue-to-cost ratio for each system configuration throughout the project's duration. The analysis considers different levels of electricity reliability (ER) rates.

Table 42 The economic analysis results for Danish case study (land lease cost included).

	BF Vertical APV system			
	ER_{APV} 25%	ER_{APV} 30%	ER_{APV} 35%	ER_{APV} 40%
LCC (M€)	6.30	6.23	6.62	8.62
LCR (M€)	95.71	97.57	103.99	131.47
LCR/LCC	15.20	15.66	15.72	15.25

In the Danish case study for the vertical bifacial APV system, the total revenue-to-cost ratio reaches its peak at an Electricity Reliability (ER) of 35% before declining at ER 40%. This suggests that ER 35% is the most optimal level for this mounting system.

The decline beyond ER 35% is primarily due to a sharp increase in land lease costs. While a higher APV capacity at ER 40% (1.24 MW_p) represents a 145% increase compared to ER 35% (506 kWp, Table 40), this results in reduced grid electricity purchases by 7.7% (€21,060 vs. €22,814, Table 41) and significantly higher electricity sales, increasing by 306% (€196,961 vs. €48,497). However, this higher capacity also requires 3.25 hectares of land, which is 144% more than the 1.33 hectares used at ER 35%. Consequently, the Life Cycle Cost (LCC) increases by 30% (€8.62 million vs. €6.62 million), and although the Life Cycle Revenue (LCR) also increases by 26.4% (€131.47 million vs. €103.99 million), the higher costs reduce overall cost-effectiveness.

4.1.6 Conclusion

This study applied the optimal configuration of a vertical bifacial agrivoltaic (APV) system integrated with a biogas boiler and power grid, originally identified as the most economically viable configuration in Italy, to the Danish context. The analysis demonstrated the adaptability of the approach while underscoring the critical influence of regional variations in climatic, economic, and spatial factors.

In Denmark, the vertical bifacial APV system with a capacity of 506 kW_p achieved its optimal performance at an electricity reliability (ER) of 35%, balancing energy generation, economic viability, and land use efficiency. However, beyond this level, diminishing returns were evident due to rising land lease costs, which significantly affected the life cycle cost (LCC) and overall system efficiency. Comparatively, in the Italian case study, the optimal configuration was achieved at an ER of 30%, requiring lower PV capacity due to Italy's higher solar intensity. This highlights how climatic conditions, such as solar radiation, play a decisive role in determining the system's performance and scalability.

The findings emphasize that while the methodology developed for Italy is transferable, region-specific factors, including energy tariffs, land availability, and solar potential, are crucial for optimizing APV systems. Tailoring system design to local conditions is essential to maximize performance and ensure cost-effectiveness.

This work highlights the significant potential of APV systems to enhance energy sustainability when their implementation is guided by detailed regional analyses. Future research should build upon these insights by investigating additional regions, incorporating evolving market conditions, and accounting for policy dynamics to further validate and refine the approach.

4.1.7 References

European Commission, Eurostat. Prices of electricity for non-household consumers in Denmark from 2008 to 2022. https://www.statista.com/statistics/595800/electricity-non-household-price-denmark/ (Accessed 15 October 2024).

Martín, H., de la Hoz, J., Aliana, A., Coronas, S., & Matas, J. (2021). Analysis of the net metering schemes for PV self-consumption in Denmark. Energies, 14(7), 1990.

Lawson, N., Alvarado-Morales, M., Tsapekos, P., & Angelidaki, I. (2021). Techno-economic assessment of biological biogas upgrading based on danish biogas plants. Energies, 14(24), 8252.

Micheli, L., Sepúlveda-Vélez, F. A., & Talavera, D. L. (2024). Impact of variable economic conditions on the cost of energy and the economic viability of floating photovoltaics. Heliyon.

Campana, P.E., Stridh, B., Hörndahl, T., Svensson, S.E., Zainali, S., Lu, S.M., Zidane, T.E.K., De Luca, P., Amaducci, S. and Colauzzi, M. (2024). Experimental results, integrated model validation, and economic aspects of agrivoltaic systems at northern latitudes. Journal of Cleaner Production, 437, p.140235.

Taramasso, M. A., Motaghi, M., & Casasso, A. (2024). A techno-economic feasibility analysis of solutions to cover the thermal and electrical demands of anaerobic digesters. Renewable Energy, 236, 121485.

European Commission, Eurostat. Average rental prices of arable land and/or permanent grassland in the EU, 2022. https://ec.europa.eu/eurostat/statistics-explained/images/8/88/Land_prices_and_rents_SE_v1.2024.xlsx (Accessed 15 October 2024).

Bellone, Y., Croci, M., Impollonia, G., Zad, A. N., Colauzzi, M., Campana, P. E., & Amaducci, S. (2024). Simulation-Based Decision Support for Agrivoltaic Systems. Applied Energy, 369, 123490.

5 OVERALL CONCLUSION

This study examines the integration of agrivoltaic (APV) systems with biomethane production, focusing on optimizing renewable energy generation and enhancing sustainability both at small and large scales. The results demonstrate the significant potential of combining these technologies to address energy needs, agricultural productivity, and environmental challenges.

The integration of a vertical bifacial APV system with a biogas boiler to meet the energy demands of a biomethane plant in Piacenza, Italy, proves to be the most economically viable option at the small scale. Scenario 7, which combines a 327 kWp vertical APV system, the power grid, and a biogas boiler, provides the highest Life Cycle Revenue to Life Cycle Cost (LCR/LCC) ratio, offering a 35% energy recovery (ER). This configuration achieves a balance between energy supply and demand, minimizing costs compared to alternatives such as combined heat and power (CHP) systems or battery storage. The vertical APV system benefits from reduced capital and operational costs, while the biogas boiler facilitates increased biomethane production, boosting revenue.

The adaptability of this optimal configuration was further validated by its application in Denmark, demonstrating how region-specific factors influence system performance. In the Danish context, the vertical bifacial APV system with a capacity of 506 kW_p achieved its optimal performance at a slightly higher ER of 35%, primarily due to lower solar intensity and regional energy tariffs. While this required a higher PV capacity compared to Italy, the findings highlight the scalability and transferability of the methodology when tailored to local climatic, economic, and spatial conditions. This emphasizes the importance of region-specific analyses in maximizing the cost-effectiveness and efficiency of integrated renewable energy systems.

At the larger scale, particularly in the context of agricultural operations like dairy farming in northern Italy, APV systems show considerable promise for enhancing land use efficiency. By generating both renewable energy and supporting crop production, APV systems offer a dual benefit that improves resource use. The study finds that PV systems, when integrated into APV configurations, significantly outperform biomethane production alone in terms of energy yield, making them a more efficient solution for meeting energy demands. While crop yields under APV systems can vary depending on the configuration and irrigation strategies, the overall impact on agricultural productivity remains favourable, especially when crops are selected to suit APV conditions.

This integrated approach offers a sustainable pathway to improve energy access and reduce greenhouse gas emissions. The research highlights the importance of strategic planning to optimize APV layouts and crop management practices, ensuring the dual goals of renewable energy generation and agricultural productivity are achieved. The findings encourage policymakers and stakeholders to consider adopting APV systems as part of a broader strategy for achieving energy independence and sustainability, particularly in rural and agricultural regions. Ultimately, the study underscores the potential for APV and biomethane systems to play a crucial role in advancing a more resilient, efficient, and sustainable future.